

NAVAL POSTGRADUATE SCHOOL MONTEREY, CALIFORNIA



19961203 007

THESIS

STUDIES ON SUBMARINE CONTROL FOR PERISCOPE DEPTH OPERATIONS

by

John V. Tolliver

September 1996

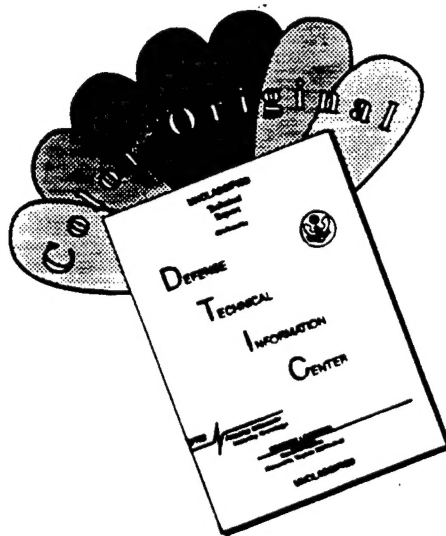
Thesis Advisor:

Fotis A. Papoulas

Approved for public release; distribution is unlimited.

DTIC QUALITY INSPECTED 4

DISCLAIMER NOTICE



THIS DOCUMENT IS BEST QUALITY AVAILABLE. THE COPY FURNISHED TO DTIC CONTAINED A SIGNIFICANT NUMBER OF COLOR PAGES WHICH DO NOT REPRODUCE LEGIBLY ON BLACK AND WHITE MICROFICHE.

REPORT DOCUMENTATION PAGE			Form Approved OMB No. 0704-0188	
Public reporting burden for this collection of information is estimated to average 1 hour per response, including the time for reviewing instruction, searching existing data sources, gathering and maintaining the data needed, and completing and reviewing the collection of information. Send comments regarding this burden estimate or any other aspect of this collection of information, including suggestions for reducing this burden, to Washington Headquarters Services, Directorate for Information Operations and Reports, 1215 Jefferson Davis Highway, Suite 1204, Arlington, VA 22202-4302, and to the Office of Management and Budget, Paperwork Reduction Project (0704-0188) Washington DC 20503.				
1. AGENCY USE ONLY (Leave blank)		2. REPORT DATE September 1996.		3. REPORT TYPE AND DATES COVERED Master's Thesis, Engineer's Thesis
4. TITLE AND SUBTITLE STUDIES ON SUBMARINE CONTROL FOR PERISCOPE DEPTH OPERATIONS			5. FUNDING NUMBERS	
6. AUTHOR(S) TOLLIVER, John V.				
7. PERFORMING ORGANIZATION NAME(S) AND ADDRESS(ES) Naval Postgraduate School Monterey CA 93943-5000			8. PERFORMING ORGANIZATION REPORT NUMBER	
9. SPONSORING/MONITORING AGENCY NAME(S) AND ADDRESS(ES)			10. SPONSORING/MONITORING AGENCY REPORT NUMBER	
11. SUPPLEMENTARY NOTES The views expressed in this thesis are those of the author and do not reflect the official policy or position of the Department of Defense or the U.S. Government.				
12a. DISTRIBUTION/AVAILABILITY STATEMENT Approved for public release; distribution is unlimited.			12b. DISTRIBUTION CODE	
13. ABSTRACT (maximum 200 words) Requirements for submarine periscope depth operations have been increased by integration with carrier battle groups, littoral operations, and contributions to joint surveillance. Improved periscope depth performance is therefore imperative. Submarine control personnel rely on a large number of analog gauges and indications. An integrated digital display system could enhance the ergonomics of the human control interface and display additional parameters. This thesis investigates the required feedbacks for robust automatic depth control at periscope depth, and thus indirectly determines the additional parameters desired for an integrated display. A model of vertical plane submarine dynamics is coupled with first and second order wave force solutions for a particular submarine hull form. Sliding mode control and several schemes of state feedback are used for automatic control. Head and beam seas at sea states three and four are investigated. The automatic control effectiveness provides insight into the indications used by the ship's control party in operations at periscope depth. One possible display system is proposed, with several additional enhancements to improve ship's safety, reduce operator fatigue, and enable accurate reconstruction of the events leading to a loss of depth control.				
14. SUBJECT TERMS Submarine, periscope depth, control optimization, wave forces			15. NUMBER OF PAGES	
			16. PRICE CODE	
17. SECURITY CLASSIFICATION OF REPORT Unclassified	18. SECURITY CLASSIFICATION OF THIS PAGE Unclassified	19. SECURITY CLASSIFICATION OF ABSTRACT Unclassified	20. LIMITATION OF ABSTRACT UL	

Approved for public release; distribution is unlimited.

**STUDIES ON SUBMARINE CONTROL
FOR PERISCOPE DEPTH OPERATIONS**

John V. Tolliver
Lieutenant, United States Navy
B.S., Montana State University, 1988

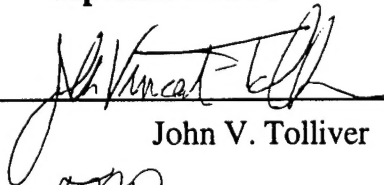
Submitted in partial fulfillment
of the requirements for the degrees of

**MASTER OF SCIENCE IN MECHANICAL ENGINEERING
and
MECHANICAL ENGINEER**

from the

**NAVAL POSTGRADUATE SCHOOL
September 1996**

Author:

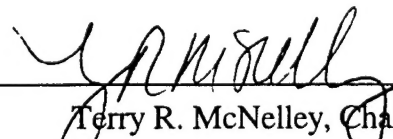


John V. Tolliver

Approved by:



Fotis A. Papoulas, Thesis Advisor



Terry R. McNelley, Chairman
Department of Mechanical Engineering

ABSTRACT

Requirements for submarine periscope depth operations have been increased by integration with carrier battle groups, littoral operations, and contributions to joint surveillance. Improved periscope depth performance is therefore imperative. Submarine control personnel rely on a large number of analog gauges and indications. An integrated digital display system could enhance the ergonomics of the human control interface and display additional parameters. This thesis investigates the required feedbacks for robust automatic depth control at periscope depth, and thus indirectly determines the additional parameters desired for an integrated display.

A model of vertical plane submarine dynamics is coupled with first and second order wave force solutions for a particular submarine hull form. Sliding mode control and several schemes of state feedback are used for automatic control. Head and beam seas at sea states three and four are investigated. The automatic control effectiveness provides insight into the indications used by the ship's control party in operations at periscope depth. One possible display system is proposed, with several additional enhancements to improve ship's safety, reduce operator fatigue, and enable accurate reconstruction of the events leading to a loss of depth control.

TABLE OF CONTENTS

I. INTRODUCTION.....	1
A. GENERAL	1
B. AIM OF THIS STUDY	2
C. THESIS OUTLINE	2
II. SUBMARINE DYNAMICS MODEL	3
A. INTRODUCTION	3
B. DEEPLY SUBMERGED EQUATIONS OF MOTION	3
1. Definition of coordinate system and states	3
2. Hydrodynamic coefficients review	4
3. Vertical plane equations of motion	5
C. EXTENSION TO VERTICAL PLANE PATHKEEPING	9
D. THE DARPA SUBOFF	10
1. Background	10
2. SUBOFF known parameters and coefficients	10
E. CONCLUDING REMARKS	12
III. WAVE FORCE MODELING	15
A. INTRODUCTION	15
B. REVIEW OF LINEAR DEEP WATER WAVES	16
C. WAVE FORCE REGIMES	18
D. SOLUTION FROM SLENDER BODY THEORY	20
1. Seaway model	20
2. First order forces	24
3. Second order forces	26
4. Inclusion of wave forces in equations of motion	27
E. CONCLUDING REMARKS	28
IV. STATE FEEDBACK CONTROL AT PERISCOPE DEPTH	29
A. INTRODUCTION	29
1. State feedback control	29
2. SUBOFF simulation parameters	30
3. State feedback implementation with SIMULINK®	31
4. Integral control on depth	33
5. Feedforward of wave forces	33
6. Optimization algorithm and parameters	36
B. FEEDBACK OF DEPTH AND PITCH ANGLE	37
1. Basic control	37
2. Disturbance feedforward	40
3. Integral control	43
C. FULL STATE FEEDBACK WITH PARTIAL DISTRIBUTION	46
1. Basic control	46
2. Disturbance feedforward	49
3. Integral Control	52
D. FULL STATE FEEDBACK	55
1. Basic control	55
2. Disturbance feedforward	58

3. Integral control	61
E. CONCLUDING REMARKS	64
V. SLIDING MODE CONTROL	67
A. INTRODUCTION	67
1. Overview of MIMO sliding mode control	67
2. Utkin's method for MIMO sliding mode control law design	69
3. Control of chatter	73
B. SIMO SLIDING MODE CONTROL RESPONSE TO DISTURBANCES	74
1. Basic sliding mode disturbance response	75
C. MIMO SLIDING MODE CONTROL AT PERISCOPE DEPTH	89
1. Introduction	89
2. Basic sliding mode controller	90
3. Disturbance feedforward	97
4. Integral control	101
D. CONCLUDING REMARKS	104
VI. GRAPHICAL DISPLAY	105
A. INTRODUCTION	105
B. CURRENT DIVING OFFICER INTERFACE	105
C. PROPOSED DISPLAY	107
D. CONCLUDING REMARKS	110
VII. CONCLUSIONS AND RECOMMENDATIONS	111
A. CONCLUSIONS	111
B. RECOMMENDATIONS	111
LIST OF REFERENCES	113
APPENDIX A. COMPUTER CODE	115
APPENDIX B. MAPLE® SOLUTIONS	125
DISTRIBUTION LIST	139

LIST OF FIGURES

Figure 1. Coordinate System Definition.....	4
Figure 2. Submerged body in pure heave.....	5
Figure 3. SIMULINK® model of vertical plane submarine dynamics.....	8
Figure 4. DARPA SUBOFF model, Roddy (1990).....	13
Figure 5. Coordinate Definition for plane progressive wave, adapted from Sarpkaya and Isaacson (1981, p. 151)	16
Figure 6. Wave force regimes (Sarpkaya and Isaacson, 1981, pg. 385).....	19
Figure 7. Example Sea State three spectrum	21
Figure 8. Spectra area division and mean frequencies	23
Figure 9. Sea surface approximation for sea state three using nineteen sinusoids.....	24
Figure 10. Submarine response to first order accelerations, and expected response	26
Figure 11. State feedback control block diagram.....	32
Figure 12. SIMULINK® trim model.....	32
Figure 13. SIMULINK® state feedback control submarine model.....	33
Figure 14. Filtered wave forces for sea state three (head seas).....	35
Figure 15. Filtered wave moments for sea state three (head seas)	35
Figure 16. SIMULINK® model of feedforward calculator.....	36
Figure 17. SIMULINK® model of system with feedforward term	36
Figure 18. Simulation with depth and pitch angle control in sea state three (head sea direction).....	40
Figure 19. Simulation with depth and pitch angle control with disturbance feedforward, sea state three (head seas)	43
Figure 20. Simulation with depth, pitch angle, and integral control, sea state three (head seas).....	46
Figure 21. Simulation with full state partial distribution feedback control, sea state three (head seas)	49
Figure 22. Simulation with full state partial distribution control and disturbance feedforward, sea state three (head seas).....	52
Figure 23. Simulation with full state partial distribution feedback integral control, sea state three (head seas)	55
Figure 24. Full state feedback optimized control simulation, sea state three (head seas).....	58
Figure 25. Full state feedback control with disturbance feedforward optimized control simulation, sea state three (head seas).....	61
Figure 26. Optimized full state feedback with integral control simulation, sea state three (head seas)	64
Figure 27. SIMULINK® model sliding mode controller	74
Figure 28. Nonlinear simulation of vertical plane response to a pure moment disturbance	81
Figure 29. Nonlinear simulation of vertical plane response to a pure force disturbance	82
Figure 30. Nonlinear simulation of vertical plane response to a pure moment disturbance with a feedforward term based on nonlinear steady state	84
Figure 31. Nonlinear simulation of vertical plane response to a pure force disturbance with a feedforward term based on nonlinear steady state	85
Figure 32. Nonlinear simulation of moment disturbance using sliding mode integral control	88
Figure 33. Nonlinear simulation of force disturbance using sliding mode integral control.....	89
Figure 34. SIMULINK® model of submarine with wave forces and trim	92
Figure 35. Basic sliding mode performance, step change approach to PD	93

Figure 36. State parameters for basic sliding mode approach to periscope depth	94
Figure 37. Simulation with basic sliding mode control in sea state three (head sea direction) ..	95
Figure 38. Simulation using sliding mode control with disturbance feedforward	100
Figure 39. Simulation with sliding mode integral control in sea state three (head seas)	102
Figure 40. USS Nautilus planes position indications.....	106
Figure 41. USS Nautilus pitch angle indication.....	106
Figure 42. Proposed graphical display of submarine control status	107
Figure 43. SIMULINK® animation of depth, pitch angle, and planes angles.....	108
Figure 44. Graphical display data paths.....	110

LIST OF TABLES

Table 1. SUBOFF Assumed and modified parameters	12
Table 2. Estimated Wave Loading Parameters	19
Table 3. Optimized pitch and depth control law results and performance	39
Table 4. Optimized pitch and depth control law with disturbance feedforward results and performance.....	42
Table 5. Optimized pitch and depth integral control law results and performance	45
Table 6. Full state feedback (partial distribution) control law optimization results and performance.....	48
Table 7. Full state feedback (partial distribution) with disturbance feedforward control law optimization results and performance	51
Table 8. Full state feedback (partial distribution) integral control law optimization results and performance.....	54
Table 9. Full state feedback control law optimization results and performance	57
Table 10. Full state feedback control law with disturbance feedforward optimization results and performance.....	60
Table 11. Full state feedback integral control law optimization results and performance	63
Table 12. Optimized RMS error (feet) of state feedback control schemes.....	65
Table 13. Steady state nonlinear solutions for $M_d = 0.001$ radians/second ²	80
Table 14. Steady state nonlinear solutions for $F_d = 0.05$	81
Table 15. Optimized basic sliding mode control law results and performance	96
Table 16. Optimized sliding mode control with disturbance feedforward results and performance.....	99
Table 17. Optimized sliding mode integral control law results and performance	103
Table 18. Optimized RMS error (feet) of sliding mode control and full state feedback	104

ACKNOWLEDGMENTS

I owe my deepest thanks to my wife Kelly and her parents Harvey and Janet for their support, and my children Jacob and Micaela for their love.

Special acknowledgment is due to Randy Dean of the Johns Hopkins Applied Physics Laboratory for his support in providing wave force solutions.

Finally, I owe deep appreciation to Professor Fotis Papoulas for his guidance during the course of this thesis.

I. INTRODUCTION

A. GENERAL

The need for attack submarines to operate at periscope depth has been increased by integration with carrier battle groups, operations in the shallow littoral, and contributions to joint surveillance.

Operating at periscope depth beneath a seaway, a submarine is in an unstable condition. As the free surface is approached, the seaway forces increase, trying to pull the submarine to the surface. To counter these forces, the ship's ballast is changed and control surfaces are used. Because of the seaway's stochastic nature, manual operation for long periods at periscope depth taxes the ship's control party.

Operators must remain aware of the environmental conditions. If the sea becomes quiescent, the submarine will sink out. If the sea suction forces are greater than the ballast and planes authority, the submarine will broach the free surface increasing detection risk by several orders of magnitude. Other events, like temperature or salinity changes, can also have major effects on reliable depth keeping. Contributing to the environmental issues, the need to use minimum speed for a given sea state to control the detectable mast feather reduces the available planes authority, and increases the difficulty of depth control.

However, the current submarine force is not optimized for these operations. One inexpensive area for improvement is the display system for the ship's control party. Modern digital display systems offer ergonomic improvements over current gauges and readouts.

Given a requirement to conduct submarine ship control manually, a fundamental question is that of how to display the state of the ship to the operators. Aside from the obvious indications like ship's pitch angle, depth, and control surface positions what else would be useful? Candidates include the net force acting on the ship, accelerations, and various time averaged values. Implied in this is that a nontraditional means of display will be used to show these parameters, so that the operators will not have to rely on a number of gauges or meters, with averaging of results only available only by the calibrated eye.

An intelligent assistant to the ship's control party would show items of current concern, and issue alerts based on an operator programmable doctrine. Issues like mast exposure, ship's relationship to the bottom, and trim state could be shown in an intuitive, logical manner.

Current evolutions and other items relating to the tactical employment could be included as required.

B. AIM OF THIS STUDY

Although the ship's control party currently relies on a small number of indications, the ability to sense "by the seat of the pants" cannot be discounted. This thesis investigates required feedbacks for robust automatic depth control at periscope depth, and thus indirectly evaluates the additional indications to be added to an integrated display.

This approach assumes that the best ship's control parties already use system states for control which are not explicitly displayed.

C. THESIS OUTLINE

Chapter II contains the development of the deeply submerged submarine dynamics model. Chapter III gives the development and source of the wave forces used to simulate operations at periscope depth. In Chapter IV, optimization studies are performed for nine different cases of state feedback control. This gives a feeling for the quality of depth control achievable by the use of different levels of sensors. Chapter V explores the use of sliding mode control for periscope depth operations. In Chapter VI, current ships control technology is reviewed and an integrated display is proposed. Conclusions and recommendations are given in Chapter VII.

II. SUBMARINE DYNAMICS MODEL

A. INTRODUCTION

When a submarine is deeply submerged, many of its maneuvering characteristics can be determined from application of Morison's equation to model test data. A series of trials, often done with a planar motion mechanism (PMM), give the damping and inertia coefficients for small maneuvers in each of the six degrees of freedom. This method is not without limits. For trials done in the horizontal and vertical planes only, nonlinear cross coupling effects are ignored. The hydrodynamic coefficients work poorly for prediction of high speed maneuvers and control surface casualties. Here the large crossflow velocities, vortex hull interaction, and flow separation all have effects which are not predicted by the hydrodynamic coefficients. It is possible, however, to include some of these effects as additional nonlinear terms.

As the submarine approaches the free surface, several complexities are introduced into the hydrodynamic coefficient approach. First, the inertia terms change as an acceleration will no longer act upon an effectively infinite region. Second, an inviscid form of damping exists near the free surface. This comes about from the generation of waves by the body, and depends on the body depth and character of motion. Finally, the interaction between the incident waves and the submarine introduces added forces and moments. These effects combine to make designing for periscope depth vexing for engineers and operating at periscope depth an art for the ship's crew.

The approach in this thesis will be to first establish a dynamics model appropriate for a deeply submerged submarine at low to moderate speeds. The forces and moments resulting from the seaway will then be superimposed on this model to provide a reasonable approximation to the submarine motion beneath waves.

B. DEEPLY SUBMERGED EQUATIONS OF MOTION

1. Definition of coordinate system and states

The coordinate system defined in Figure 1 will be used. The origin of the global coordinate system is fixed at the ocean surface. The z axis is positive downward, towards the ocean bottom. The x axis is positive in the direction of intended submarine motion. The body fixed coordinates are rotated from the global coordinates by the angle θ . Body fixed velocities

w (heave), u (surge), and q (pitch) are shown. The control surface deflections, δ_b (bow planes) and δ_s (stern planes) are also defined.

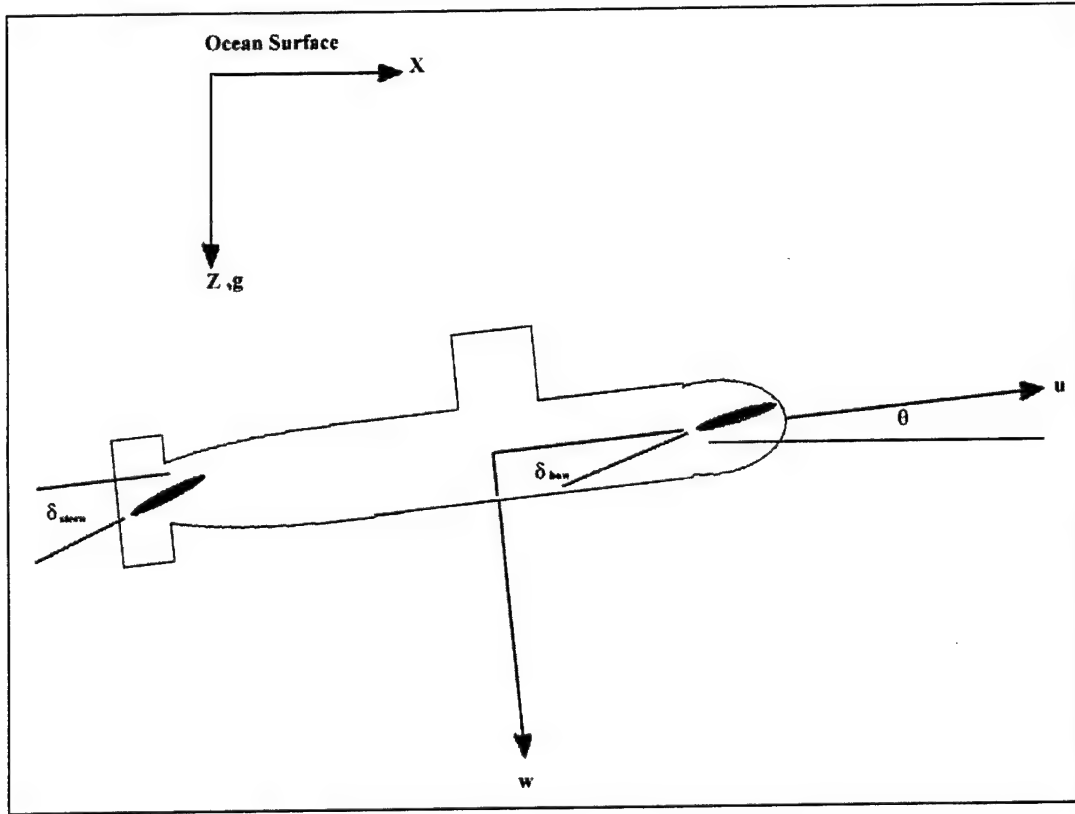


Figure 1. Coordinate System Definition

2. Hydrodynamic coefficients review

For a deeply submerged submarine, small motions can be analyzed using the concept of hydrodynamic coefficients. These represent a Taylor series expansion of the functional relationship between body movements and the resulting fluid forces. For example, given the deeply submerged body in Figure 2 undergoing pure heave, resulting body forces can be expressed in the following manner:

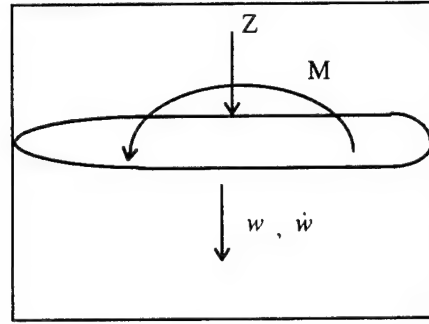


Figure 2. Submerged body in pure heave

$$M = M_w w + M_{w|w|} w|w| + M_{\dot{w}} \dot{w} \quad (1)$$

$$Z = Z_w w + Z_{w|w|} w|w| + Z_{\dot{w}} \dot{w} \quad (2)$$

This method is extended to the six degrees of freedom of the body, and done for velocity and acceleration components of the movement. This includes representations of added mass, viscous drag, and square law drag.

3. Vertical plane equations of motion

By using this system of notation, and applying Newton's second law to the body fixed coordinates, and transforming to global coordinates, the equations of pitch and heave may be obtained in the vertical plane. The general case is quite complex, having centers of mass and buoyancy that are separate from each other and the coordinate system origin. This, along with cross coupled hydrodynamic coefficients, results in a nonlinear, coupled set of differential equations.

These equations of pitch and heave may be simplified considerably by several reasonable assumptions. Assuming that the submarine motion is constrained to the vertical plane, the equations of motion for heave and pitch are (Smith, Crane, and Summey (1978)):

$$m[\dot{w} - uq - x_G \dot{q} - z_G q^2] = \quad (3)$$

$$Z_q \dot{q} + Z_w \dot{w} + Z_q uq + Z_w w$$

$$+ u^2 (Z_{\delta_b} \delta_b + Z_{\delta_s} \delta_s)$$

$$\begin{aligned}
I_y \dot{q} - m[x_G(\dot{w} - uq) - z_G(\dot{u} + wq)] = & \quad (4) \\
& M_{\dot{q}} \dot{q} + M_{\dot{w}} \dot{w} + M_q uq + M_w uw \\
& + u^2 (M_{\delta_b} \delta_b + M_{\delta_s} \delta_s) \\
& - (x_G mg - x_B B) \cos(\theta) \\
& - (z_G mg - z_B B) \sin(\theta)
\end{aligned}$$

It is apparent that Equations (3) and (4) are nonlinear, coupled differential equations in w and q and u . To reduce this coupling, terms involving the derivatives of w and q can be collected, resulting in a mass matrix.

$$\bar{M} = \begin{bmatrix} m - Z_{\dot{w}} & -Z_{\dot{q}} \\ -M_{\dot{w}} & I_y - M_{\dot{q}} \end{bmatrix} \quad (5)$$

The mass matrix can be readily inverted:

$$\bar{M}^{-1} = \frac{\begin{bmatrix} I_y - M_{\dot{q}} & Z_{\dot{q}} \\ M_{\dot{w}} & m - Z_{\dot{w}} \end{bmatrix}}{(m - Z_{\dot{w}})(I_y - M_{\dot{q}}) - Z_{\dot{q}} M_{\dot{w}}} \quad (6)$$

By applying Equation (6), the cross coupling of terms in \dot{w} and \dot{q} can be removed from Equations (3) and (4). To allow the introduction of external forces and moments, the system was augmented by force and moment disturbances acting at the origin of the body fixed coordinates. They were multiplied by the cosine of the pitch angle for conversion to the body fixed coordinate system. These disturbances can be used to input external effects, such as changes in trim and wave forces. By further assuming that the center of buoyancy is at the body fixed coordinate system origin, the center of mass is directly below, and that the forward speed u is constant, the equations of motion can be reduced to the following:

$$\dot{w} = a_{11}uw + a_{12}uq + a_{13} \sin(\theta) + b_{11}u^2 \delta_b + b_{12}u^2 \delta_s + F_d \cos(\theta) + e_{11}q^2 + e_{12}qw \quad (7)$$

$$\dot{q} = a_{21}uw + a_{22}uq + a_{23} \sin(\theta) + b_{21}u^2 \delta_b + b_{22}u^2 \delta_s + M_d \cos(\theta) + e_{21}q^2 + e_{22}qw \quad (8)$$

$$\dot{\theta} = q \quad (9)$$

$$\dot{z} = w \cos(\theta) - u \sin(\theta) \quad (10)$$

$$\dot{x} = w \sin(\theta) + u \cos(\theta) \quad (11)$$

where:

$$a_{11} = \frac{Z_w(I_y - M_{\dot{q}}) + Z_{\dot{q}}M_w}{(m - Z_w)(I_y - M_{\dot{q}}) - Z_{\dot{q}}M_w}$$

$$a_{12} = \frac{(Z_q + m)(I_y - M_{\dot{q}}) + Z_{\dot{q}}M_q}{(m - Z_w)(I_y - M_{\dot{q}}) - Z_{\dot{q}}M_w}$$

$$a_{21} = \frac{M_{\dot{w}}Z_{\dot{w}} + (m - Z_w)M_w}{(m - Z_w)(I_y - M_{\dot{q}}) - Z_{\dot{q}}M_w}$$

$$a_{22} = \frac{M_{\dot{w}}(Z_q + m) + (m - Z_w)M_q}{(m - Z_w)(I_y - M_{\dot{q}}) - Z_{\dot{q}}M_w}$$

$$a_{13} = \frac{Z_{\dot{q}}z_Gmg}{(m - Z_w)(I_y - M_{\dot{q}}) - Z_{\dot{q}}M_w}$$

$$a_{23} = \frac{(m - Z_w)z_Gmg}{(m - Z_w)(I_y - M_{\dot{q}}) - Z_{\dot{q}}M_w}$$

$$b_{11} = \frac{(I_y - M_{\dot{q}})Z_{\delta_b} + Z_{\dot{q}}M_{\delta_b}}{(m - Z_w)(I_y - M_{\dot{q}}) - Z_{\dot{q}}M_w}$$

$$b_{21} = \frac{M_{\dot{w}}Z_{\delta_b} + M_{\delta_b}(m - Z_w)}{(m - Z_w)(I_y - M_{\dot{q}}) - Z_{\dot{q}}M_w}$$

$$b_{12} = \frac{(I_y - M_{\dot{q}})Z_{\delta_s} + Z_{\dot{q}}M_{\delta_s}}{(m - Z_w)(I_y - M_{\dot{q}}) - Z_{\dot{q}}M_w}$$

$$b_{22} = \frac{M_{\dot{w}}Z_{\delta_s} + M_{\delta_s}(m - Z_w)}{(m - Z_w)(I_y - M_{\dot{q}}) - Z_{\dot{q}}M_w}$$

$$e_{11} = \frac{(I_y - M_{\dot{q}})z_Gm}{(m - Z_w)(I_y - M_{\dot{q}}) - Z_{\dot{q}}M_w}$$

$$e_{12} = \frac{Z_{\dot{q}}z_Gm}{(m - Z_w)(I_y - M_{\dot{q}}) - Z_{\dot{q}}M_w}$$

$$e_{21} = \frac{M_{\dot{w}}z_Gm}{(m - Z_w)(I_y - M_{\dot{q}}) - Z_{\dot{q}}M_w}$$

$$e_{22} = \frac{(m - Z_{\dot{w}})z_G m}{(m - Z_{\dot{w}})(I_y - M_{\dot{q}}) - Z_{\dot{q}} M_{\dot{w}}}$$

Equations (7) through (11) are the governing equations of motion for this thesis. It is of note that the disturbance force and moment terms represent accelerations due to the disturbances. To provide ease of use, the equations of motion were implemented in the SIMULINK® model shown in Figure 3. This building block approach was very effective for conducting studies on the effectiveness of different types of controllers.

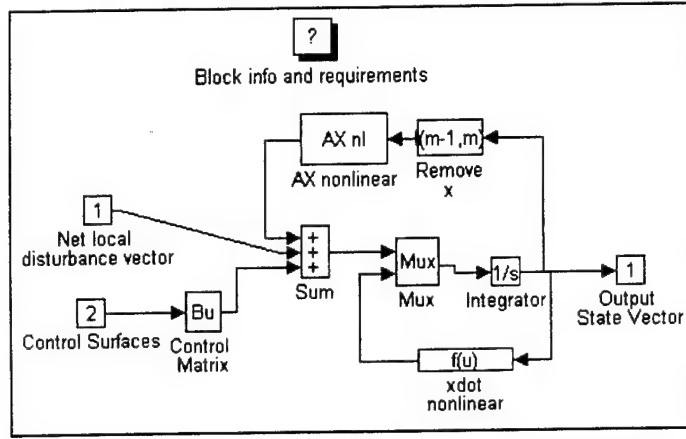


Figure 3. SIMULINK® model of vertical plane submarine dynamics

For control design, it is convenient to use a linear state space representation of the system. This allows the use of a variety of controller design tools including pole placement and linear quadratic regulator algorithms. Equations (7) through (11) can be linearized about a level flight condition. This results in the linear state space representation:

$$\dot{w} = a_{11}uw + a_{12}uq + a_{13}\theta + b_{11}u^2\delta_b + b_{11}u^2\delta_s + F_d \quad (12)$$

$$\dot{q} = a_{21}uw + a_{22}uq + a_{23}\theta + b_{21}u^2\delta_b + b_{22}u^2\delta_s + M_d \quad (13)$$

$$\dot{\theta} = q \quad (14)$$

$$\dot{z} = w - u\theta \quad (15)$$

$$\dot{x} = w\theta + u \quad (16)$$

Equations (12) through (15) can be rewritten in matrix form. This form of the linear submarine vertical plane dynamics equations will be used for controller design. For controller design, Equation (16) was excluded from the matrix form. Because of the constant forward speed u assumption, there was no direct means of control for x .

$$\begin{bmatrix} \dot{w} \\ \dot{q} \\ \dot{\theta} \\ \dot{z} \end{bmatrix} = \begin{bmatrix} a_{11}u & a_{12}u & a_{13} & 0 \\ a_{21}u & a_{22}u & a_{23} & 0 \\ 0 & 1 & 0 & 0 \\ 1 & 0 & u & 0 \end{bmatrix} \begin{bmatrix} w \\ q \\ \theta \\ z \end{bmatrix} + \begin{bmatrix} b_{11}u^2 & b_{12}u^2 \\ b_{21}u^2 & b_{22}u^2 \\ 0 & 0 \\ 0 & 0 \end{bmatrix} \begin{bmatrix} \delta_b \\ \delta_s \end{bmatrix} + \begin{bmatrix} F_d \\ M_d \\ 0 \\ 0 \end{bmatrix} \quad (17)$$

C. EXTENSION TO VERTICAL PLANE PATHKEEPING

Equations (7) through (10) and the corresponding SIMULINK® model are linearized around a constant commanded depth, or level flight. They can be extended to a two dimensional pathkeeping simulation by a coordinate transformation. After coordinate rotation by an angle β (positive in the same direction as θ), the resulting system is:

$$\dot{w} = a_{11}uw + a_{12}uq + a'_{13} \sin(\theta') + b_1 u^2 \delta + F'_d \quad (18)$$

$$\dot{q} = a_{21}uw + a_{22}uq + a'_{23} \sin(\theta') + b_2 u^2 \delta + M'_d \quad (19)$$

$$\dot{\theta}' = q \quad (20)$$

$$\dot{z}' = w \cos(\theta') - u \sin(\theta') \quad (21)$$

$$\dot{x}' = w \sin(\theta') + u \cos(\theta') \quad (22)$$

where:

$$\theta' = \theta - \beta \quad (23)$$

$$x' = -z \sin(\beta) + x \cos(\beta) \quad (24)$$

$$z' = z \cos(\beta) + x \sin(\beta) \quad (25)$$

$$a'_{13} = a_{13} \cos(\beta) \quad (26)$$

$$a'_{23} = a_{23} \cos(\beta) \quad (27)$$

$$F_d' = F_d + a_{13} \cos(\theta') \sin(\beta) \quad (28)$$

$$M_d' = M_d + a_{23} \cos(\theta') \sin(\beta) \quad (29)$$

If the expected angular deviation from the planned path is small, Equations (28) and (29) can be simplified by assuming that $\cos(\theta')$ is equal to one. Then the rotated equation set, Equations (18) through (22), is identical in form to Equations (7) through (11).

Equations (23) through (29) allow any vertical plane path consisting of a series of straight line segments to be simulated one segment at a time.

D. THE DARPA SUBOFF

1. Background

For the purpose of this work, it was desired to have a vertical plane model of submarine dynamics which would give a similar response to a modern fast attack nuclear submarine (SSN). Several sets of unclassified hydrodynamic coefficients were available, these being for the swimmer delivery vehicle (SDV) detailed in Smith, Crane, and Summey (1978) and for the DARPA SUBOFF model detailed in Roddy (1990).

The SDV had a very complete set of hydrodynamic coefficients which have been used in a large number of Autonomous Underwater Vehicle (AUV) research projects. Among these is the Naval Postgraduate School (NPS) AUV sliding mode controller, Hawkinson (1990). Despite these advantages, the SDV hydrodynamic coefficients were not used because the wing like hull of the SDV bore little resemblance to an axisymmetric submarine hull.

The SUBOFF hydrodynamic coefficients detailed in Roddy (1990) lacked some of the cross coupling coefficients. The documentation also lacked details on the models metacentric height. Because the SUBOFF represented a submarine hull form and most of the vertical plane coefficients and parameters were available, it was chosen as the model for this thesis.

2. SUBOFF known parameters and coefficients

The SUBOFF was developed to allow comparison between flow field predictions and model test data (Roddy, 1990). The available coefficients were based on planar motion mechanism tests conducted on the model.

Because the aim of the study was to examine full scale submarine motions, the model and its hydrodynamic coefficients were scaled to a length of 300 feet. After scaling, several parameters had to be modified or assumed to give control and response comparable to a modern fast attack submarine. The force coefficients of the stern planes was doubled to provide a more realistic level force. Bow planes were assumed to have one half the force and one quarter the moment authority of the stern planes. Finally, a metacentric height of one foot was assumed, as it provided a realistic point of stern planes reversal. The resulting parameters are shown in Table 1.

Parameter	SUBOFF Model	Scaled / Modified Result
Length (Feet)	14.2917	300
Displacement (tons)	0.7704	7,7145
Maximum Diameter (Feet)	1.667	35
Metacentric Height (Feet)	Not Provided	1
XG	0.00975	0
ZG	Not Provided	1
XB	-0.006669	0
ZB	Not Provided	0
Z'_{δ_s}	-0.005603	-0.011206
M'_{δ_s}	-0.002409	-0.004818
Z'_{δ_b}	Not Provided	-0.005603
M'_{δ_b}	Not Provided	0.0012045

Table 1. SUBOFF Assumed and modified parameters

E. CONCLUDING REMARKS

A simplified model of submarine vertical plane dynamics was derived. The coefficients for use in this model were obtained from the DARPA SUBOFF model, which is a representative axisymmetric submarine hull form. The simplified nonlinear equations of motion were incorporated in a SIMULINK® model to allow easy integration with wave force models and different controllers.



III. WAVE FORCE MODELING

A. INTRODUCTION

As a submarine operates near the free surface, it encounters complex forces which may cause unsatisfactory or unstable depth control. The lift and moment from incident waves increase in an exponential manner as the surface is approached. To maintain a desired depth, the ship's ballast is adjusted to counteract steady forces. Control surfaces are used to counter dynamic changes. A small depth excursion or change in forces can overwhelm the planes and cause a loss of depth control. The consequences range from losing radio reception to compromising the ship's mission.

The effects of incident waves on a submerged body can be divided up in several categories. The largest, the first order forces act at the incident wave frequency. These forces move the submarine, but usually result in oscillations about a mean state. Second order forces, which are the result of wave diffraction and wave interaction, have several different frequency components.

Wave diffraction of a single frequency wave results in a steady force and a varying force at twice the wave frequency. The double frequency force is typically neglected, as the large inertia of the submarine effectively filters it. Interactions of waves at different frequencies also results in forces. These consist of a component acting at the sum of the wave frequencies and a component acting at the difference of the wave frequencies. The sum frequency force is typically neglected, as it is also filtered by submarine's inertia. The difference frequency component results in a slowly varying force on the submarine.

The slowly varying forces are the principle cause of difficult periscope depth control (Ni, Zhang, and Dai, 1994). They are compensated for using control surfaces and occasional adjustments of trim.

During the design phase, engineering decisions are made which will determine the ship's ability to remain at periscope depth. Of these, the most critical are the height of the sail and control surface sizes. Every foot added to the sail gives a deeper periscope depth. Larger planes improve the operator's ability to compensate for changes in suction forces. However, these improvements are not without cost. The sail and other appendages are a large fraction of the total drag, and can restrict the ship's top speed. Larger movable control surfaces can adversely affect the high speed casualty recoverability (Jackson, 1992, p. 15-9).

The goal of this thesis is not to provide new tools for the designer, but rather new means to enhance control for the operators of current submarines. Due to this focus, simplified means of modeling the wave forces for a few specific cases will be used.

B. REVIEW OF LINEAR DEEP WATER WAVES

The pertinent features of linear deep water waves will be reviewed to provide background for the following sections. The coordinate system used for the examples is shown in Figure 5. For the examples in this section, it will be assumed that the submarine is oriented with the bow pointing into the page. Consistent with the global coordinate system from Chapter II, the distance from the surface to the submarine centerline is z . The submarine diameter is D .

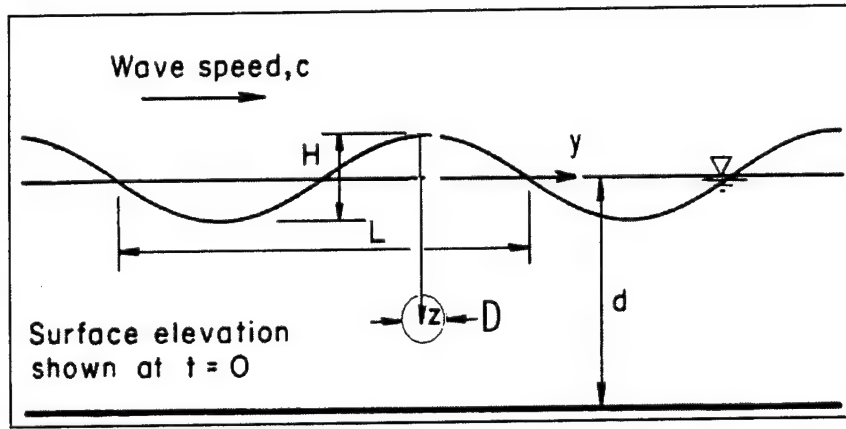


Figure 5. Coordinate Definition for plane progressive wave, adapted from Sarpkaya and Isaacson (1981, p. 151)

For a wave of wavelength L , a wave number, k , can be defined.

$$k = \frac{2\pi}{L} \quad (30)$$

Assuming that fluid is incompressible and inviscid Laplace's equation can be applied.

It is thus desired to find a solution to:

$$\frac{\partial^2 \phi}{\partial x^2} + \frac{\partial^2 \phi}{\partial z^2} = 0 \quad (31)$$

To this, the boundary conditions at the free surface, and the bottom must be applied:

$$\frac{\partial \phi}{\partial z} = 0, \text{ at } z = d \text{ (no flow through ocean bottom)} \quad (32)$$

$$\frac{\partial \eta}{\partial t} + \frac{\partial \phi}{\partial x} \frac{\partial \eta}{\partial x} + \frac{\partial \phi}{\partial z} = 0, \text{ at } z = \eta \text{ (zero velocity normal to ocean surface)} \quad (33)$$

$$\frac{\partial \phi}{\partial t} + \frac{1}{2} \left[\left(\frac{\partial \phi}{\partial x} \right)^2 + \left(\frac{\partial \phi}{\partial z} \right)^2 \right] + g\eta = f(t), \text{ at } z = \eta \quad (34)$$

For small amplitude waves in deep water, the following solution can be obtained
(adapted from Sarpkaya and Isaacson, 1981, p. 159):

$$\phi = \frac{\pi H}{kT} e^{-kz} \sin(\omega t) \quad (35)$$

$$c^2 = \frac{\omega^2}{k^2} = \frac{g}{k} \quad (36)$$

$$L = \frac{gT^2}{2\pi} \quad (37)$$

$$\eta = \frac{H}{2} \cos(\omega t) \quad (38)$$

$$\zeta = -\frac{H}{2} e^{-kz} \cos(\omega t) \quad (39)$$

$$\dot{\zeta} = \omega \frac{H}{2} e^{-kz} \sin(\omega t) \quad (40)$$

$$\ddot{\zeta} = \omega^2 \frac{H}{2} e^{-kz} \cos(\omega t) \quad (41)$$

$$\xi = -\frac{H}{2} e^{-kz} \sin(\omega t) \quad (42)$$

$$\dot{\xi} = -\omega \frac{H}{2} e^{-kz} \cos(\omega t) \quad (43)$$

$$\ddot{\xi} = \omega^2 \frac{H}{2} e^{-kz} \sin(\omega t) \quad (44)$$

where η is the distance from the surface to the average level ($z = 0$), ω is the angular frequency of the incident wave, ζ is the displacement of a particle in the x direction, and ξ is the displacement of a particle in the z direction.

A key parameter in oscillating flows is the Keulegan-Carpenter number:

$$K = \frac{U_{mean} T}{D} \quad (45)$$

where U_{mean} is the average velocity across the characteristic dimension D .

By taking the average of the velocity given in Equation (40), and substitution into Equation (45), the expression for the Keulegan-Carpenter can be reduced to the following:

$$K = \frac{2H}{D} e^{-kz} \quad (46)$$

Equation (46) is the Keulegan-Carpenter number based on the cross flow velocity of the undisturbed wave at the same depth as the centerline of the submarine hull.

C. WAVE FORCE REGIMES

There are different regimes of interaction between a submerged body and a wave field. Broadly, they can be broken into several areas. Inertial interaction, where the body acts like a particle in the wave field. Wave diffraction, where the bodies influence upon the wave field is accounted for. Finally, there are flow separation (viscous) effects. The relative importance of each of these effects can be determined by examining the relationship the body size to the wave parameters. (Sarpkaya and Isaacson, 1981, pp. 381-386)

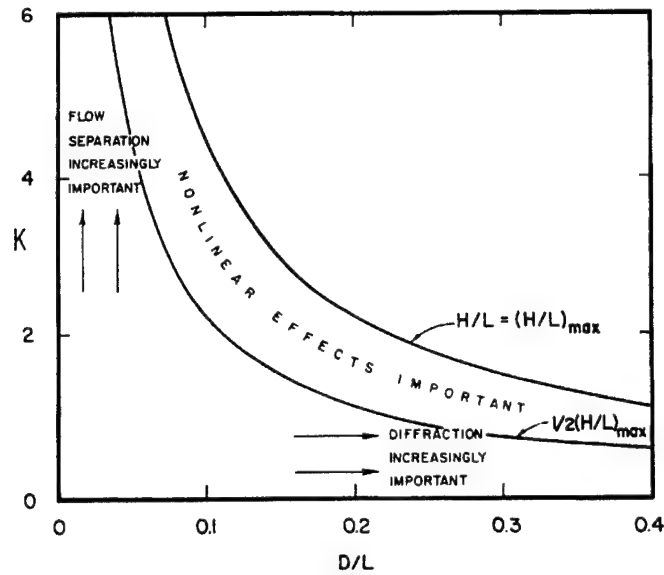


Figure 6. Wave force regimes (Sarpkaya and Isaacson, 1981, pg. 385)

To estimate the significant effects for a typical SSN, a typical operating condition is assumed. For a 300 foot submarine with a 35 foot diameter, a typical periscope operating depth would be about 50 feet from the centerline of the ship to the free surface. Using average values for sea states three and four and assuming deep water compared to the wavelength, the following quantities were calculated at a depth of 50 feet:

Parameter	Sea State 3	Sea State 4
Significant Wave Height	3	6
Average Period	6.623501	7.154522
Wave Length	224.6467	262.1114
Wave Number	0.027969	0.023971
K	0.042339	0.103414
D/L	0.1558	0.133531

Table 2. Estimated Wave Loading Parameters

The Diameter/Wavelength (D/L) ratios and the Keulegan-Carpenter numbers of Table 2 show that for the sea states of interest, wave diffraction much more significant than viscous forces. It can be concluded that an inviscid analysis should give good results for the wave forces. However, this is only rigorous for an unappended hull, as the control surfaces and sail on an actual submarine will experience viscous effects.

D. SOLUTION FROM SLENDER BODY THEORY

Wave force solutions for several specific cases were generated for the SUBOFF by the SSBN Security Department of the Johns Hopkins University Applied Physics Laboratory. A slender body solution with some three dimensional corrections was used. The specific method used for the generation of the first order motions and second order forces is detailed by O'Dea and Barr (1976, pp. 7-25).

A seaway approximation consisting of a small number of regular waves was used to model sea states three and four. For each sea state, the resulting data were separated into two categories. The effects of the first order forces were given in terms of body motions. The effects of the steady second order forces and the difference interaction forces were provided in pounds force.

1. Seaway model

A random seaway can be represented by the superposition of a large number of regular waves. The seaway was approximated by superimposing n regular waves. The frequency and height of these waves was determined using the Bretschneider spectrum. It gives the spectral density in terms of the significant wave height, H_s , and the peak frequency, ω_o .

$$S(\omega) = \frac{5H_s^2}{16\omega_o(\omega / \omega_o)^5} e^{\left[-\frac{5}{4}\left(\frac{\omega}{\omega_o}\right)^4 \right]} \quad (47)$$

To model sea state three, a significant wave height of three feet was used, with a central frequency of 0.836 radians per second. This results in the following spectrum:

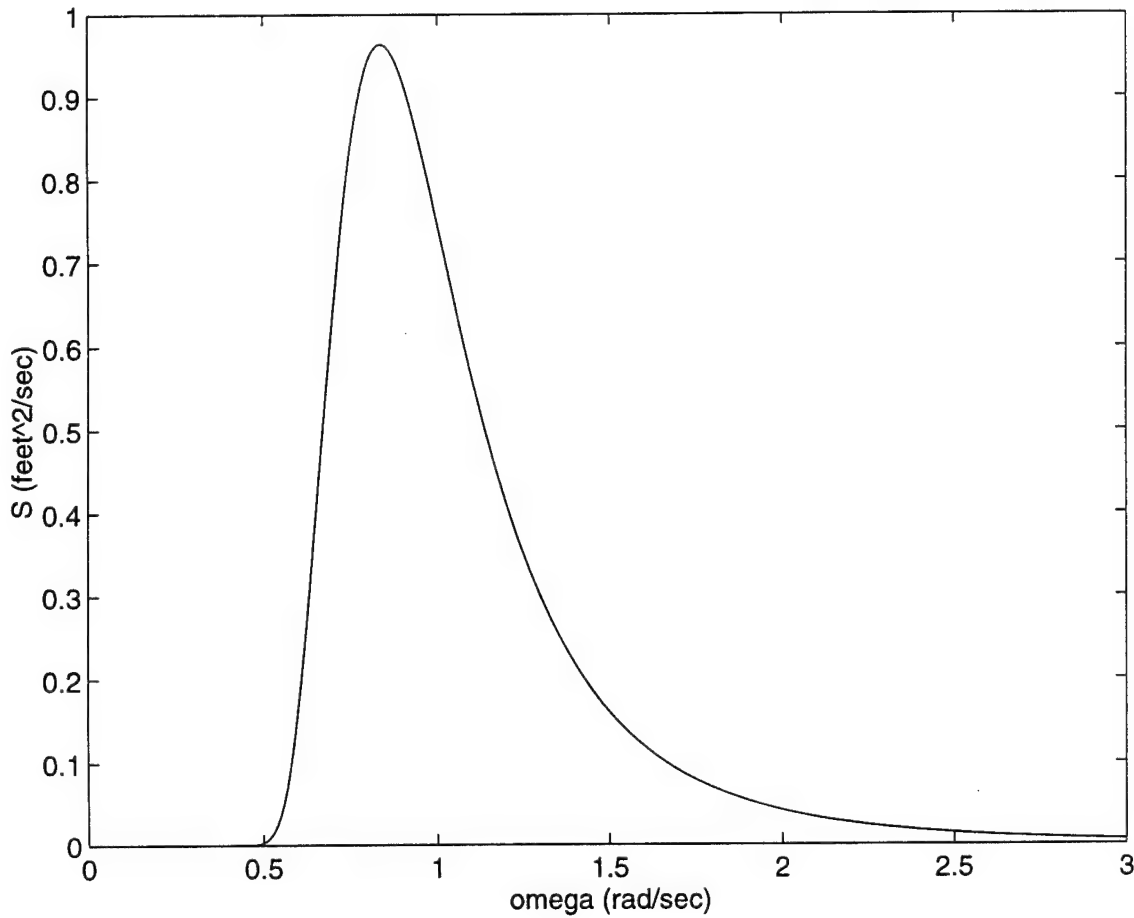


Figure 7. Example Sea State three spectrum

Figure 7 gives a statistical picture of the seaway, but is not immediately useful for time domain simulation. One way to obtain a time history is to represent this stationary process as a the sum of a series of sine waves:

$$\eta(t) = \sum_{i=1}^n A_i \sin(\omega_i t + \alpha_i) \quad (48)$$

Where A_i is the amplitude of the i^{th} wave, and α_i is its randomly chosen phase angle.

If the number of sine waves is reasonable large, and the frequencies and amplitudes of each component are chosen to achieve the same energy as the section of spectrum it represents, Equation (48) will give a good representation of the ocean surface.

The method chosen was to divide the spectra into n segments of equal areas. This results in n sine waves all with equal amplitudes. Integration of Equation (48) yields:

$$\int_0^{\infty} S(\omega) d\omega = \frac{H_s^2}{16} \quad (49)$$

Because the spectrum extends to infinity, it was chosen truncate the spectrum at a point where the area was a fraction C of the total area. The amount of area to be represented by each sine wave is equal to its mean square value. So the amplitude of each sine wave is equal to the square root of the area it represents times the square root of two.

$$A_i = \frac{H_s}{2} \sqrt{\frac{C}{2n}} \quad (50)$$

Equation (48) can be integrated up to some frequency $\hat{\omega}_i$, which represents the frequency at which the spectral area is equal to iC/n times the total area.

$$\int_0^{\hat{\omega}_i} S(\omega) d\omega = \frac{H_s^2}{16} \frac{i}{n} C \quad (51)$$

Solving Equation (51) for $\hat{\omega}_i$ yields:

$$\hat{\omega}_i = \omega_o \left[\frac{4}{5} \ln \left(\frac{Ci}{N} \right) \right]^{\frac{1}{4}} \quad (52)$$

Because the spectral level is insignificant below ω equal to $0.6\omega_o$, the frequency of the first segment was determined as follows:

$$\omega_1 = \frac{(0.6\omega_o + \hat{\omega}_1)}{2} \quad (53)$$

The remainder of the frequencies were determined by taking the midpoint of the frequencies at either side of the area segment.

$$\omega_i = \frac{\hat{\omega}_{i-1} + \omega_i}{2}, \text{ for } i = 2 \text{ to } n \quad (54)$$

Figure 8 illustrates the method used, approximating the spectrum with sinusoids. Nineteen equal area sections are divided, with the center frequency of each segment marked with a circle.

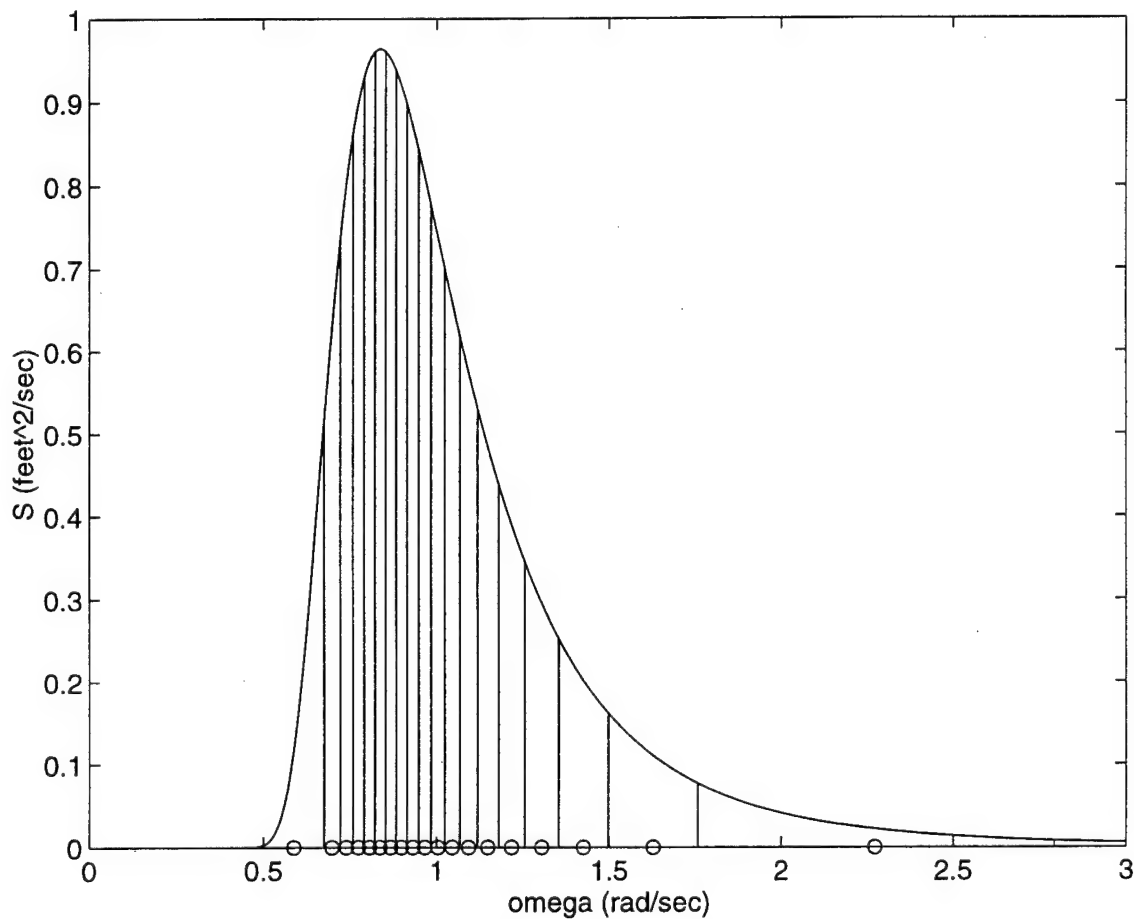


Figure 8. Spectra area division and mean frequencies

Figure 9 shows the ocean surface which results from the use of this method for the case of sea state three, peak frequency of 0.862 radians per second. Nineteen sinusoids were used to approximate the spectra, and the phase angles were randomly chosen.

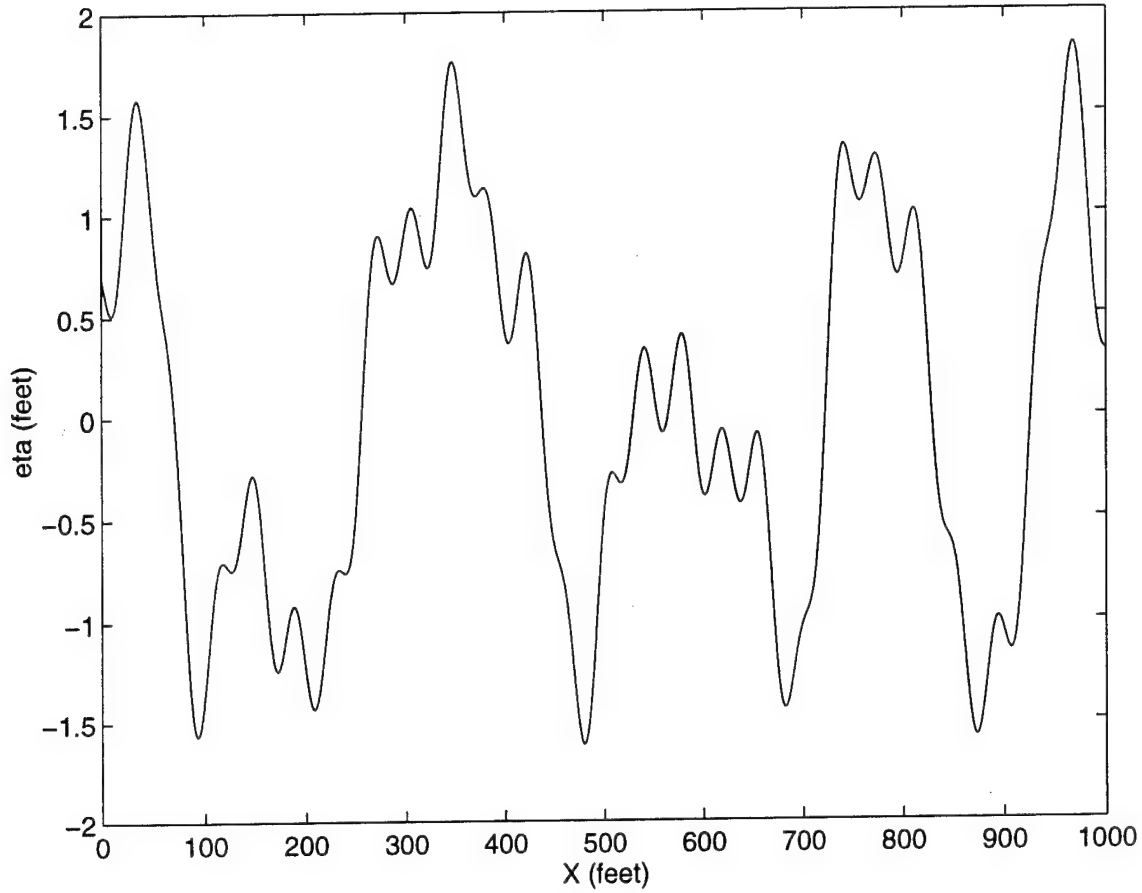


Figure 9. Sea surface approximation for sea state three using nineteen sinusoids

2. First order forces

The first order wave effects were provided in the form of submarine motions. They were given as a series of phasors, the real part of the summation representing the actual perturbation caused by the first order wave forces.

$$z(t) = \sum_{i=1}^n Z_i e^{-i(\omega_i t + \alpha_i)} \quad (55)$$

$$\theta(t) = \sum_{i=1}^n \theta_i e^{-i(\omega_i t + \alpha_i)} \quad (56)$$

Because the first order motions were provided for a specific depth, it was required to correct Equations (55) and (56) for depth. The first order motions roughly correspond to the particle motions given by Equation (42), so an exponential decay was used to derive the following correction factor:

$$\frac{e^{-k_i z}}{e^{-k_i z_0}} \quad (57)$$

Application of Equation (57) to Equations (55) and (56) results in:

$$z(t) = \sum_{i=1}^n Z_i e^{-\sqrt{-1}(\omega_i t + \alpha_i) - k_i(z - z_0)} \quad (58)$$

$$\theta(t) = \sum_{i=1}^n \theta_i e^{-\sqrt{-1}(\omega_i t + \alpha_i) - k_i(z - z_0)} \quad (59)$$

The displacements given by Equations (58) and (59) are not suitable for inclusion in the submarine equations of motion. For this, an acceleration is required. Differentiating twice with respect to time results in:

$$\ddot{z}(t) = -\sum_{i=1}^n \omega_i^2 Z_i e^{-i(\omega_i t + \alpha_i) - k_i(z - z_0)} \quad (60)$$

$$\ddot{\theta}(t) = -\sum_{i=1}^n \omega_i^2 \theta_i e^{-i(\omega_i t + \alpha_i) - k_i(z - z_0)} \quad (61)$$

Equations (60) and (61) were incorporated as force and moment disturbances in the equations of motion found in Chapter II. To test the validity of this approach, an open loop simulation was performed using the accelerations from Equations (60) and (61) for one sea state and heading. Figure 10 shows the results of this simulation, as well as the expected first order motions. The upper curve shows the expected first order motions, and the lower curve shows the results of integrating Equations (7) through (11) with the accelerations from Equations (60) and (61). Although there was some drifting motion, the character of motion and the approximate amplitude of each cycle of motion very close. The drifting motion was a result lack of the lack of open loop depth stability, which is characteristic of submarines.

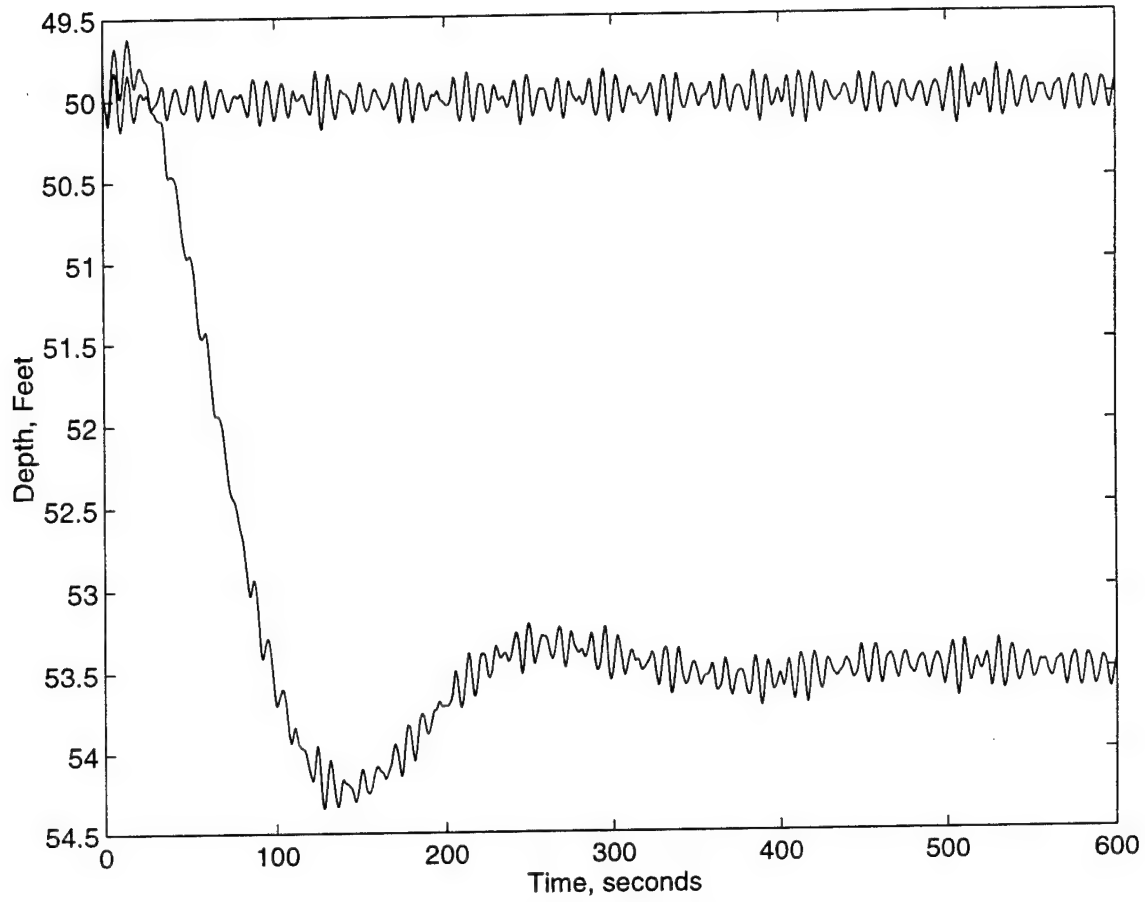


Figure 10. Submarine response to first order accelerations, and expected response

3. Second order forces

For a particular depth and wave time history, the second order forces were given in the following form:

$$Z(t) = \sum_{i=1}^n \sum_{j=1}^n F_{ij} e^{i(\omega_i - \omega_j)t + \alpha_i + \alpha_j} \quad (62)$$

$$M(t) = \sum_{i=1}^n \sum_{j=1}^n M_{ij} e^{i(\omega_i - \omega_j)t + \alpha_i + \alpha_j} \quad (63)$$

$Z(t)$ represents the force acting at the body fixed coordinate system in the z direction and $M(t)$ is the moment acting about the y axis. It should be noted that Equations (63) and (65) include the slowly varying forces ($i \neq j$) and the steady forces ($i = j$).

It can be determined from analysis of the changes of second order forces with respect to depth given by Crook (1994, pp. 61,62) that the steady forces with the following exponential decay factor:

$$e^{-2kz} \quad (64)$$

The slowly varying order wave forces vary with depth according to the sum of the wave numbers:

$$\frac{e^{-(k_i+k_j)z}}{e^{-(k_i+k_j)z_0}} \quad (65)$$

Application of Equations (64) and (65) to Equations (62) and (63) results in:

$$Z(t) = \sum_{i=1}^n \sum_{j=1}^n F_{ij} e^{i((\omega_i - \omega_j)t + \alpha_i + \alpha_j) - (k_i + k_j)(z - z_0)} \quad (66)$$

$$M(t) = \sum_{i=1}^n \sum_{j=1}^n M_{ij} e^{i((\omega_i - \omega_j)t + \alpha_i + \alpha_j) - (k_i + k_j)(z - z_0)} \quad (67)$$

The real portion of Equations (66) and (67) represents the steady and slowly varying second order wave forces acting on the submarine, with correction for depth.

4. Inclusion of wave forces in equations of motion

The first order accelerations and second order forces had to be combined to form the force and moment disturbance accelerations for use in the deeply submerged equations of motion (Equations (7) and (8)).

$$\begin{bmatrix} F_d(t) \\ M_d(t) \end{bmatrix}_{Incident \atop Waves} = \begin{bmatrix} \ddot{z}(t) \\ \ddot{\theta}(t) \end{bmatrix} + \overline{M}^{-1} \begin{bmatrix} Z(t) \\ M(t) \end{bmatrix} \quad (68)$$

E. CONCLUDING REMARKS

An elementary review of linear wave theory was presented. The case of interest, a submarine at periscope depth, was examined to determine the salient elements of its interaction with the incident waves. The parameters suggested that the major features of the incident wave effects on the submarine could be determined by using a potential analysis with inertial and diffraction forces accounted for.

The Bretschneider spectrum was used to determine the spectral density functions of the sea states of interest. For the purpose of time domain simulation, the spectrum was approximated by the superposition of a number of regular waves with randomly chosen phase angles.

The first order force transfer function and second order forces response amplitude operators were provided for the SUBOFF for a nominal speed and depth. Approximate depth scaling was introduced to allow use at depths other than nominal.

IV. STATE FEEDBACK CONTROL AT PERISCOPE DEPTH

A. INTRODUCTION

1. State feedback control

One popular means of control is to feed back the system states after the application of linear gains. System response of linear systems subjected to this type of control is predictable, and a variety of tools are available for control law gain selection.

The ship's control party on a submarine with conventional indications does not have the full state of the ship to operate from. Although the actual instrumentation may vary somewhat, in general a few analog indications are used in conjunction with a digital depth indication. For this reason, various levels of partial state feedback were used to evaluate the effects of missing indications.

The use of different state feedback schemes was felt to be appropriate to model human operators. The treatment of airplane pilots as a control law "has come to be recognized as a quasilinear element for random-appearing tracking tasks related to piloting. At the same time, the pilot retains spectacular nonlinear gain changing, mode switching, and goal seeking precognitive control capabilities as yet only partially explored." (Graham and McRuer, 1991, p. 1093) In this context, it was assumed submarine "pilots" could be treated in a similar fashion, with feedback from each operating state determined with linear gains.

The use of a first order lag was considered to model the combined human and control surface response time. It was found that reasonable lag values (on the order of a half second) had minimal effect on the control response and corresponding submarine motions. Because of the computational expense, the control response time was neglected.

State feedback control of the linear system

$$\dot{x} = Ax + Bu \quad (69)$$

where:

$A \in \mathbb{R}^{m \times m}$, state matrix

$B \in \mathbb{R}^{m \times n}$, control matrix

$x \in \mathbb{R}^{m \times 1}$, state vector

$u \in \mathcal{R}^{n \times 1}$, control vector

can be expressed as:

$$u = Kx \quad (70)$$

where:

$$K \in \mathcal{R}^{n \times m} \quad (71)$$

The system given by Equation (69) subject to the control law given by Equation (70) has the following closed loop dynamics matrix:

$$A_c = (A + BK) \quad (72)$$

The eigenvalues of the closed loop dynamics matrix will be related to the system stability and responsiveness. In general, the real portion of the eigenvalues must be negative for system stability. Also the more negative the eigenvalues, the faster the system response.

2. SUBOFF simulation parameters

Wave force data was available for the SUBOFF for four different cases. These were sea states three and four with head and beam directions. All were valid at a speed of six knots and depths greater than fifty feet.

At six knots, the linear state representation used for eigenvalue determination and control law design is:

$$\begin{bmatrix} \dot{w} \\ \dot{q} \\ \dot{\theta} \\ \dot{z} \end{bmatrix} = \begin{bmatrix} -0.0179 & 3.7101 & 0.0196 & 0 \\ 0.0006 & -0.0680 & -0.0034 & 0 \\ 0 & 1 & 0 & 0 \\ 1 & 0 & -10.1269 & 0 \end{bmatrix} \begin{bmatrix} w \\ q \\ \theta \\ z \end{bmatrix} + \begin{bmatrix} -0.0628 & -0.1009 \\ 0.009 & -0.0027 \\ 0 & 0 \\ 0 & 0 \end{bmatrix} \begin{bmatrix} \delta_b \\ \delta_s \end{bmatrix} + \begin{bmatrix} F_d(t) \\ M_d(t) \\ 0 \\ 0 \end{bmatrix} \quad (73)$$

where:

$$F_d(t) = F_{trim} + F_{wave}(t)$$

$$M_d(t) = M_{trim} + M_{wave}(t)$$

All simulations were performed using the nonlinear equations of submarine dive plane motion:

$$\dot{w} = a_{11}uw + a_{12}uq + a_{13}\sin(\theta) + b_{11}u^2\delta_b + b_{12}u^2\delta_s + F_d \cos(\theta) + e_{11}q^2 + e_{12}qw \quad (74)$$

$$\dot{q} = a_{21}uw + a_{22}uq + a_{23}\sin(\theta) + b_{21}u^2\delta_b + b_{22}u^2\delta_s + M_d \cos(\theta) + e_{21}q^2 + e_{22}qw \quad (75)$$

$$\dot{\theta} = q \quad (76)$$

$$\dot{z} = w \cos(\theta) - u \sin(\theta) \quad (77)$$

$$\dot{x} = w \sin(\theta) + u \cos(\theta) \quad (78)$$

The simulations were performed using a commanded depth of 55 feet and using a zero error initial state vector. Commanded pitch angle, heave and pitch rate were all zero. The depth was chosen to provide a good representation of actual submarine periscope operating depth.

3. State feedback implementation with SIMULINK®

The state feedback controller was implemented in the SIMULINK® model shown in Figure 11. This block was designed to use an optional feedforward signal, and also to facilitate the use of integral control (Both feedforward and integral control are discussed later in this chapter). Deflection limits were placed on the control surfaces. Control surface rate limits were not included, but could be easily added. These limits are of interest because of the relationships between control surface rates, hydraulic plant size requirements and noise from control surface operations.

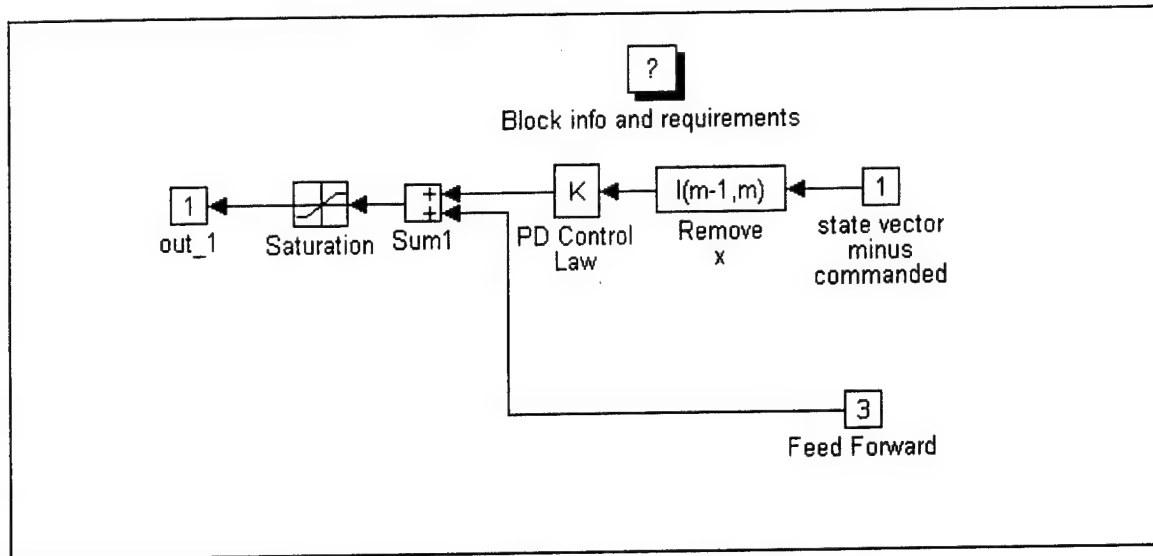


Figure 11. State feedback control block diagram

A SIMULINK® model was developed to incorporate the submarine dynamics of Chapter II, the wave forces of Chapter III, and the state feedback control law. Also included was a logical means of adjusting the submarine's trim. This was done by adding ballast in units of thousands of pounds at the center of buoyancy, and shifting ballast from the forward trim tank to the after trim tank in units of thousands of pounds. The details of the trim model are shown in Figure 12, while the overall model is shown in Figure 13.

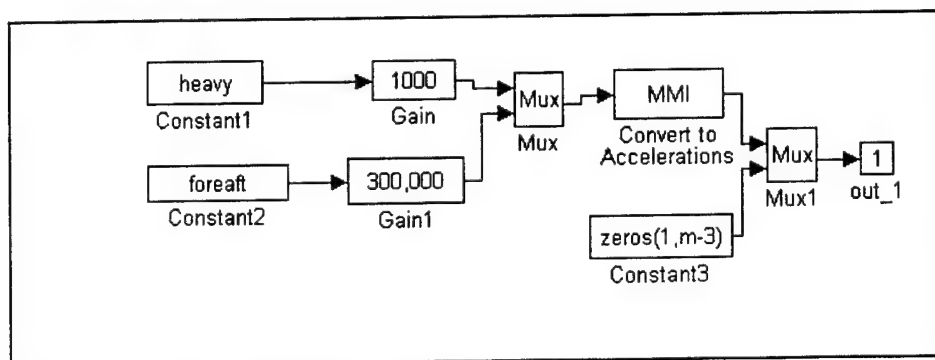


Figure 12. SIMULINK® trim model

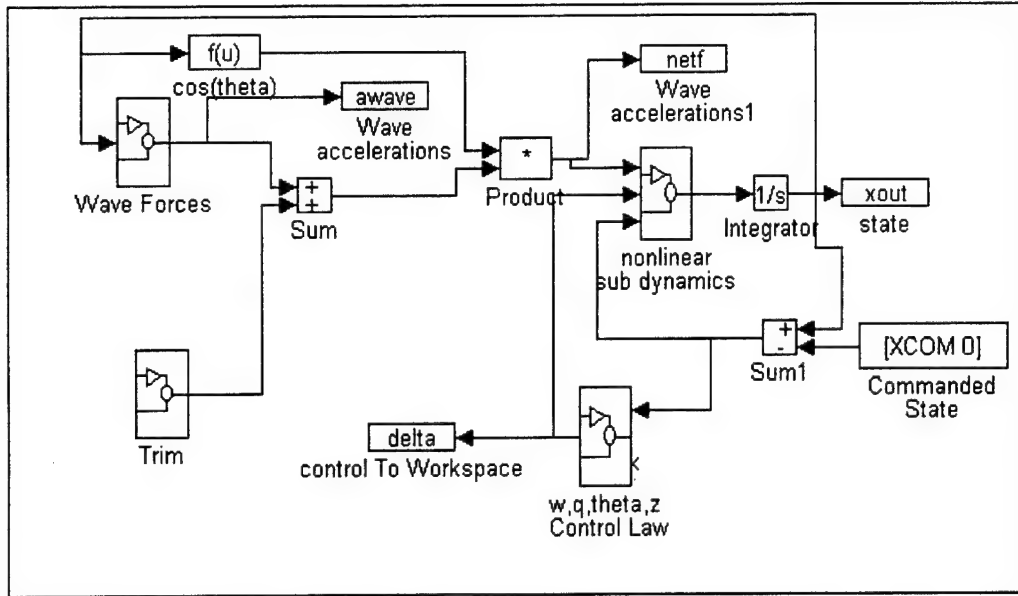


Figure 13. SIMULINK® state feedback control submarine model

4. Integral control on depth

To apply integral control, an additional state is introduced. Equations (74) through (77) are augmented by:

$$\dot{z}_I = z - z_{commanded} \quad (79)$$

which is used to provide state feedback. This forces the steady state value of z to zero. In general, this approach is satisfactory as long as the control effort does not become saturated and the eigenvalues of the integral state are slower than the state which is being zeroed.

5. Feedforward of wave forces

Given the wave forces values, control effort can be directly applied to eliminate the average depth error. With a constant disturbance, a steady state value of the depth error can be determined (Appendix B). Using the linear equations of motion, the steady state depth error can be written as a linear combination of the net force and moment disturbances:

$$z_{ss} - z_{commanded} = C_1 F_d + C_2 M_d \quad (80)$$

To eliminate the depth error, it is required to apply the control effort it applied:

$$K_5 = z_{ss} \begin{bmatrix} K_{14} \\ K_{24} \end{bmatrix} \quad (81)$$

Equations (80) and (81) can be combined to give a matrix gain relationship between the net disturbance and the feedforward:

$$K_5 = \begin{bmatrix} K_{14} \\ K_{24} \end{bmatrix} \begin{bmatrix} C_1 & C_2 \end{bmatrix} \begin{bmatrix} F_d \\ M_d \end{bmatrix} = \begin{bmatrix} C_1 K_{14} & C_2 K_{14} \\ C_1 K_{24} & C_2 K_{24} \end{bmatrix} \begin{bmatrix} F_d \\ M_d \end{bmatrix} \quad (82)$$

The state feedback control law with feedforward is:

$$\begin{bmatrix} \delta_{bp} \\ \delta_{sp} \end{bmatrix} = Kx + K_5 \quad (83)$$

It has been suggested (Musker, Loader, and Butcher, 1988), (Ni, Zhang, and Dai, 1994) that effective periscope depth control can be achieved by feeding forward the average second order wave forces. Because wave forces are a dynamic disturbance and the feedforward was calculated for a steady disturbance, a filter was employed to cut out the high frequency components of the wave forces. The filter employed was a first order Butterworth filter with a cut off frequency ω_{co} . The cut off frequency was initially chosen as one radian/second. This was well below the maximum frequency wave force components (around 2.2 radians/second). Figure 14 and Figure 15 show the effects of the first order Butterworth filter on the wave forces at a depth of 55 feet in sea state three. It is apparent that with a cutoff frequency of ten radians per second, the filtered forces and moments are very close to the unfiltered. At the lower cutoff frequency, 0.1 radians per second, the filtered forces and moments are much closer to the average values.

To implement the feedforward control law, it was assumed that the net external force and moment were known quantities. Equation (82) was implemented in the SIMULINK® model shown in Figure 16 while the complete system model is shown in Figure 17.

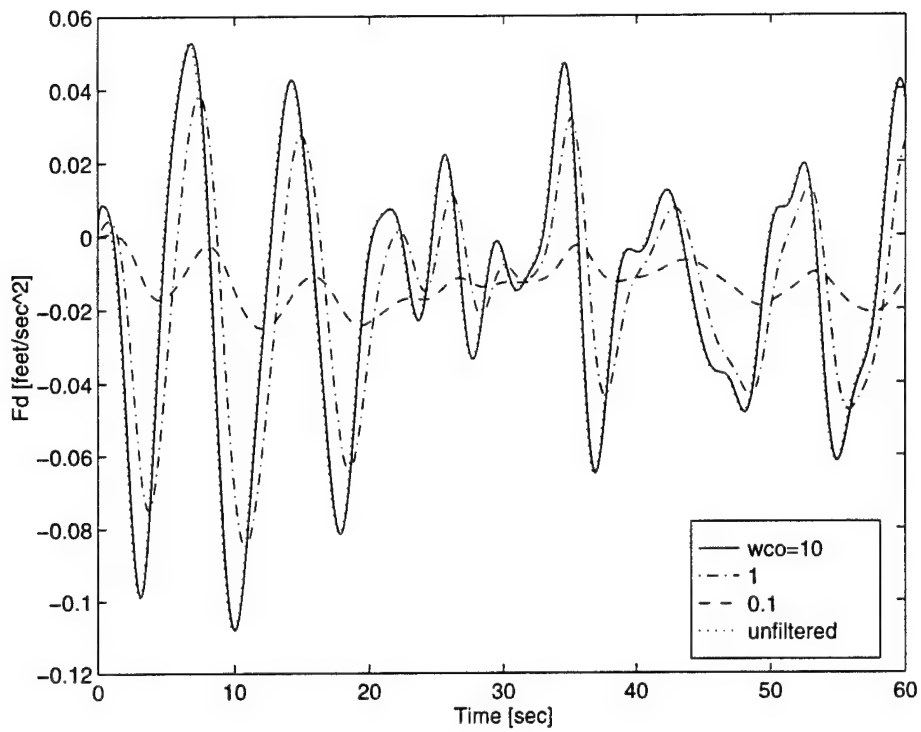


Figure 14. Filtered wave forces for sea state three (head seas)

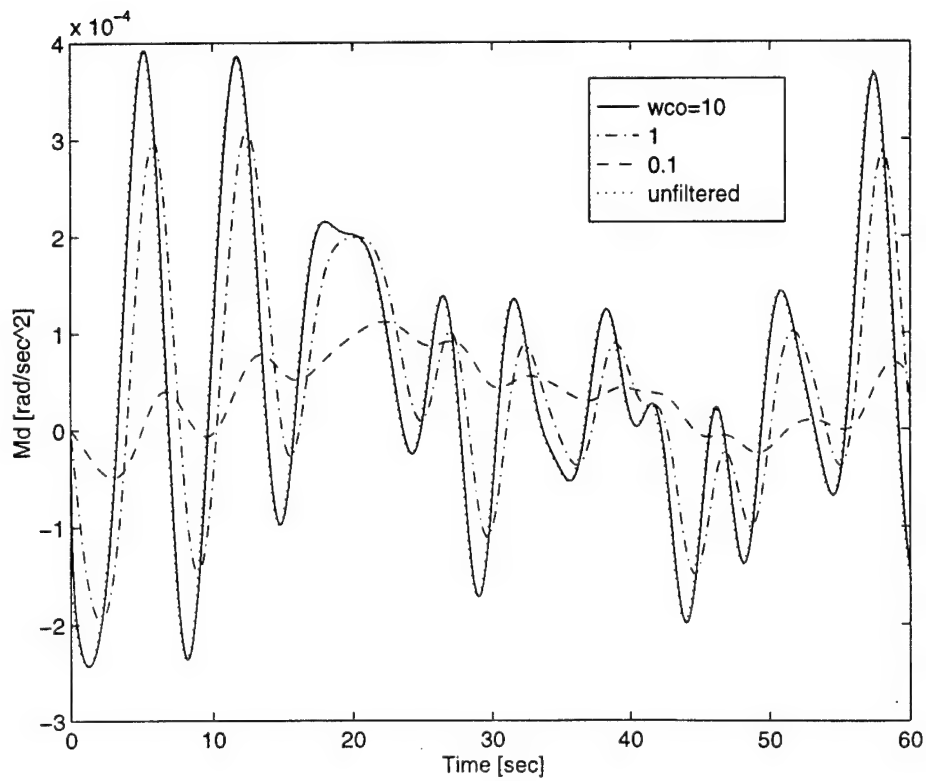


Figure 15. Filtered wave moments for sea state three (head seas)

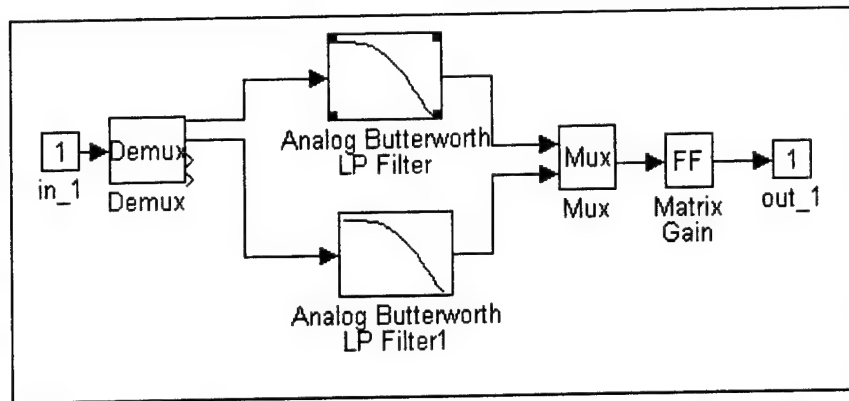


Figure 16. SIMULINK® model of feedforward calculator

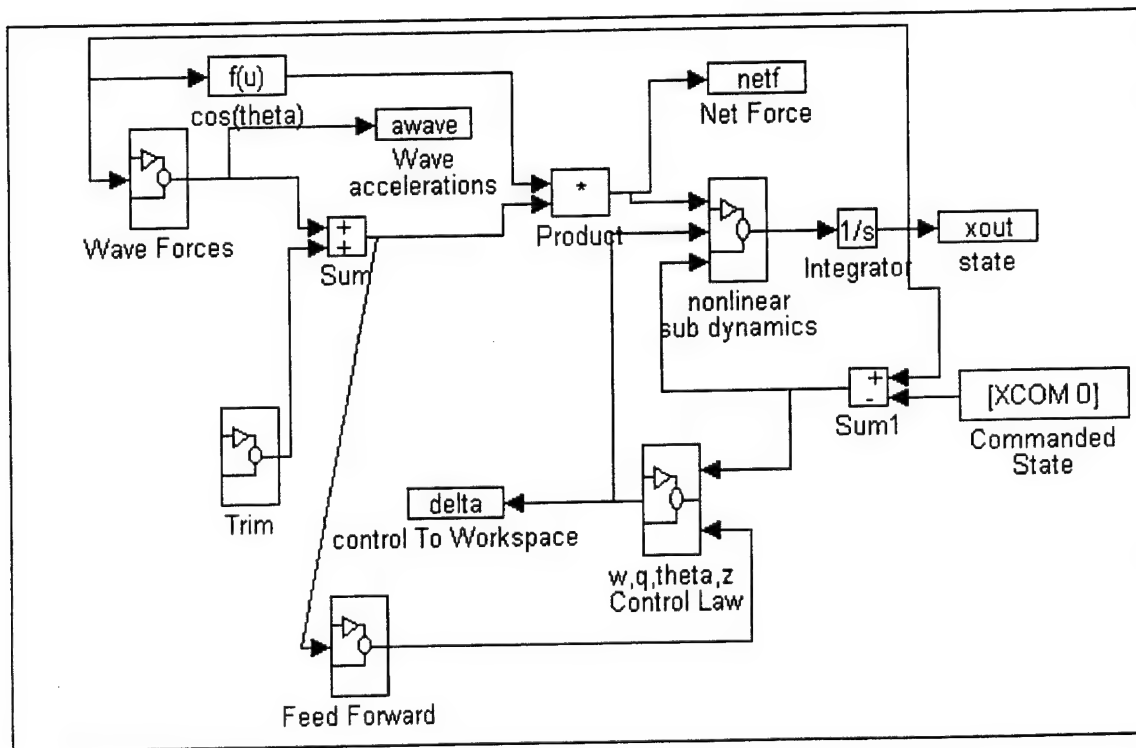


Figure 17. SIMULINK® model of system with feedforward term

6. Optimization algorithm and parameters

One difficulty of using partial state feedback is that conventional pole placement or linear quadratic regulator algorithms can not be used to determine the gains. The gains in question were selected randomly, and gain combinations which gave stable eigenvalues were

simulated. Because of the clamping on the maximum planes angle, some gains which yielded stable eigenvalues resulted in unstable ship control.

Randomly selected gains certainly provide less than optimum depthkeeping. Because of this, each feedback case was optimized to provide the best case for a particular sea state and commanded depth combination. In conjunction with the feedback optimization, the trim was optimized.

The MATLAB® function CONSTR was used to perform the optimizations. CONSTR uses the Broyden-Fletcher-Goldfarb-Shanno variable metric method, and supports constrained optimization problems. To prevent the optimizer from selecting unstable systems, a constraint was placed on the eigenvalues. The real part of the eigenvalues was required to be less than a maximum value, usually -10^{-3} .

The objective of the optimizations was to reduce the root mean square (RMS) value of the depth error. For the basic state feedback control, the average depth was expected to differ somewhat from the commanded depth of 55 feet. Because of this, the objective for these optimizations was to minimize the RMS value of the difference between the depth and the mean depth.

Because the optimizations were performed without regard for minimizing control effort and or rates, large gains with attendant control chatter was expected. Although control chatter is not consistent with normal submarine operations, it was neglected to provide a clear basis of comparison between the differing levels of feedback.

B. FEEDBACK OF DEPTH AND PITCH ANGLE

1. Basic control

An elementary level of ship control can be conducted with the stern and bow planesman, each operating to control one particular state. The logical approach to this is for the stern planesman to control the ship's angle, and the bow planesman to control depth. This results in the following control law:

$$\begin{bmatrix} \delta_{bp} \\ \delta_{sp} \end{bmatrix} = \begin{bmatrix} 0 & 0 & 0 & K_{14} \\ 0 & 0 & K_{23} & 0 \end{bmatrix} \begin{bmatrix} w - w_{commanded} \\ q - q_{commanded} \\ \theta - \theta_{commanded} \\ z - z_{commanded} \end{bmatrix} \quad (84)$$

$$|\delta| \leq \delta_{\max} \quad (85)$$

After a stable set of random gains was determined, the controller was optimized to minimize the deviation from the average depth. The formal optimization statement (Vanderplaats, 1984, p. 9) is:

Minimize:

$$F(K_{14}, K_{23}, H, F) = \sqrt{\frac{\int_0^{t_f} (z - z_{\text{mean}})^2 dt}{t_f}} \quad (86)$$

where:

$z = \text{depth}$, determined by nonlinear simulation

$$z_{\text{mean}} = \frac{\int_0^{t_f} (z) dt}{t_f},$$

$H = \text{Ballast added to center of buoyancy, thousands of pounds}$

$F = \text{Ballast shifted from forward to aft, thousands of pounds}$

Subject to:

$$\text{real}(\text{eigenvalues}(A_c)) \leq E_{\max} \quad (87)$$

Deviation from the mean value of depth, vice the commanded was used because of the expected average depth error.

This approach was used for each of the four sea state cases. For sea state three (head seas), the optimized response is shown in Figure 18. The results of the four optimizations are shown in Table 3. For the RMS error and maximum error, the optimized values are given, along with their percentage of the initial values.

In all cases, use of the optimization resulted in reduction of the mean square depth error (measured from the average depth). Reduction of the maximum error was also achieved.

Sea State/Direction	3/head	3/beam	4/head	4/beam
Initial Values				
K ₁₄	0.1465	0.1465	0.1465	0.1465
K ₂₃	17.51	17.51	17.51	17.51
H/F (10 ³ pounds)	15/0	15/0	15/0	15/0
Mean Depth (feet)	55.15	55.20	55.09	55.29
RMS Error (feet)	0.9220	0.9210	1.23	1.30
Maximum Error (feet)	2.46	2.47	3.86	4.76
Eigenvalues	-0.0074 + 0.2096i -0.0074 - 0.2096i -0.0356 + 0.1144i -0.0356 - 0.1144i	-0.0074 + 0.2096i -0.0074 - 0.2096i -0.0356 + 0.1144i -0.0356 - 0.1144i	-0.0074 + 0.2096i -0.0074 - 0.2096i -0.0356 + 0.1144i -0.0356 - 0.1144i	-0.0074 + 0.2096i -0.0074 - 0.2096i -0.0356 + 0.1144i -0.0356 - 0.1144i
Optimized Values				
K ₁₄	0.567	0.2293	0.4708	0.2016
K ₂₃	63.83	22.5724	48.6186	19.58
H/F (10 ³ pounds)	9.9 / 2.0	15.8/-4.9	15.6/-1.5	4.9/-5
Mean Depth (feet)	54.7	55.99	55.12	55.44
RMS Error (feet)	0.4550 (49%)	0.7549 (82%)	0.657 (53%)	1.23 (95%)
Maximum Error (feet)	1.533 (62%)	2.03 (82%)	2.54 (66%)	4.15 (87%)
Eigenvalues	-0.0388 + 0.2392i -0.0388 - 0.2392i -0.0042 + 0.3911i -0.0042 - 0.3911i	-0.0419 + 0.1464i -0.0419 - 0.1464i -0.0010 + 0.2346i -0.0010 - 0.2346i	-0.0419 + 0.2178i -0.0419 - 0.2178i -0.0010 + 0.3397i -0.0010 - 0.3397i	-0.0010 + 0.2194i -0.0010 - 0.2194i -0.0419 + 0.1358i -0.0419 - 0.1358i

Table 3. Optimized pitch and depth control law results and performance

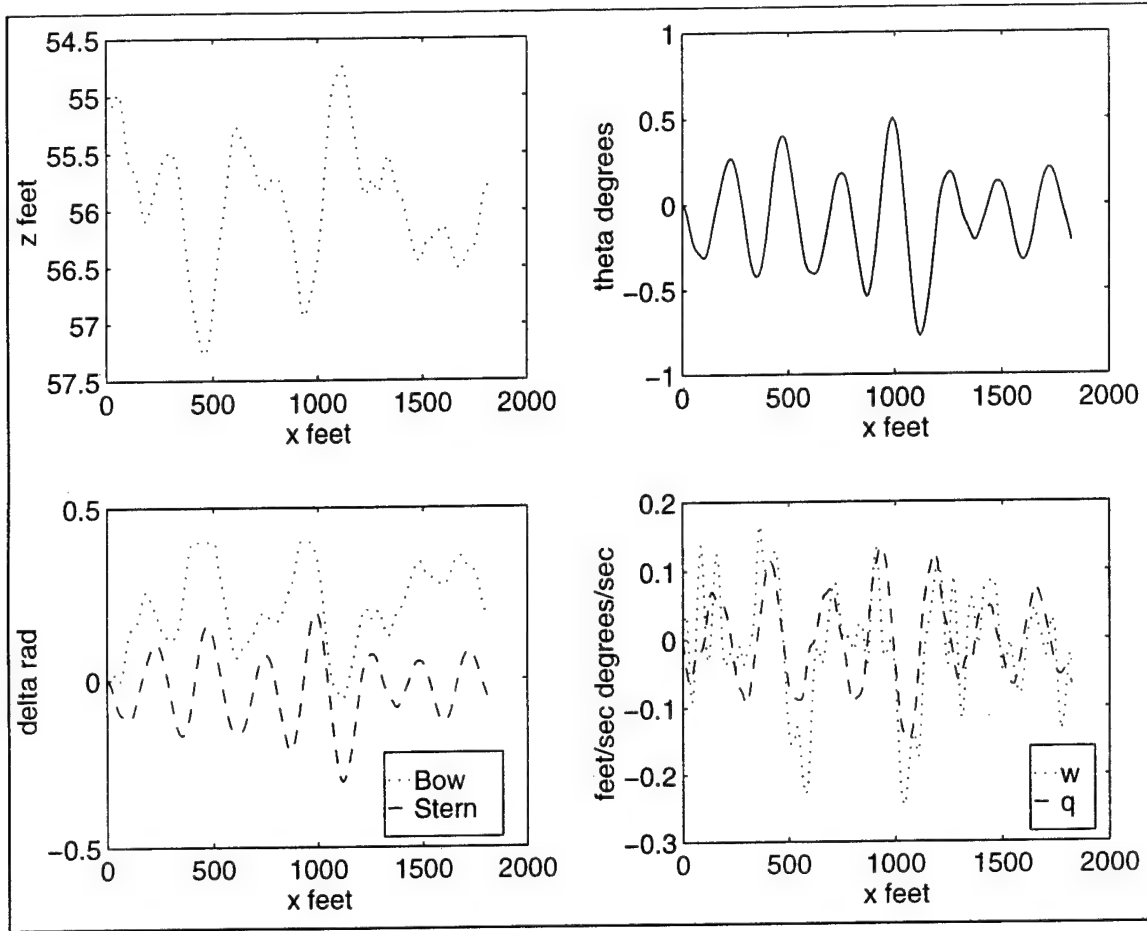


Figure 18. Simulation with depth and pitch angle control in sea state three (head sea direction)

2. Disturbance feedforward

The pitch angle and depth feedback control can be implemented with a disturbance feedforward to correct average depth error. This results in the following control law:

$$\begin{bmatrix} \delta_{bp} \\ \delta_{sp} \end{bmatrix} = \begin{bmatrix} 0 & 0 & 0 & K_{14} \\ 0 & 0 & K_{23} & 0 \end{bmatrix} \begin{bmatrix} w - w_{commanded} \\ q - q_{commanded} \\ \theta - \theta_{commanded} \\ z - z_{commanded} \end{bmatrix} + \begin{bmatrix} C_1 K_{14} & C_2 K_{14} \\ 0 & 0 \end{bmatrix} \begin{bmatrix} \hat{F}_d \\ \hat{M}_d \end{bmatrix} \quad (88)$$

$$|\delta| \leq \delta_{\max} \quad (89)$$

where K_5 is given by Equation (82) and the force and moment disturbances are filtered.

After a stable set of random gains was determined, the controller was optimized to minimize the deviation from the average depth. The formal optimization statement is:

$$F(K_{14}, K_{23}, \omega_{co}, H, F) = \sqrt{\frac{\int_0^{t_f} (z - z_{commanded})^2 dt}{t_f}} \quad (90)$$

Subject to:

$$real(eigenvalues(A_c)) \leq E_{\max} \quad (91)$$

This approach was used for each of the four sea state cases. For sea state three (head seas), the optimized response is shown in Figure 19. The results of the four optimizations are shown in Table 4. For the RMS error and maximum error, the optimized values are given, along with their percentage of the initial values.

Sea State/Direction	3/head	3/beam	4/head	4/beam
Initial Values				
K_{14}	0.1465	0.1465	0.1465	0.1465
K_{23}	17.51	17.51	17.51	17.51
ω_{co} (rad/sec)	1	1	1	1
H/F (10 ³ pounds)	20/0	20/0	20/0	20/0
Mean Depth (feet)	55.07	56.7	55.826	61.33
RMS Error (feet)	0.408	2.24	1.71	6.93
Maximum Error (feet)	1.104	5.27	3.71	13.46
Eigenvalues	-0.0074 + 0.2096i -0.0074 - 0.2096i -0.0356 + 0.1144i -0.0356 - 0.1144i	-0.0074 + 0.2096i -0.0074 - 0.2096i -0.0356 + 0.1144i -0.0356 - 0.1144i	-0.0074 + 0.2096i -0.0074 - 0.2096i -0.0356 + 0.1144i -0.0356 - 0.1144i	-0.0074 + 0.2096i -0.0074 - 0.2096i -0.0356 + 0.1144i -0.0356 - 0.1144i
Optimized Values				
K_{14}	1.116	3.5763	7.40	3.396
K_{23}	151.00	454.7	1,073.6	979.02
ω_{co} (rad/sec)	0.743	3.30	6.83	6.43
H/F (10 ³ pounds)	19.5/3.5	22.1/1.3	26.5/3.25	8.4/-4.0
Mean Depth (feet)	54.996	55.14	55.04	55.21
RMS Error (feet)	0.102 (25%)	0.556 (25%)	0.810 (47%)	0.883 (13%)
Maximum Error (feet)	0.322 (29%)	2.24 (43%)	0.560 (15%)	3.36 (25%)
Eigenvalues	-0.0337 + 0.3345i -0.0337 - 0.3345i -0.0092 + 0.6088i -0.0092 - 0.6088i	-0.0354 + 0.6055i -0.0354 - 0.6055i -0.0076 + 1.0490i -0.0076 - 1.0490i	-0.0322 + 0.8604i -0.0322 - 0.8604i -0.0107 + 1.6296i -0.0107 - 1.6296i	-0.0250 + 0.5675i -0.0250 - 0.5675i -0.0179 + 1.6019i -0.0179 - 1.6019i

Table 4. Optimized pitch and depth control law with disturbance feedforward results and performance

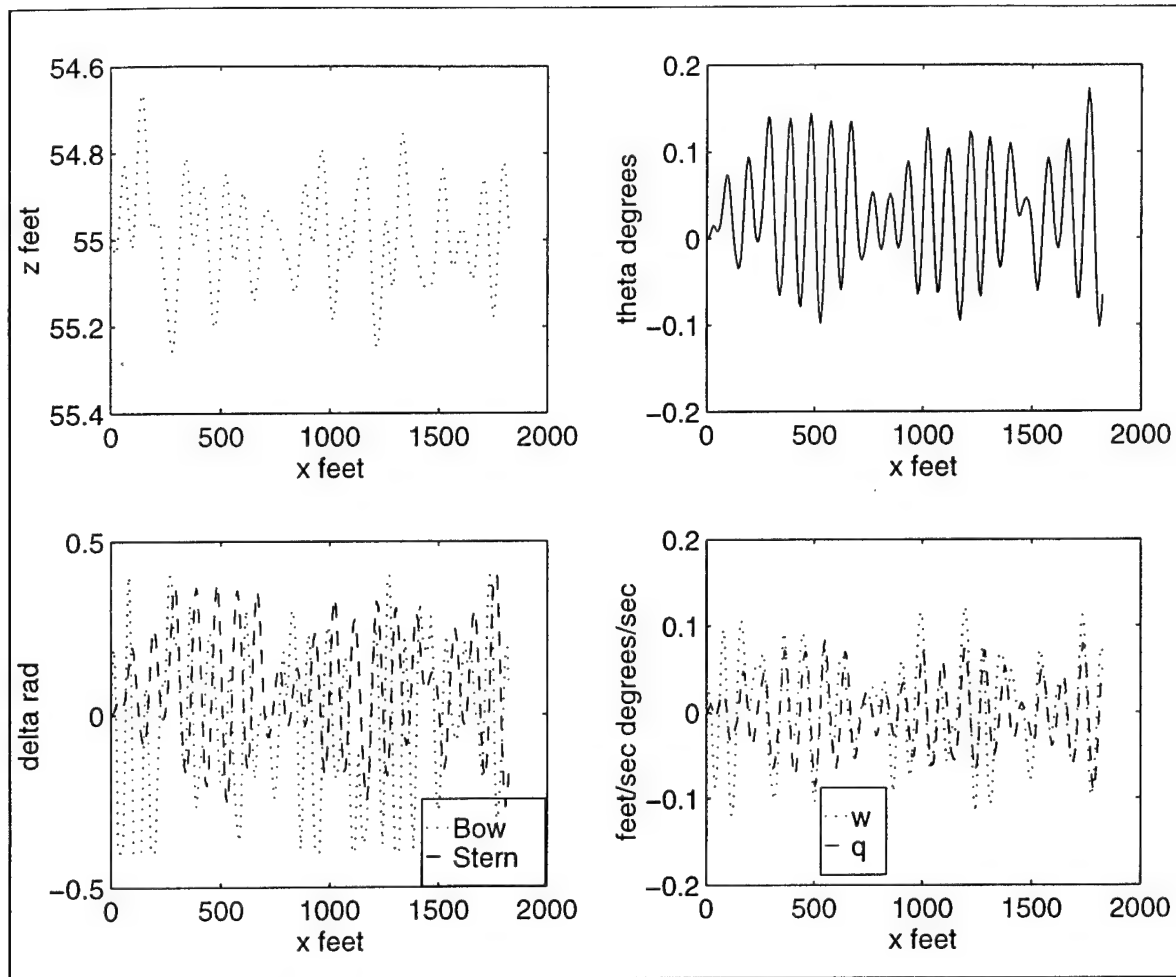


Figure 19. Simulation with depth and pitch angle control with disturbance feedforward, sea state three (head seas)

3. Integral control

The feedback of depth and pitch angle can be augmented with integral control on depth to remove the average depth error. Since the bow planes are principally used for the control of depth, the integral control was applied to the bow planes only. This results in the following control law:

$$\begin{bmatrix} \delta_{bp} \\ \delta_{sp} \end{bmatrix} = \begin{bmatrix} 0 & 0 & 0 & K_{14} & K_{15} \\ 0 & 0 & K_{23} & 0 & 0 \end{bmatrix} \begin{bmatrix} w - w_{commanded} \\ q - q_{commanded} \\ \theta - \theta_{commanded} \\ z - z_{commanded} \\ z_I \end{bmatrix} \quad (92)$$

$$|\delta| \leq \delta_{\max} \quad (93)$$

After a stable set of random gains was determined, the controller was optimized to minimize the deviation from the commanded depth. The formal optimization statement is:

Minimize:

$$F(K_{14}, K_{15}, K_{23}, H, F) = \sqrt{\frac{\int_0^{t_f} (z - z_{commanded})^2 dt}{t_f}} \quad (94)$$

Subject to:

$$real(eigenvalues(A_c)) \leq E_{\max} \quad (95)$$

This approach was used for each of the four sea state cases. For sea state three (head seas), the optimized response is shown in Figure 20. The results of the four optimizations are shown in Table 5.

Sea State/Direction	3/head	3/beam	4/head	4/beam
Initial Values				
K ₁₄	0.1465	0.1465	0.1465	0.1465
K ₁₅	0.001	0.001	0.001	0.001
K ₂₃	17.51	17.51	17.51	17.51
H/F (10 ³ pounds)	20/0	20/0	20/0	20/0
Mean Depth (feet)	55.15	55.16	55.19	55.24
RMS Error (feet)	0.987	0.986	1.29	1.39
Maximum Error (feet)	2.614	2.63	4.01	5.12
Eigenvalues	-0.0077 + 0.2088i -0.0077 - 0.2088i -0.0318 + 0.1148i -0.0318 - 0.1148i -0.0070	-0.0077 + 0.2088i -0.0077 - 0.2088i -0.0318 + 0.1148i -0.0318 - 0.1148i -0.0070	-0.0077 + 0.2088i -0.0077 - 0.2088i -0.0318 + 0.1148i -0.0318 - 0.1148i -0.0070	-0.0077 + 0.2088i -0.0077 - 0.2088i -0.0318 + 0.1148i -0.0318 - 0.1148i -0.0070
Optimized Values				
K ₁₄	1.5609	0.6329	0.2906	0.296
K ₁₅	0.0019	0.0012	0.0004	0.0005
K ₂₃	304.5	107.76	28.46	76.53
H/F (10 ³ pounds)	18.2/1.4	20.0/0.1	18.1/-3.4	12.2/-4.2
Mean Depth (feet)	55.01	55.09	55.05	55.11
RMS Error (feet)	0.455 (46%)	0.3811 (39%)	0.865 (67%)	1.05 (76%)
Maximum Error (feet)	2.035 (78%)	1.0138 (39%)	3.38 (84%)	3.53 (69%)
Eigenvalues	-0.0149 + 0.8824i -0.0149 - 0.8824i -0.0274 + 0.3887i -0.0274 - 0.3887i -0.0012	-0.0134 + 0.5221i -0.0134 - 0.5221i -0.0286 + 0.2475i -0.0286 - 0.2475i -0.0020	-0.0001 + 0.2615i -0.0001 - 0.2615i -0.0421 + 0.1675i -0.0421 - 0.1675i -0.0015	-0.0163 + 0.4296i -0.0163 - 0.4296i -0.0258 + 0.1707i -0.0258 - 0.1707i -0.0015

Table 5. Optimized pitch and depth integral control law results and performance

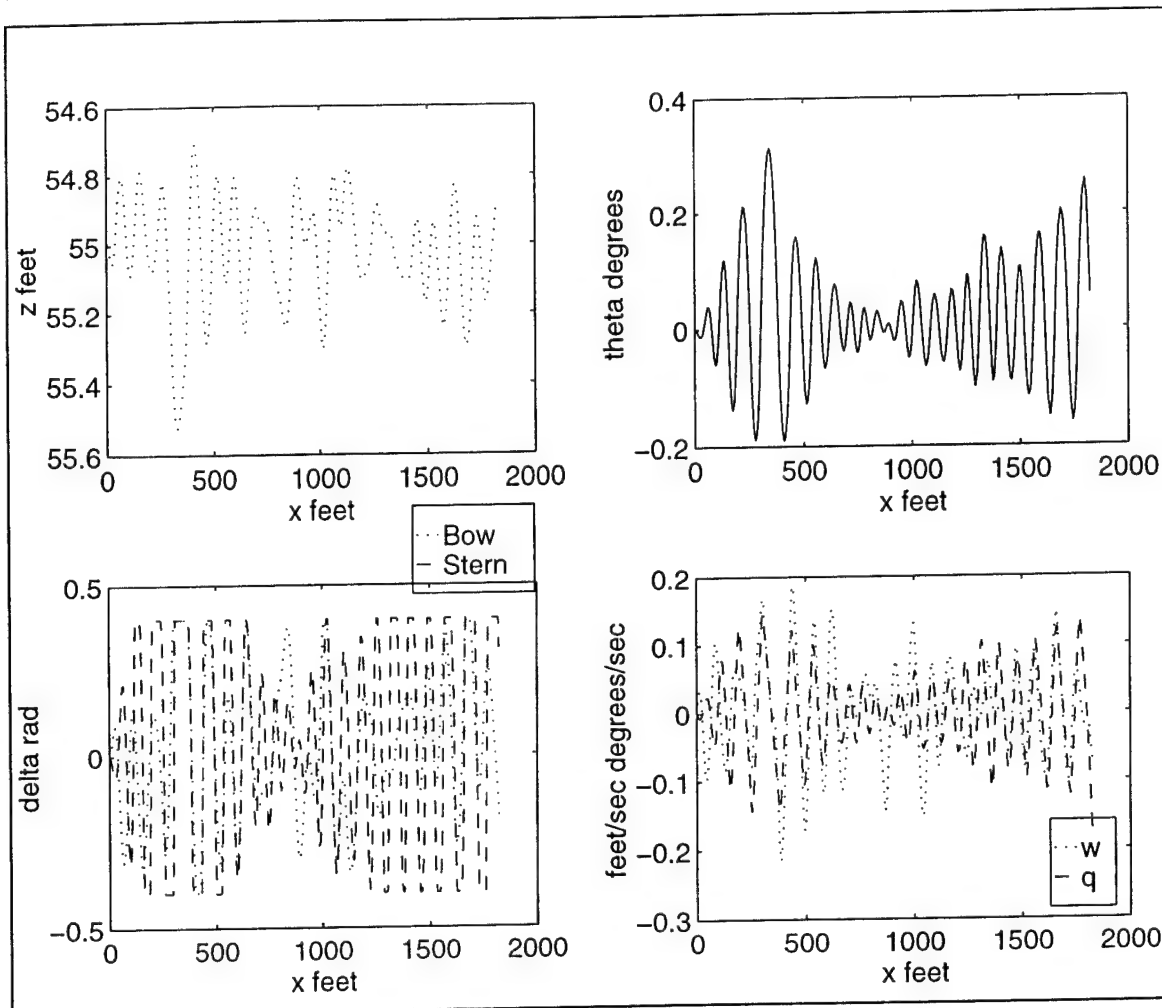


Figure 20. Simulation with depth, pitch angle, and integral control, sea state three (head seas)

C. FULL STATE FEEDBACK WITH PARTIAL DISTRIBUTION

1. Basic control

The poor depth control of the previous section can be improved by adding to the number of states fed back. In keeping with previous logic, the bow planes will be controlled by the depth and heave, while the stern planes will be controlled by pitch and pitch rate. This results in the following control law:

$$\begin{bmatrix} \delta_{bp} \\ \delta_{sp} \end{bmatrix} = \begin{bmatrix} K_{11} & 0 & 0 & K_{14} \\ 0 & K_{22} & K_{23} & 0 \end{bmatrix} \begin{bmatrix} w - w_{commanded} \\ q - q_{commanded} \\ \theta - \theta_{commanded} \\ z - z_{commanded} \end{bmatrix} \quad (96)$$

$$|\delta| \leq \delta_{\max} \quad (97)$$

After a stable set of random gains was determined, the controller was optimized to minimize the deviation from the average depth. The formal optimization statement is:

Minimize:

$$F(K_{11}, K_{14}, K_{22}, K_{23}, H, F) = \sqrt{\frac{\int_0^{t_f} (z - z_{mean})^2 dt}{t_f}} \quad (98)$$

Subject to:

$$real(eigenvalues(A_c)) \leq E_{\max} \quad (99)$$

This approach was used for each of the four sea state cases. For sea state three (head seas), the optimized response is shown in Figure 21. The results of the four optimizations are shown in Table 6.

Sea State/Direction	3/head		3/beam		4/head		4/beam	
Initial Values								
K^T	12.5543	0	12.5543	0	12.5543	0	12.5543	0
	0	22.5268	0	22.5268	0	22.5268	0	22.5268
	0	24.9900	0	24.9900	0	24.9900	0	24.9900
	2.5490	0	2.5490	0	2.5490	0	2.5490	0
H/F (103 pounds)	20/0		20/0		20/0		20/0	
Mean Depth (feet)	55.06		55.33		55.21		55.73	
RMS Error (feet)	0.216		0.425		0.412		1.06	
Maximum Error (feet)	0.796		1.38		1.26		3.38	
Eigenvalues	-0.6743		-0.6743		-0.6743		-0.6743	
	$-0.0413 + 0.3587i$		$-0.0413 + 0.3587i$		$-0.0413 + 0.3587i$		$-0.0413 + 0.3587i$	
	$-0.0413 - 0.3587i$		$-0.0413 - 0.3587i$		$-0.0413 - 0.3587i$		$-0.0413 - 0.3587i$	
	-0.1789		-0.1789		-0.1789		-0.1789	
Optimized Values								
K^T		0	7.035	0	13.265	0	16.58	0
	0	1366.3	0	91.224	0	91.49	0	96.44
	0	1163.3	0	20.87	0	51.15	0	82.43
	89.26	0	3.813	0	2.1048	0	15.33	0
H/F (103 pounds)	14.6/-1.4		12.3/-0.4		20.0/0.1		16.8/0.0	
Mean Depth (feet)	55.02		55.01		55.21		55.09	
RMS Error (feet)	0.1969 (91%)		0.350 (82%)		0.358 (87%)		0.821 (77%)	
Maximum Error (feet)	1.17 (147%)		0.99 (72%)		1.13 (90%)		3.46 (102%)	
Eigenvalues	-3.3197		$-0.1266 + 0.4709i$		-0.7286		$-0.2213 + 0.8861i$	
	$-0.0693 + 1.2522i$		$-0.1266 - 0.4709i$		$-0.1458 + 0.4700i$		$-0.2213 - 0.8861i$	
	$-0.0693 - 1.2522i$		$-0.2619 + 0.0179i$		$-0.1458 - 0.4700i$		$-0.3797 + 0.4819i$	
	-0.1879		$-0.2619 - 0.0179i$		-0.1514		$-0.3797 - 0.4819i$	

Table 6. Full state feedback (partial distribution) control law optimization results and performance

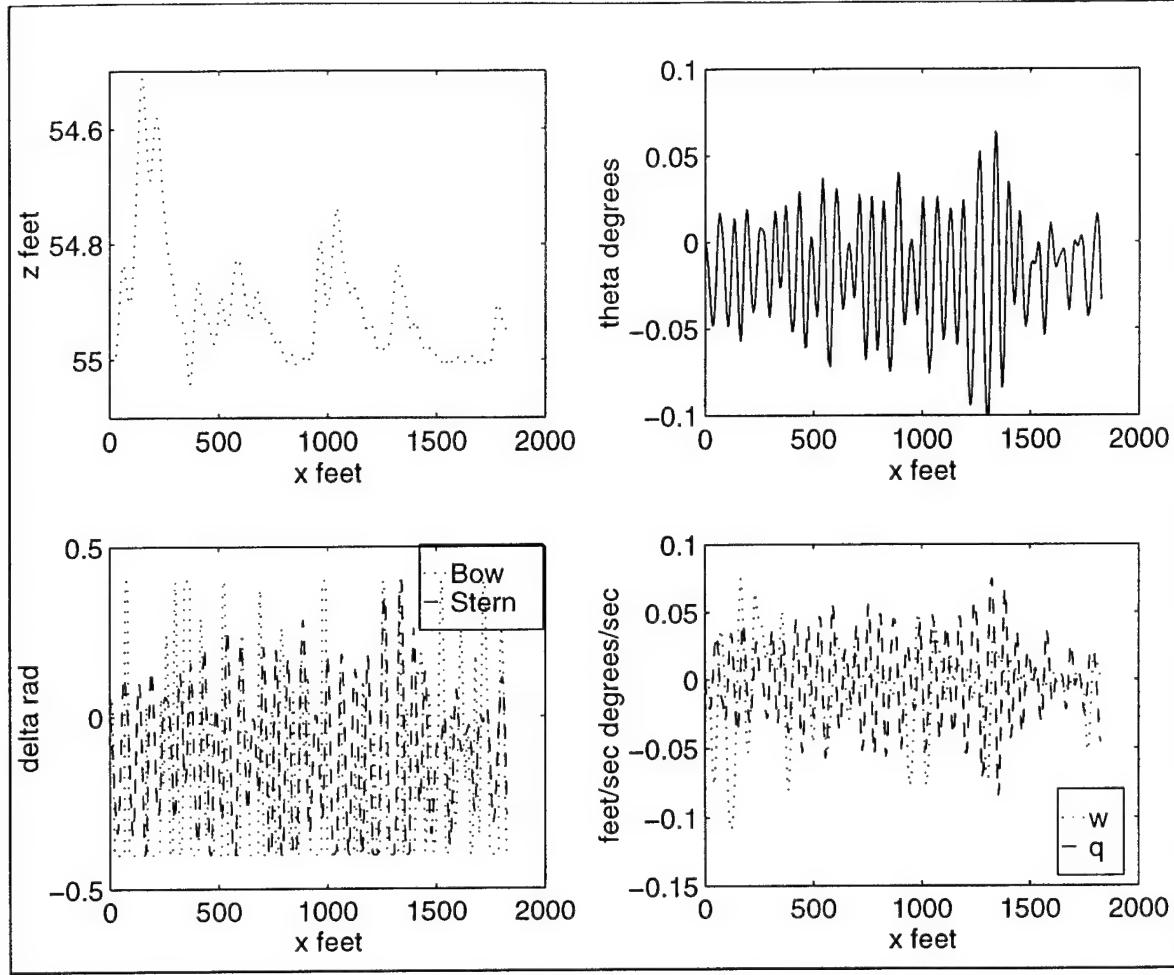


Figure 21. Simulation with full state partial distribution feedback control, sea state three (head seas)

2. Disturbance feedforward

As before, the basic control law can be modified to include a feedforward term to correct the average depth error.

$$\begin{bmatrix} \delta_{bp} \\ \delta_{sp} \end{bmatrix} = \begin{bmatrix} K_{11} & 0 & 0 & K_{14} \\ 0 & K_{22} & K_{23} & 0 \end{bmatrix} \begin{bmatrix} w - w_{commanded} \\ q - q_{commanded} \\ \theta - \theta_{commanded} \\ z - z_{commanded} \end{bmatrix} + \begin{bmatrix} C_1 K_{14} & C_2 K_{14} \\ 0 & 0 \end{bmatrix} \begin{bmatrix} \hat{F}_d \\ \hat{M}_d \end{bmatrix} \quad (100)$$

$$|\delta| \leq \delta_{max} \quad (101)$$

After a stable set of random gains was determined, the controller was optimized to minimize the deviation from the average depth. The formal optimization statement is:

Minimize:

$$F(K_{11}, K_{14}, K_{22}, K_{23}, \omega_{co}, H, F) = \sqrt{\frac{\int_0^{t_f} (z - z_{commanded})^2 dt}{t_f}} \quad (102)$$

Subject to:

$$real(eigenvalues(A_c)) \leq E_{\max} \quad (103)$$

This approach was used for each of the four sea state cases. For sea state three (head seas), the optimized response is shown in Figure 22. The results of the four optimizations are shown in Table 7.

Sea State/Direction	3/head		3/beam		4/head		4/beam	
Initial Values								
K^T	12.5543	0	12.5543	0	12.5543	0	12.5543	0
	0	22.5268	0	22.5268	0	22.5268	0	22.5268
	0	24.9900	0	24.9900	0	24.9900	0	24.9900
	2.5490	0	2.5490	0	2.5490	0	2.5490	0
ω_{co} (rad/sec)	1		1		1		1	
H/F (103 pounds)	20/0		20/0		20/0		20/0	
Mean Depth (feet)	55.16		55.35		55.23		55.82	
RMS Error (feet)	0.371		0.533		0.551		1.40	
Maximum Error (feet)	1.264		1.83		1.72		3.50	
Eigenvalues	-0.6743		-0.6743		-0.6743		-0.6743	
	-0.0413 + 0.3587i		-0.0413 + 0.3587i		-0.0413 + 0.3587i		-0.0413 + 0.3587i	
	-0.0413 - 0.3587i		-0.0413 - 0.3587i		-0.0413 - 0.3587i		-0.0413 - 0.3587i	
	-0.1789		-0.1789		-0.1789		-0.1789	
Optimized Values								
K^T	25.81	0	15.73	0	12.74	0	16.87	0
	0	175.77	0	230.65	0	18.09	0	9.197
	0	26.1	0	535.98	0	20.1	0	18.12
	3.5847	0	9.446	0	2.70	0	3.714	0
ω_{co} (rad/sec)	0.481		3.80		0.998		0.999	
H/F (10 ³ pounds)	7.1/-3.3		19.7/-2.5		20.0/0.0		19.7/0.0	
Mean Depth (feet)	55.01		55.23		55.18		55.63	
RMS Error (feet)	0.0785 (21%)		0.3624 (68%)		0.5171 (94%)		1.25 (89%)	
Maximum Error (feet)	0.246 (19%)		1.07 (58%)		2.03 (118%)		3.26 (93%)	
Eigenvalues	-1.1709		-0.1692 + 1.3601i		-0.6730		-0.9159	
	-0.5214		-0.1692 - 1.3601i		-0.0429 + 0.3320i		-0.0386 + 0.3173i	
	-0.0948		-0.6826 + 0.4529i		-0.0429 - 0.3320i		-0.0386 - 0.3173i	
	-0.3993		-0.6826 - 0.4529i		-0.1767		-0.1769	

Table 7. Full state feedback (partial distribution) with disturbance feedforward control law optimization results and performance

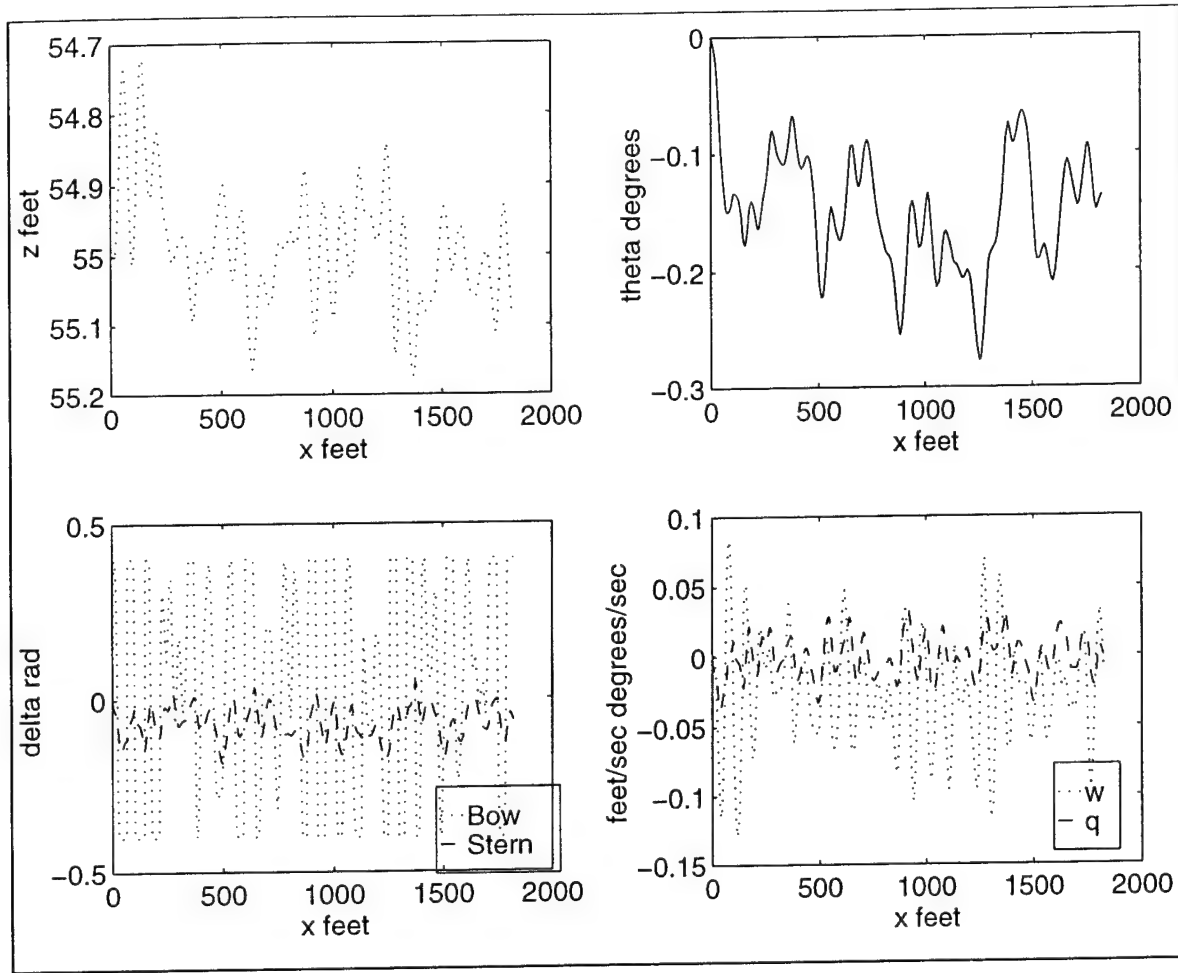


Figure 22. Simulation with full state partial distribution control and disturbance feedforward, sea state three (head seas)

3. Integral Control

This full state feedback with partial distribution was augmented with integral control on depth to remove the average depth error. As before, the integral control was done using the bow planes only. This results in the following control law:

$$\begin{bmatrix} \delta_{bp} \\ \delta_{sp} \end{bmatrix} = \begin{bmatrix} K_{11} & 0 & 0 & K_{14} & K_{15} \\ 0 & K_{22} & K_{23} & 0 & 0 \end{bmatrix} \begin{bmatrix} w - w_{commanded} \\ q - q_{commanded} \\ \theta - \theta_{commanded} \\ z - z_{commanded} \\ z_I \end{bmatrix} \quad (104)$$

$$|\delta| \leq \delta_{max} \quad (105)$$

After a stable set of random gains was determined, the controller was optimized to minimize the deviation from the average depth. The formal optimization statement is as follows:

Minimize:

$$F(K_{11}, K_{14}, K_{15}, K_{22}, K_{23}, H, F) = \sqrt{\frac{\int_0^{t_f} (z - z_{mean})^2 dt}{t_f}} \quad (106)$$

Subject to:

$$real(eigenvalues(A_c)) \leq E_{max} \quad (107)$$

This approach was used for each of the four sea state cases. For sea state three (head seas), the optimized response is shown in Figure 23. The results of the four optimizations are shown in Table 8.

Sea State/Direction	3/head		3/beam		4/head		4/beam	
Initial Values								
K^T	12.5543 0 0 2.5490 0.0010	0 22.5268 24.9900 0 0	12.5543 0 0 2.5490 0.0010	0 22.5268 24.9900 0 0	12.5543 0 0 2.5490 0.0010	0 22.526 8 24.990 0	12.5543 0 0 2.5490 0.0010	0 22.526 8 24.99 0
H/F (10^3 pounds)	20/0		20/0		20/0		20/0	
Mean Depth (feet)	55.05		55.31		55.21		55.74	
RMS Error (feet)	0.2106		0.533		0.4868		1.205	
Maximum Error (feet)	0.866		1.723		1.82		3.43	
Eigenvalues	-0.6744 -0.0412 + 0.3587i -0.0412 - 0.3587i -0.1785 -0.0004		-0.6744 -0.0412 + 0.3587i -0.0412 - 0.3587i -0.1785 -0.0004		-0.6744 -0.0412 + 0.3587i -0.0412 - 0.3587i -0.1785 -0.0004		-0.6744 -0.0412 + 0.3587i -0.0412 - 0.3587i -0.1785 -0.0004	
Optimized Values								
K^T	523.12 0 0 89.26 .04016	0 1366.3 1163.3 0 0	385.2 0 0 254.4 0.0077	0 874.3 1400.5 0 0	14.074 0 0 2.146 0.0003	0 73.89 21.85 0 0	79.08 0 0 52.88 0.0032	0 353.83 54.45 0 0
H/F (10^3 pounds)	14.6/-1.4		26.7/4.6		21.2/-0.2		10.5/-2.6	
Mean Depth (feet)	55.02		55.05		55.25		55.18	
RMS Error (feet)	0.059 (28%)		0.3017 (57%)		0.4274 (88%)		0.909 (75%)	
Maximum Error (feet)	0.248 (29%)		0.862 (50%)		1.16 (64%)		3.59 (105%)	
Eigenvalues	-30.7579 -4.6840 -1.0562 -0.1695 -0.0005		-22.3751 -1.8146 + 1.6555i -1.8146 - 1.6555i -0.6572 0.00003		-0.7495 -0.1526 + 0.3297i -0.1526 - 0.3297i -0.1168 -0.0001		-3.4631 -1.4563 -0.9504 -0.1490 -0.0001	

Table 8. Full state feedback (partial distribution) integral control law optimization results and performance

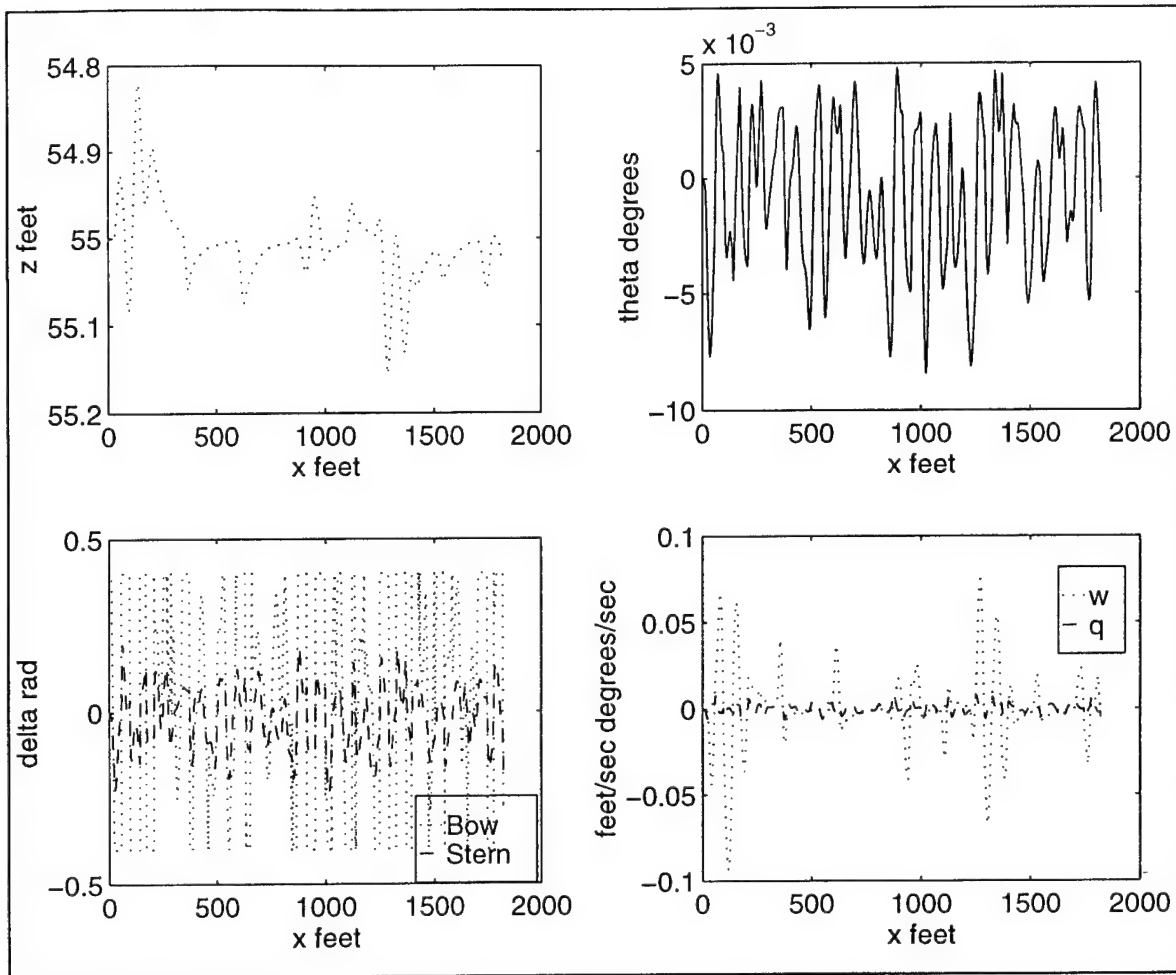


Figure 23. Simulation with full state partial distribution feedback integral control, sea state three (head seas)

D. FULL STATE FEEDBACK

1. Basic control

The best control possible using state feedback should result from the use of all four states by each control. This results in the following control law:

$$\begin{bmatrix} \delta_{bp} \\ \delta_{sp} \end{bmatrix} = \begin{bmatrix} K_{11} & K_{12} & K_{13} & K_{14} \\ K_{21} & K_{22} & K_{23} & K_{24} \end{bmatrix} \begin{bmatrix} w - w_{commanded} \\ q - q_{commanded} \\ \theta - \theta_{commanded} \\ z - z_{commanded} \end{bmatrix} \quad (108)$$

$$|\delta| \leq \delta_{\max} \quad (109)$$

After a stable set of gains was determined using a linear quadratic regulator algorithm, the controller was optimized to minimize the deviation from the average depth. The formal optimization statement was:

Minimize:

$$F(K_{11}, K_{12}, K_{13}, K_{14}, K_{21}, K_{22}, K_{23}, K_{24}, H, F) = \sqrt{\frac{\int_0^{t_f} (z - z_{mean})^2 dt}{t_f}} \quad (110)$$

Subject to:

$$real(eigenvalues(A_c)) \leq E_{\max} \quad (111)$$

This approach was used for each of the four sea state cases. For sea state three (head seas), the optimum response is shown in Figure 24. The results of the four optimizations are shown in Table 9.

Sea State/Direction	3/head		3/beam		4/head		4/beam	
Initial Values								
K^T	6.847	5.1622	6.847	5.1622	6.847	5.1622	6.847	5.1622
	-168.26	121.32	-168.26	121.32	-168.26	121.32	-168.26	121.32
	-65.795	27.744	-65.795	27.744	-65.795	27.744	-65.795	27.744
	0.9740	-0.0789	0.9740	-0.0789	0.9740	-0.0789	0.9740	-0.0789
H/F (10 ³ pounds)	20/0		20/0		20/0		20/0	
Mean Depth (feet)	55.09		55.37		55.21		56.16	
RMS Error (feet)	0.0914		0.3605		0.355		1.60	
Maximum Error (feet)	0.262		1.34		1.09		4.55	
Eigenvalues	-0.8859		-0.8859		-0.8859		-0.8859	
	-0.2854		-0.2854		-0.2854		-0.2854	
	-0.1630 + 0.2247i		-0.1630 + 0.2247i		-0.1630 + 0.2247i		-0.1630 + 0.2247i	
	-0.1630 - 0.2247i		-0.1630 - 0.2247i		-0.1630 - 0.2247i		-0.1630 - 0.2247i	
Optimized Values								
K^T	10.300	9.638	4.591	11.31	4.591	11.306	3.503	11.5734
	45.790	170.45	-283.9	78.91	-283.9	78.91	-374.02	178.92
	-135.16	39.390	125.7	-1.333	-125.7	-1.333	-66.65	40.760
	3.6389	0.0308	1.457	0.1568	1.457	0.1568	0.446	0.0221
H/F (10 ³ pounds)	20.1/-0.9		18.0/-0.3		18.0/-0.33		19.9/0.0	
Mean Depth (feet)	55.03		55.13		55.13		56.54	
RMS Error (feet)	0.037 (40%)		0.2638 (73%)		0.2683 (76%)		1.24 (78%)	
Maximum Error (feet)	0.119 (45%)		0.961 (72%)		0.961 (88%)		4.06 (89%)	
Eigenvalues	-1.7613		-1.0446		-1.0446		-1.0313 + 0.4218i	
	-0.2510		-0.3493 + 0.2881i		-0.3493 + 0.2881i		-1.0313 - 0.4218i	
	-0.0617 + 0.5264i		-0.3493 - 0.2881i		-0.3493 - 0.2881i		-0.0936 + 0.0741i	
	-0.0617 - 0.5264i		-0.2053		-0.2053		-0.0936 - 0.0741i	

Table 9. Full state feedback control law optimization results and performance

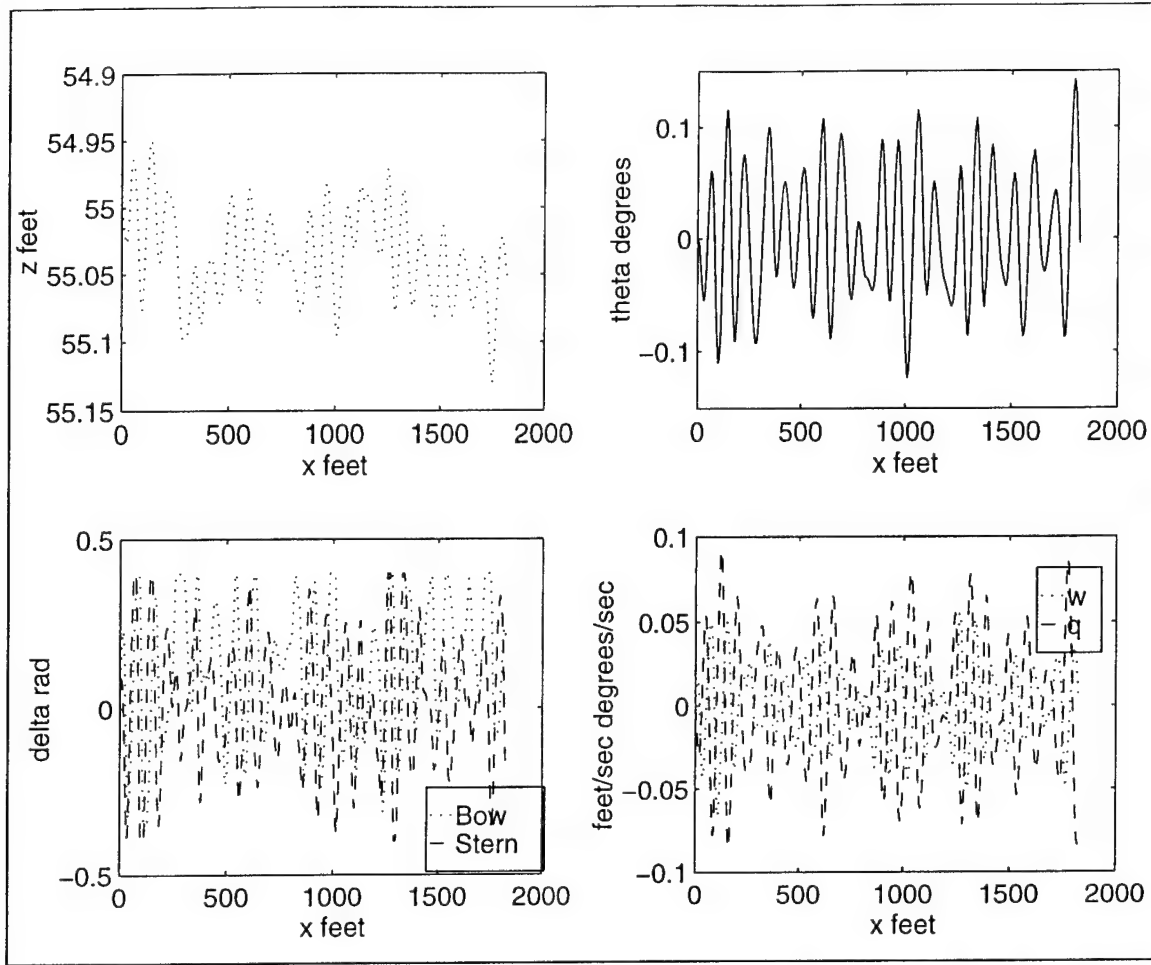


Figure 24. Full state feedback optimized control simulation, sea state three (head seas)

2. Disturbance feedforward

The state feedback control law was modified to include disturbance feedforward. This results in the following control law:

$$\begin{bmatrix} \delta_{bp} \\ \delta_{sp} \end{bmatrix} = \begin{bmatrix} K_{11} & K_{12} & K_{13} & K_{14} \\ K_{21} & K_{22} & K_{23} & K_{24} \end{bmatrix} \begin{bmatrix} w - w_{commanded} \\ q - q_{commanded} \\ \theta - \theta_{commanded} \\ z - z_{commanded} \end{bmatrix} + \begin{bmatrix} C_1 K_{14} & C_2 K_{14} \\ C_1 K_{24} & C_2 K_{24} \end{bmatrix} \begin{bmatrix} \hat{F}_d \\ \hat{M}_d \end{bmatrix} \quad (112)$$

$$|\delta| \leq \delta_{max} \quad (113)$$

After a stable set of gains was determined using a linear quadratic regulator algorithm, the controller was optimized to minimize the deviation from the average depth. The formal optimization statement was:

Minimize:

$$F(K_{11}, K_{12}, K_{13}, K_{14}, K_{21}, K_{22}, K_{23}, K_{24}, \omega_{co}, H, F) = \sqrt{\frac{\int_0^{t_f} (z - z_{commanded})^2 dt}{t_f}} \quad (114)$$

Subject to:

$$real(eigenvalues(A_c)) \leq E_{max} \quad (115)$$

This approach was used for each of the four sea state cases. For sea state three (head seas), the optimum response is shown in Figure 25. The results of the four optimizations are shown in Table 10.

Sea State/Direction	3/head		3/beam		4/head		4/beam	
Initial Values								
K^T	6.847	5.1622	6.847	5.1622	6.847	5.1622	6.847	5.1622
	-168.26	121.32	-168.26	121.32	-168.26	121.32	-168.26	121.32
	-65.795	27.744	-65.795	27.744	-65.795	27.744	-65.795	27.744
	0.9740	-0.0789	0.9740	-0.0789	0.9740	-0.0789	0.9740	-0.0789
ω_{co} (rad/sec)	1		1		1		1	
H/F (10 ³ pounds)	20/0		20/0		20/0		20/0	
Mean Depth (feet)	55.06		55.937		55.21		56.70	
RMS Error (feet)	0.1428		1.343		0.430		2.393	
Maximum Error (feet)	0.4897		3.46		1.11		5.49	
Eigenvalues	-0.8859		-0.8859		-0.8859		-0.8859	
	-0.2854		-0.2854		-0.2854		-0.2854	
	-0.1630 + 0.2247i		-0.1630 + 0.2247i		-0.1630 + 0.2247i		-0.1630 + 0.2247i	
	-0.1630 - 0.2247i		-0.1630 - 0.2247i		-0.1630 - 0.2247i		-0.1630 - 0.2247i	
Optimized Values								
K^T	-26.2	96.5	0.3964	11.08	20.60	-2.681	5.00	-3.94
	-1633	914.4	-879.14	329.16	-194.6	181.5	-452.53	609.1
	-368.8	91.9	-297.0	-91.096	27.66	48.6	25.47	449.5
	5	-1.2	3.52	0.215	-0.276	-0.238	6.66	0.318
ω_{co} (rad/sec)	1.4046		1.033		0.983		1.739	
H/F (10 ³ pounds)	13.5/-0.8		19.16/-0.2134		19.0/-0.1		18.8/-0.1	
Mean Depth (feet)	55.0013		55.18		55.18		55.22	
RMS Error (feet)	0.0928 (65%)		0.4121 (31%)		0.400 (36%)		0.792 (33%)	
Maximum Error (feet)	0.2852 (58%)		1.62 (47%)		1.117 (101%)		2.23 (41%)	
Eigenvalues	-7.0391		-0.8095 + 0.5268i		-1.1927		-0.0898 + 0.9297i	
	-4.6280		-0.8095 - 0.5268i		-0.2499 + 0.3312i		-0.0898 - 0.9297i	
	-0.1322 + 0.1329i		-1.1529		-0.2499 - 0.3312i		-1.1834	
	-0.1322 - 0.1329i		-0.0315		-0.0618		-0.6517	

Table 10. Full state feedback control law with disturbance feedforward optimization results and performance

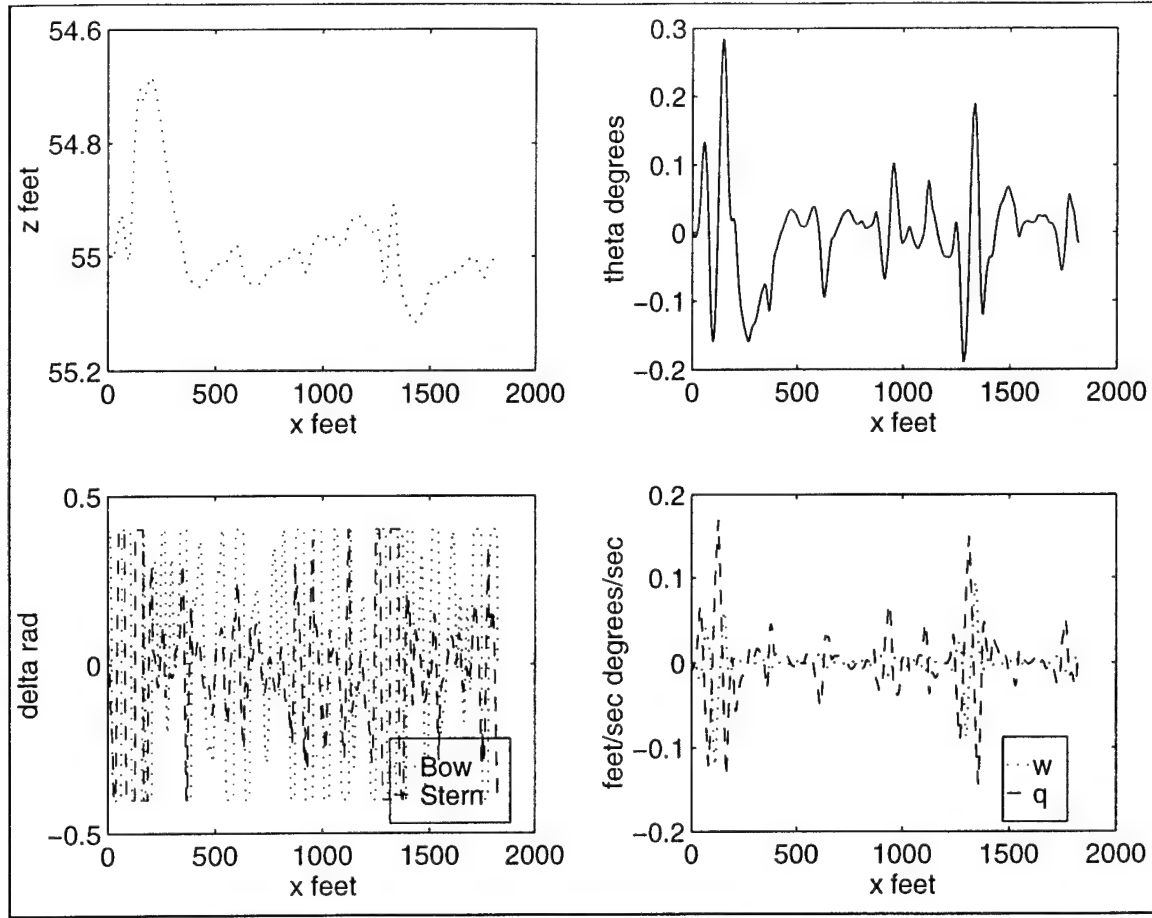


Figure 25. Full state feedback control with disturbance feedforward optimized control simulation, sea state three (head seas)

3. Integral control

This full state feedback with partial distribution was augmented with integral control on depth to remove the average depth error. Since the bow planes are principally used for the control of depth, the integral control was done using the bow planes only. This results in the following control law:

$$\begin{bmatrix} \delta_{bp} \\ \delta_{sp} \end{bmatrix} = \begin{bmatrix} K_{11} & K_{12} & K_{13} & K_{14} & K_{15} \\ K_{21} & K_{22} & K_{23} & K_{24} & K_{25} \end{bmatrix} \begin{bmatrix} w - w_{commanded} \\ q - q_{commanded} \\ \theta - \theta_{commanded} \\ z - z_{commanded} \\ z_I \end{bmatrix} \quad (116)$$

$$|\delta| \leq \delta_{max} \quad (117)$$

After a stable set of random gains was determined, the controller was optimized to minimize the deviation from the average depth. The formal optimization statement is:

Minimize:

$$F(K_{11}, K_{12}, K_{13}, K_{14}, K_{15}, K_{21}, K_{22}, K_{23}, K_{24}, K_{25}, H, F) = \sqrt{\frac{\int_0^{t_f} (z - z_{commanded})^2 dt}{t_f}} \quad (118)$$

Subject to:

$$real(eigenvalues(A_c)) \leq E_{\max} \quad (119)$$

This approach was used for each of the four sea state cases. For sea state three (head seas), the optimum response is shown in Figure 26. The results of the four optimizations are shown in Table 11.

Sea State/Direction	3/head		3/beam		4/head		4/beam	
Initial Values								
K^T	6.847	5.1622	6.847	5.1622	6.847	5.1622	6.847	5.1622
	-168.26	121.32	-168.26	121.32	-168.26	121.32	-168.26	121.32
	-65.795	27.744	-65.795	27.744	-65.795	27.744	-65.795	27.744
	0.9740	-0.0789	0.9740	-0.0789	0.9740	-0.0789	0.9740	-0.0789
	0.01	-0.01	0.01	-0.01	0.01	-0.01	0.01	-0.01
H/F (10 ³ pounds)	20/0		20/0		20/0		20/0	
Mean Depth (feet)	55.01		55.02		54.78		54.68	
RMS Error (feet)	0.101		0.415		0.573		2.483	
Maximum Error (feet)	0.3065		1.545		1.79		6.927	
Eigenvalues	-0.8854		-0.8854		-0.8854		-0.8854	
	-0.2693		-0.2693		-0.2693		-0.2693	
	-0.1652 + 0.2153i		-0.1652 + 0.2153i		-0.1652 + 0.2153i		-0.1652 + 0.2153i	
	-0.1652 - 0.2153i		-0.1652 - 0.2153i		-0.1652 - 0.2153i		-0.1652 - 0.2153i	
	-0.122		-0.122		-0.122		-0.122	
Optimized Values								
K^T	240.17	24.2736	1.3875	7.5561	13.059	4.681	-1.679	6.870
	-137.3	256.28	-158.91	153.309	-146.54	155.09	-234.17	257.016
	-195.76	84.99	-52.850	39.280	-36.04	42.31	-94.42	48.260
	36.65	0.1753	0.4948	-0.0550	0.9425	-0.0484	1.140	-0.0327
	0.162	-0.0128	0.0109	0.0069	0.013	-0.0037	0.0111	-0.0105
H/F (10 ³ pounds)	20.7/1.9		19.1/0		20/0		19.9/0.0	
Mean Depth (feet)	55.00		55.00		54.99		54.92	
RMS Error (feet)	0.0414 (14%)		0.372 (90%)		0.536 (93%)		1.96 (79%)	
Maximum Error (feet)	0.175 (57%)		1.01 (65%)		1.57 (88%)		6.88 (99%)	
Eigenvalues	-17.3244		-0.8739		-1.2707		-1.0690	
	-0.7017		-0.1541 + 0.1441i		-0.2086 + 0.1628i		-0.1214 + 0.3327i	
	-0.1942 + 0.4296i		-0.1541 - 0.1441i		-0.2086 - 0.1628i		-0.1214 - 0.3327i	
	-0.1942 - 0.4296i		-0.2567		-0.2056		-0.2428	
	-0.0076		-0.0375		-0.0208		-0.0012	

Table 11. Full state feedback integral control law optimization results and performance

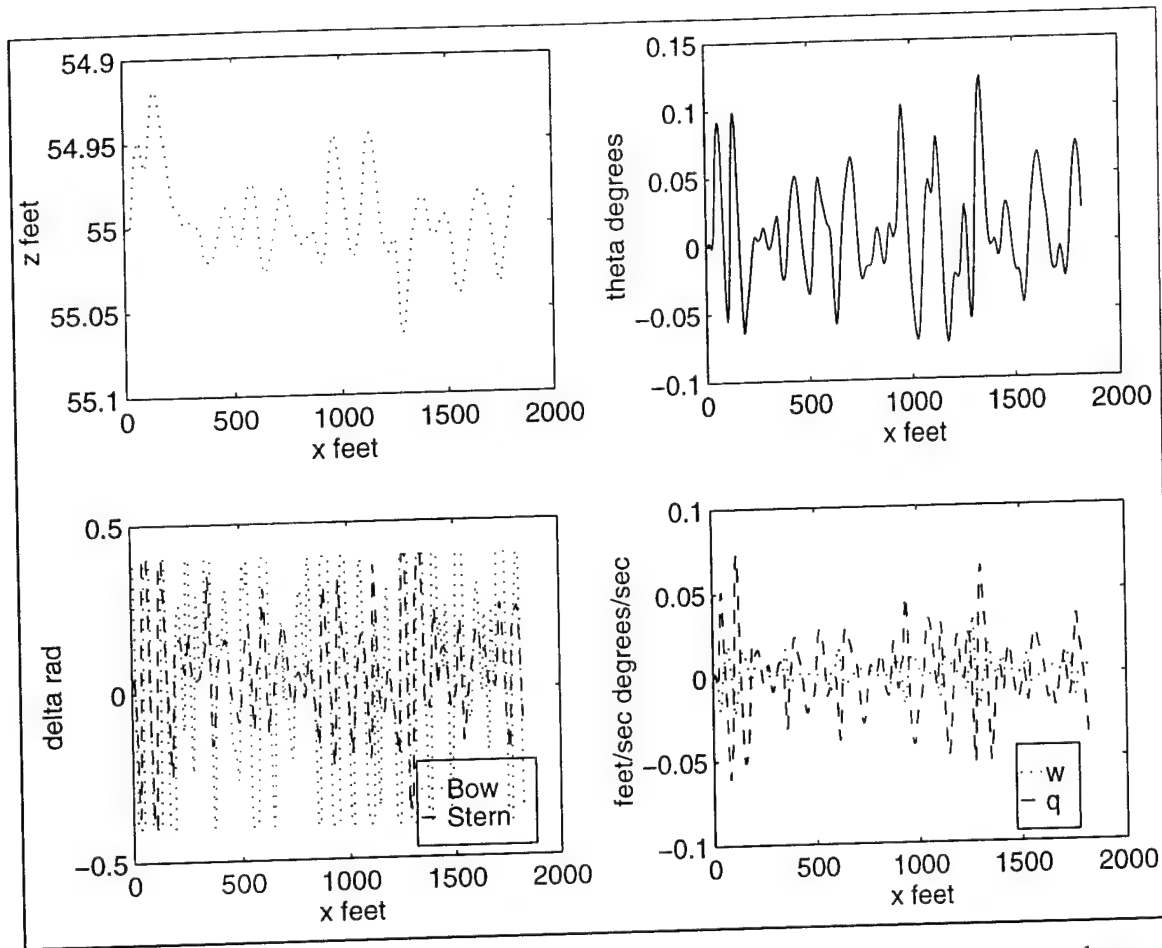


Figure 26. Optimized full state feedback with integral control simulation, sea state three (head seas)

E. CONCLUDING REMARKS

For each case of feedback control, the degree of control achieved generally improved by the additional state feedbacks. Full distribution of each state to both controls further reduced the error. Table 12 provides a summary of the optimizations performed, and the RMS error of each one.

Changes in the optimized trim and control law in all cases varied substantially with changes in sea state or direction. This is consistent with operational experience.

Each controller was optimized with only the goal of minimizing the mean square of the depth error. This resulted in large gains and excessive control effort. In addition, large rates of control were experienced. This would be detrimental for actual submarine operations, as there are rate limits associated with the control surfaces. These limits come from the sizing

of the hydraulic plants which drive the planes, and operation concerns related to plane induced noise.

Some improvements in depthkeeping were achieved by the feedforward of the disturbance forces. This is in spite of the feedforward being based on a steady state response to a constant disturbance.

Sea State/Direction	3/Head	3/Beam	4/Head	4/Beam
Control Scheme				
Depth and Pitch Angle	0.4550	0.7549	0.657	1.23
Depth and Pitch angle with feedforward	0.102	0.556	0.810	0.883
Depth and Pitch angle with integral	0.455	0.3811	0.865	1.05
Full State with partial distribution	0.1969	0.350	0.358	0.821
Full State with partial distribution and feedforward	0.0785	0.3624	0.5171	1.25
Full State with partial distribution and integral	0.059	0.3017	0.4274	0.909
Full State	0.037	0.2638	0.2683	1.24
Full State with feedforward	0.0928	0.4121	0.400	0.792
Full State integral	0.0414	0.372	0.536	1.96

Table 12. Optimized RMS error (feet) of state feedback control schemes

V. SLIDING MODE CONTROL

A. INTRODUCTION

1. Overview of MIMO sliding mode control

The controller design starts with a standard linear state space representation:

$$\dot{x} = Ax + Bu \quad (120)$$

where:

$A \in \mathbb{R}^{m \times m}$, state matrix

$B \in \mathbb{R}^{m \times n}$, control matrix

$x \in \mathbb{R}^{m \times 1}$, state vector

$u \in \mathbb{R}^{n \times 1}$, control vector

The sliding mode control law, u , is composed of two main parts:

$$u = \hat{u} + \bar{u} \quad (121)$$

The first part, \hat{u} , is a linear feedback based on the linear representation given by Equation (120). The second part, \bar{u} , are nonlinear feedbacks with their signs switching depending on the relationship of the system states to the sliding surfaces. The sliding surfaces are hyper planes in the state space, with one for each control. They are defined by:

$$\sigma(x) = S^T x = 0 \quad (122)$$

Where:

$$S \in \mathbb{R}^{n \times m}$$

To determine the nonlinear feedback functions, the concept of Liapunov stability is used. The Liapunov function is taken as:

$$V(x) = \frac{1}{2} (\sigma_1^2 + \sigma_2^2 + \dots + \sigma_n^2) \quad (123)$$

Asymptotic system stability is guaranteed provided that $\dot{V}(x)$ is a positive definite function, that is:

$$\dot{V}(x) = \dot{\sigma}_1\sigma_1 + \dot{\sigma}_2\sigma_2 + \dots + \dot{\sigma}_n\sigma_n < 0 \quad (124)$$

Equation (124) is satisfied if:

$$\dot{\sigma}_i\sigma_i < 0 \text{ for } i=1 \text{ to } n \quad (125)$$

Equation (125) can be rewritten as:

$$\dot{\sigma}_i = -\eta_i \text{sign}(\sigma_i) \quad (126)$$

where η_i is a positive gain parameter for the i^{th} sliding surface. Equation (126) can be rewritten after substituting the time derivative of Equation (122) and Equation (120) as:

$$S^T (Ax + Bu) = - \begin{bmatrix} \eta_1 \text{sign}(\sigma_1) \\ \eta_2 \text{sign}(\sigma_2) \\ \vdots \\ \eta_n \text{sign}(\sigma_n) \end{bmatrix} \quad (127)$$

Solving Equation (127) for u yields:

$$u = -(S^T B)^{-1} S^T Ax - (S^T B)^{-1} \begin{bmatrix} \eta_1 \text{sign}(\sigma_1) \\ \eta_2 \text{sign}(\sigma_2) \\ \vdots \\ \eta_n \text{sign}(\sigma_n) \end{bmatrix} \quad (128)$$

Equation (128) can be rewritten in matrix form as:

$$u = Kx + K_s \eta \text{sign}(\sigma) \quad (129)$$

where:

$$K = -(S^T B)^{-1} S^T A$$

$$K_s = -(S^T B)^{-1}$$

Equation (129) is identical in form to Equation (121), with a linear state feedback and a nonlinear switching term.

For the decomposition in Equation (128), it is required that the closed loop stability matrix, $(A-BK)$, have n zero eigenvalues. The sliding surfaces are the left eigenvectors resulting from the zero eigenvalues.

2. Utkin's method for MIMO sliding mode control law design

Determination of the sliding surfaces can be difficult, especially with a MIMO system. One technique for this is proposed by Utkin (1977). For this technique to be applied, the B matrix of the state space system (Equation (120)) must be of the form:

$$B = \begin{bmatrix} B_1 \\ 0 \end{bmatrix} \quad (130)$$

where:

$$B_1 \in \mathbb{R}^{n \times n}$$

$$0 \in \mathbb{R}^{(m-n) \times n}$$

For the MIMO cases of vertical plane depth control used in this thesis, this was the case. For the stern planes only control examples, a QR factorization was applied, to transform the state space system into this form.

Given that the B matrix is of the form defined in Equation (130), Equation (120) can be decomposed into the following:

$$x_1 = A_{11}x_1 + A_{12}x_2 + B_1u \quad (131)$$

$$x_2 = A_{21}x_1 + A_{22}x_2 \quad (132)$$

where:

$$\begin{aligned}
x_1 &\in \mathbb{R}^{n \times 1} \\
x_2 &\in \mathbb{R}^{(m-n) \times 1} \\
A_{11} &\in \mathbb{R}^{n \times n} \\
A_{12} &\in \mathbb{R}^{n \times (m-n)} \\
A_{21} &\in \mathbb{R}^{(m-n) \times n} \\
A_{22} &\in \mathbb{R}^{(m-n) \times (m-n)}
\end{aligned}$$

The sliding surfaces become:

$$\sigma = S_1^T x_1 + S_2^T x_2 = 0 \quad (133)$$

where:

$$\begin{aligned}
S_1^T &\in \mathbb{R}^{n \times n} \\
S_2^T &\in \mathbb{R}^{n \times (m-n)}
\end{aligned}$$

Because the sliding surfaces are the left eigenvectors of the n zero eigenvalues, S_1^T can be set to the identity matrix without loss of generality. Substitution of Equation (133) into Equation (148) leads to:

$$\dot{\sigma} = \dot{x}_1 + S_2^T \dot{x}_2 = -\eta \text{sign}(\sigma_1 + S_2^T x_2) \quad (134)$$

$$u = -B_1^{-1} \left[(A_{11} + S_2^T A_{21})x_1 + (A_{12} + S_2^T A_{22})x_2 \right] - B_1^{-1} \begin{bmatrix} \eta_1 \text{sign}(\sigma_1) \\ \eta_2 \text{sign}(\sigma_2) \\ \vdots \\ \eta_n \text{sign}(\sigma_n) \end{bmatrix} \quad (135)$$

When the system is on the sliding surfaces, Equation (133) can be used to solve for x_1 in terms of x_2 , resulting in:

$$x_1 = -S_2^T x_2 \quad (136)$$

Substitution of this result into Equation (132) results in:

$$\dot{x}_2 = (A_{22} - A_{21}S_2^T)x_2 \quad (137)$$

Equation (137) is the set of independent equations that the non zero eigenvalues for the control result from. For the application of pole placement algorithms to determine the sliding surfaces, it only has to be recognized that it is in the standard state space format:

$$\dot{y} = \hat{A}y + \hat{B}\hat{K}y \quad (138)$$

with:

$$\hat{A} = A_{22}$$

$$\hat{B} = -A_{21}$$

$$\hat{K} = S_2^T$$

Once S_2^T is determined, the control law can be determined by substituting it into Equation (135).

Utkin's technique also allows for the use of linear quadratic regulator methods for determination of the sliding surfaces. (Utkin 1977) For this method, it is desired to minimize a quadratic performance index:

$$I = \frac{1}{2} \int_0^{\infty} x^T Q x dt \quad (139)$$

where Q is a positive definite weighting matrix. By partitioning Q in the same manner as A was partitioned for equations (131) and (132), Equation (139) can be rewritten as:

$$I = \frac{1}{2} \int_0^{\infty} (x_1^T Q_{11} x_1 + x_2^T Q_{21} x_1 + x_1^T Q_{12} x_2 + x_2^T Q_{22} x_2) dt \quad (140)$$

or:

$$I = \frac{1}{2} \int_0^{\infty} (x_2^T Q^* x_2 + v^T Q_{11} v) dt \quad (141)$$

where:

$$Q^* = Q_{22} - Q_{21} Q_{11}^{-1} Q_{12}$$

$$A^* = A_{22} - A_{21} Q_{11}^{-1} Q_{12}$$

$$v = x_1 + Q_{11}^{-1} Q_{12} x_2$$

With the system on the sliding surfaces, Equation (140) can be rewritten as:

$$\dot{x}_2 = A^* x_2 + A_{21} v \quad (142)$$

Equations (141) and (142) are in a recognizable form for the application of any convenient linear quadratic regulator solution. The Hamiltonian is:

$$H = p^T (A^* x_2 + A_{21} v) - \frac{1}{2} (x_2^T Q^* x_2 + v^T Q_{11} v) \quad (143)$$

The algebraic Riccati equation is:

$$(A^*)^T k + kA^* - kA_{21}Q_{11}^{-1}A_{21}^T k + Q^* = 0 \quad (144)$$

The solution of Equation (144) results in:

$$v = -Q_{11}^{-1}A_{21}^T kx_2 \quad (145)$$

This result is used with the definition for v from Equation (141) to provide the relationship between x_1 and x_2 . This results in the sliding surface:

$$S_2^T = Q_{11}^{-1}(Q_{12} + A_{21}^T k) \quad (146)$$

With S_2^T determined, the control law can be determined by substitution into Equation (135).

This sliding mode LQR controller design was implemented in a MATLAB® function SMLQR.M which included provisions for a QR factorization for the cases when the B matrix was not of the form given by Equation (130). SMLQR.M is included in Appendix A.

3. Control of chatter

One undesirable aspect of sliding mode control is the chatter induced by the nonlinear switching term near the sliding surfaces. The nonlinear switching term in the sliding mode control can cause control chatter when the system is near a sliding surface. One way to reduce the chatter is to use the concept of a boundary layer around the sliding surface. First, a *satsign* function is defined:

$$satsign(x) = \begin{cases} 1, & x > 1 \\ x, & -1 \leq x \leq 1 \\ -1, & x < -1 \end{cases} \quad (147)$$

A boundary layer of thickness ϕ around each sliding surface, is applied using the *satsign* function:

$$\dot{\sigma}_i = \text{satsign}\left(\frac{\sigma_i}{\phi_i}\right) \quad (148)$$

Equation (147) can be used to replace the *sign* function used in Equation (129) with no change in the asymptotic stability of the system. There are some effects, however, because the dynamics near the sliding surface are not the same as the closed loop dynamics which exist when the system is on the sliding surface. The final control law is:

$$u = Kx + K_s \eta \text{satsign}\left(\frac{\sigma}{\phi}\right) \quad (149)$$

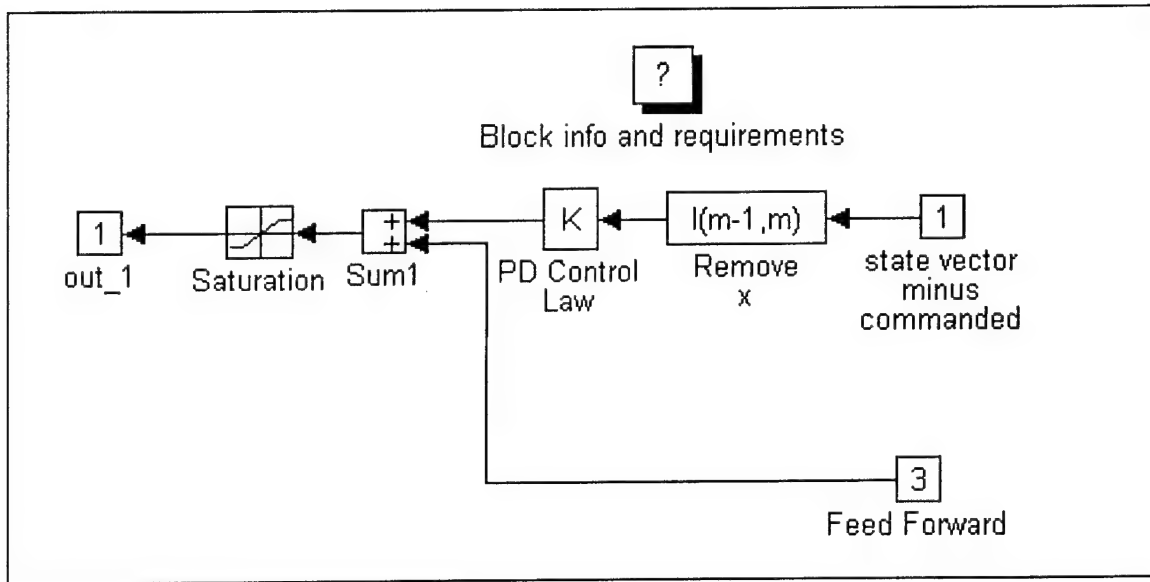


Figure 27. SIMULINK® model sliding mode controller

Equation (149) was implemented as a SIMULINK® model, shown in Figure 27.

B. SIMO SLIDING MODE CONTROL RESPONSE TO DISTURBANCES

When applied to vertical plane submarine control, sliding mode control has several nuances which are not obvious from inspection of the governing equations. In order to illustrate these, the performance of sliding mode control will be explored through several example cases. To keep the analytic derivations simple, the cases worked will be done with

stern planes control only. The general concepts, however, will be applicable to stern and bow planes control.

The response of sliding mode control to force and moment disturbances is fundamental to its application to submarine control in the vertical plane. These force and moment disturbances could result from a variety of situations. Examples of these include out of trim conditions, free surface effects, and wave forces.

1. Basic sliding mode disturbance response

The first case will use a basic sliding mode control law, that is one without a feedforward term or integral control. The resulting control law is:

$$\sigma = S_1 w + S_2 q + S_3 \theta + S_4 z \quad (150)$$

$$\delta = K_1 w + K_2 q + K_3 \theta + \eta K_s \text{sat} \text{sign}\left(\frac{\sigma}{\phi}\right) \quad (151)$$

$$|\delta| \leq \delta_{\max} \quad (152)$$

a) Linear analysis steady state

Assuming that the sliding mode control is not saturated and that the control deflection is less than the maximum, the submarine should reach an equilibrium state under the action of steady force and or moment disturbances. The linear equations of motion in the vertical plane with one control are:

$$\dot{w} = a_{11}uw + a_{12}uq + a_{13}\theta + b_1u^2\delta + F_d \quad (153)$$

$$\dot{q} = a_{21}uw + a_{22}uq + a_{23}\theta + b_2u^2\delta + M_d \quad (154)$$

$$\dot{\theta} = q \quad (155)$$

$$\dot{z} = w - u\theta \quad (156)$$

$$\dot{x} = w\theta + u \quad (157)$$

Equations (150) through (157) can be solved for the following steady state condition:

$$w_{ss} = \frac{F_d(-ub_2) + M_d(ub_1)}{b_2a_{11}u^2 + b_2a_{13} - b_1a_{21}u^2 - b_1a_{23}} \quad (158)$$

$$q_{ss} = 0 \quad (159)$$

$$\theta_{ss} = \frac{F_d(-b_2) + M_d(b_1)}{b_2a_{11}u^2 + b_2a_{13} - b_1a_{21}u^2 - b_1a_{23}} \quad (160)$$

$$z_{ss} = F_d \frac{a_{21}u^2 + K_3u^2b_2 + a_{23} + u^3\eta K_s\phi b_2S_1 + u^2\eta K_s\phi b_2S_3 + K_1u^3b_2}{u^2K_nS_4\phi(b_2a_{11}u^2 + b_2a_{13} - b_1a_{21}u^2 - b_1a_{23})} - M_d \frac{K_3u^2b_1 + a_{11}u^2 + a_{13} + u^3\eta K_s\phi b_1S_1 + K_1u^3b_1 + u^2\eta K_s\phi b_1S_3}{u^2K_nS_4\phi(b_2a_{11}u^2 + b_2a_{13} - b_1a_{21}u^2 - b_1a_{23})} \quad (161)$$

$$\delta_{ss} = \frac{F_d(a_{21}u^2 + a_{23}) + M_d(-a_{11}u^2 - a_{13})}{u^2(b_2a_{11}u^2 + b_2a_{13} - b_1a_{21}u^2 - b_1a_{23})} \quad (162)$$

If the sliding mode is just saturated, that is $|\sigma / \phi| = 1$, the system will still be stable, however the gain parameter η will be at a critical value. If further reduced, the system will be unstable. Assuming the sliding mode is just saturated this critical value, η_{crit} , can be determined.

$$\eta_{crit} = \left| \frac{F_d \frac{a_{21}u^2 + a_{23} + K_3u^2b_2 + K_1u^3b_2}{K_su^2(b_2a_{11}u^2 + b_2a_{13} - b_1a_{21}u^2 - b_1a_{23})} - M_d \frac{a_{11}u^2 + a_{13} + K_3u^2b_1 + K_1u^3b_1}{K_su^2(b_2a_{11}u^2 + b_2a_{13} - b_1a_{21}u^2 - b_1a_{23})} \right| \quad (163)$$

For cases with the gain parameter η less than critical, a steady state \dot{z} results, along with steady state values in all states other than z . By assuming a steady state \dot{z} and solving Equations (150) through (157) for equilibrium, the following equations result:

$$\theta_{ss} = \frac{F_d(-a_{21} - b_2uK_1) + Md(b_1uK_1 + a_{11}) + u^2K_s\eta(b_2a_{11} - b_1a_{21})}{u^2K_3(b_1a_{21} - b_2a_{11}) + uK_1(a_{13}b_2 - a_{23}b_1) + a_{13}a_{21} - a_{23}a_{11}} \quad (164)$$

$$\dot{z}_{ss} = - \frac{F_d + b_1u^2K_s\eta + \theta_{ss}(a_{13} + a_{11}u^2 + b_1u^3K_1 + b_1u^2K_3)}{u(b_1uK_1 + a_{11})} \quad (165)$$

$$w_{ss} = u\theta_{ss} + \dot{z}_{ss} \quad (166)$$

$$q_{ss} = 0 \quad (167)$$

$$\delta_{ss} = \frac{-(a_{11}uw_{ss} + a_{13}\theta_{ss} + F_d)}{b_1u^2} \quad (168)$$

Inspection of Equation (164) may cause the reader to incorrectly assume that a nonzero steady state value of θ will exist in the absence of disturbances. This is not the case, however, because the use of Equation (164) implies the lack of a steady state z , and therefore a disturbance.

b) Nonlinear analysis steady state

An analysis similar to that conducted on the linear equations can be conducted to determine the system steady state response under a constant disturbance. The nonlinear equations of motion in the vertical plane with one control are:

$$\dot{w} = a_{11}uw + a_{12}uq + a_{13}\sin(\theta) + b_1u^2\delta + F_d\cos(\theta) + e_{11}q^2 + e_{12}qw \quad (169)$$

$$\dot{q} = a_{21}uw + a_{22}uq + a_{23}\sin(\theta) + b_2u^2\delta + M_d\cos(\theta) + e_{21}q^2 + e_{22}qw \quad (170)$$

$$\dot{\theta} = q \quad (171)$$

$$\dot{z} = w\cos(\theta) - u\sin(\theta) \quad (172)$$

$$\dot{x} = w\sin(\theta) + u\cos(\theta) \quad (173)$$

Once again, the basic sliding mode control of Equations (150) and (151) is used. Assuming that steady state is possible (sliding mode control is not saturated, and the control deflection is less than the maximum) Equations (169) through (173) subject to the basic sliding mode control law can be reduced to the following nonlinear equation:

$$\begin{aligned} & a_{11}\sin(\theta)u^2b_2 + a_{13}\sin(\theta)\cos(\theta)b_2 + F_d\cos^2(\theta)b_2 - \\ & b_1a_{21}\sin(\theta)u^2 - b_1a_{23}\sin(\theta)\cos(\theta) - b_1M_d\cos^2(\theta) = 0 \end{aligned} \quad (174)$$

Solution of Equation (174) yields the steady state value of θ . It is of note that Equation (174) is independent of the control law. The correct root is readily determined by using the value closest to the linear analysis (Equation (160)). Substitution of this value into Equations (169) through (173) yields following steady state results:

$$w_{ss} = u \tan(\theta_{ss}) \quad (175)$$

$$q_{ss} = 0 \quad (176)$$

$$\delta_{ss} = \frac{-(a_{11}uw_{ss} + a_{13}\sin(\theta_{ss}) + F_d)}{b_1u^2} \quad (177)$$

$$z_{ss} = \frac{\frac{\phi}{\eta K_s}(\delta_{ss} - K_1w_{ss} - K_3\theta_{ss}) - S_1w_{ss} - S_3\theta_{ss}}{S_4} \quad (178)$$

The steady state value of z given by Equation (178) is dependent upon the control law gains. Following the example of the linear analysis, a critical value of the gain parameter, η_{crit} can be determined.

$$\eta_{crit} = \left| \frac{\delta_{ss} - K_1w_{ss} - K_3\theta_{ss}}{K_s} \right| \quad (179)$$

Unlike the linear analysis, the critical value of the gain parameter is not just a linear combination of the disturbance forces, but rather requires nonlinear solution for each possible case.

If $|\sigma / \phi| > 1$ the sliding mode control will be saturated, and a nonzero steady state \dot{z}_{ss} will exist. For this case, the control law control law reduces to:

$$\delta = K_1w + K_2q + K_3\theta + \eta K_s \text{sign}(\sigma) \quad (180)$$

Given the steady state final condition in all state variables with the exception of z , Equations (169) through (173) and (180) can be reduced to finding a root of the following nonlinear equation:

$$\frac{u^2 (b_1 K_3 a_{21} \theta + b_1 K_n a_{21} - b_2 K_3 a_{11} \theta - b_2 K_2 a_{11}) + u \sin(\theta) (a_{13} b_2 K_1 - a_{23} b_1 K_1)}{b_2 u K_1 + a_{21}} + \frac{F_d \cos(\theta) (b_2 u K_1 + a_{21}) - M_d \cos(\theta) (b_1 u K_1 + a_{11}) + \sin(\theta) (a_{13} a_{21} - a_{23} a_{11})}{b_2 u K_1 + a_{21}} = 0 \quad (181)$$

This can be accomplished using the linear value of θ_{ss} from Equation (164) as the initial guess. It follows that:

$$\dot{z}_{ss} = - \frac{F_d \cos^2(\theta_{ss}) + a_{13} \sin(\theta_{ss}) \cos(\theta_{ss})}{u(b_1 u K_1 + a_{11})} - \frac{u^2 (a_{11} \sin(\theta_{ss}) + b_1 u K_1 \sin(\theta_{ss}) + b_1 K_3 \theta_{ss} \cos(\theta_{ss}) + b_1 K_s \eta \cos(\theta_{ss}))}{u(b_1 u K_1 + a_{11})} \quad (182)$$

$$w_{ss} = u \tan(\theta_{ss}) + \dot{z}_{ss} \quad (183)$$

$$\delta_{ss} = K_1 w_{ss} + K_3 \theta_{ss} + \eta K_s \text{sign}(\sigma) \quad (184)$$

c) *Disturbance response simulation with basic sliding mode*

These results can then be applied to the SUBOFF hydrodynamic coefficients. For the modified coefficients used in this thesis, the linear state space system at six knots with stern planes only is:

$$\begin{bmatrix} \dot{w} \\ \dot{q} \\ \dot{\theta} \\ \dot{z} \end{bmatrix} = \begin{bmatrix} -0.0179 & 3.7101 & 0.0196 & 0 \\ 0.0006 & -0.0680 & -0.0034 & 0 \\ 0 & 1 & 0 & 0 \\ 1 & 0 & -10.1269 & 0 \end{bmatrix} \begin{bmatrix} w \\ q \\ \theta \\ z \end{bmatrix} + \begin{bmatrix} -0.1009 \\ -0.0027 \\ 0 \\ 0 \end{bmatrix} \delta + \begin{bmatrix} F_d \\ M_d \\ 0 \\ 0 \end{bmatrix} \quad (185)$$

A sliding mode control law is determined using Utkin's method. After some experimentation, the diagonal of the minimization matrix Q was selected as $Q_{11} = 100$, $Q_{22} = 100$, $Q_{33} = 100$, $Q_{44} = 1$. This yielded the following control law:

$$\sigma = 1.0w - 67.5592q - 15.4082\theta + 0.0830z \quad (186)$$

$$\delta = -0.2803w + 84.8572q + 7.0612\theta + K_s \eta \text{sat} \text{sign}\left(\frac{\sigma}{\phi}\right) \quad (187)$$

$$|\delta| \leq 0.4 \quad (188)$$

A moment disturbance was chosen to be controllable but give a nontrivial response. The application of a force of five thousand pounds and moment of 4,573 thousand foot pounds resulted in a pure angular acceleration, $M_d = 0.001$ radians/second². For this state space system, control law, and disturbance set, the value of η_{crit} was (0.0661). Application of the nonlinear solutions yielded the steady state solutions in Table 13.

η / η_{crit}	$w_{ss}(\text{Feet / Sec})$	$q_{ss}(\text{Rad / sec})$	$\theta_{ss}(\text{Degrees})$	$z_{ss}(\text{Feet})$	$\delta_{ss}(\text{Radians})$	$\dot{z}_{ss}(\text{Feet / Sec})$
0	-0.9606	0	-0.8271	Infinity	0.1673	-0.8143
0.5	-1.1791	0	-4.3402	Infinity	0.1941	-0.4094
1.1	-1.3965	0	-7.8518	-19.5783	0.2208	0
2	-1.3965	0	-7.8518	-14.6467	0.2208	0
4	-1.3965	0	-7.8518	-11.6330	0.2208	0

Table 13. Steady state nonlinear solutions for $M_d = 0.001$ radians/second²

The system transient response was simulated using the RK45 function of the SIMULINK® toolbox. Figure 28 shows the resulting paths. The response is given for six values of the ratio of η and η_{crit} . As expected, for values of η less than critical the control law is unable to maintain a steady depth.

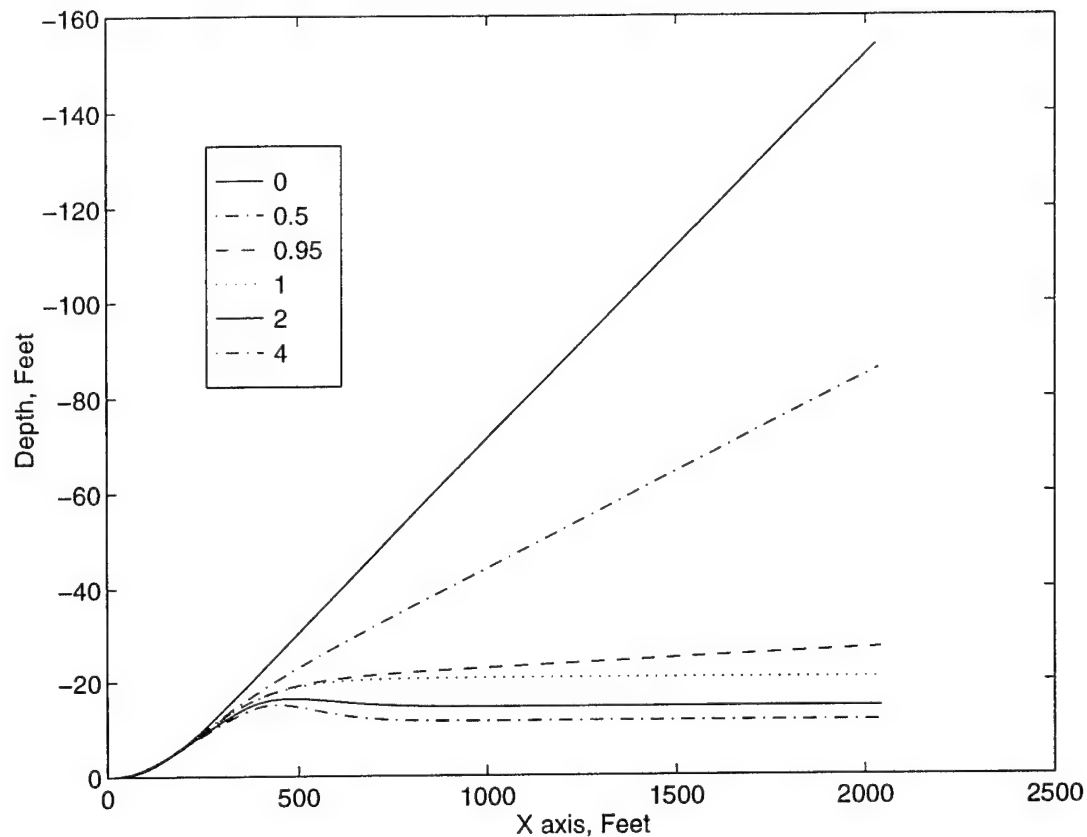


Figure 28. Nonlinear simulation of vertical plane response to a pure moment disturbance

The calculations and simulations were repeated for a pure force disturbance. A force of 43 thousand pounds and a moment of 220.4 foot thousand pounds resulted in a pure vertical acceleration of 0.005 feet/second². For this state space system, control law, and disturbance set, the value of η_{crit} was (0.0466).

η / η_{crit}	w_u (Feet / Sec)	q_u (Rad / sec)	θ_u (Degrees)	z_u (Feet)	δ_u (Radians)	\dot{z}_u (Feet / Sec)
0	1.5724	0	5.4888	Infinity	0.2357	0.5966
0.5	1.4156	0	2.9632	Infinity	0.2549	0.8902
1.1	1.8836	0	10.5368	22.4107	0.1976	0
2	1.8836	0	10.5368	17.4792	0.1976	0
4	1.8836	0	10.5368	14.4654	0.1976	0

Table 14. Steady state nonlinear solutions for $F_d = 0.05$

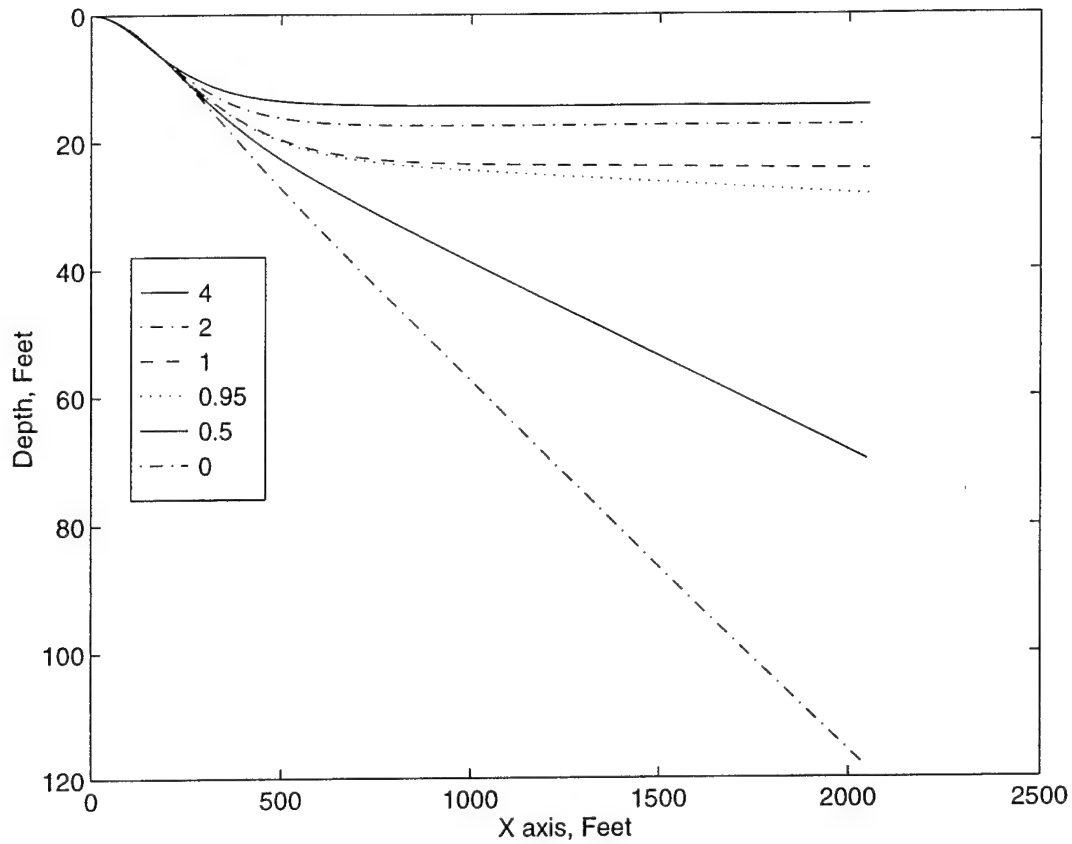


Figure 29. Nonlinear simulation of vertical plane response to a pure force disturbance

d) Disturbance response with sliding mode feedforward control

To eliminate the steady state error induced by a disturbance, several techniques may be employed. Using a feedforward function in the sliding mode control law is one technique. A feedforward term works by using knowledge of the external disturbance and using applying some degree of control effort. This provides a steady state control effort to oppose the disturbance without a steady state error. This approach is limited as it requires one control per zero error state and may be limited in other ways. A feedforward term can be added to the sliding mode control law by changing the sliding surface to the following:

$$\sigma = S_1 w + S_2 q + S_3 \theta + S_4 z + S_5 \quad (189)$$

The value of S_5 is such that it will equal the control effort that is applied by the steady state quantity that is desired to be zeroed. Since the main priority is to obtain zero

depth error, S_5 is selected to equal the control effort introduced by the previously calculated value of steady state depth error:

$$S_5 = \frac{\phi}{\eta K_s} (\delta_{ss} - K_1 w_{ss} - K_3 \theta_{ss}) - S_1 w_{ss} - S_3 \theta_{ss} \quad (190)$$

The steady state values needed for Equation (190) can be determined from linear or nonlinear analysis, although the linear analysis will result in a non-zero depth error. The linear analysis gives the following:

$$S_5 = C_1 M_d + C_2 F_d \quad (191)$$

where:

$$C_1 = \frac{-\left(\frac{\phi}{S_4 K_s \eta} \left(a_{11} + \frac{a_{13}}{u^2} + K_3 b_1 + K_1 u b_1\right) + \frac{S_3 b_1}{S_4} + \frac{S_1 u b_1}{S_4}\right)}{a_{11} u^2 b_2 + a_{13} b_2 - b_1 a_{21} u^2 - b_1 a_{23}} \quad (192)$$

$$C_2 = \frac{\left(\frac{\phi}{S_4 K_s \eta} \left(a_{21} + \frac{a_{23}}{u^2} + K_3 b_2 + K_1 u b_2\right) + \frac{S_3 b_2}{S_4} + \frac{S_1 u b_2}{S_4}\right)}{a_{11} u^2 b_2 + a_{13} b_2 - b_1 a_{21} u^2 - b_1 a_{23}} \quad (193)$$

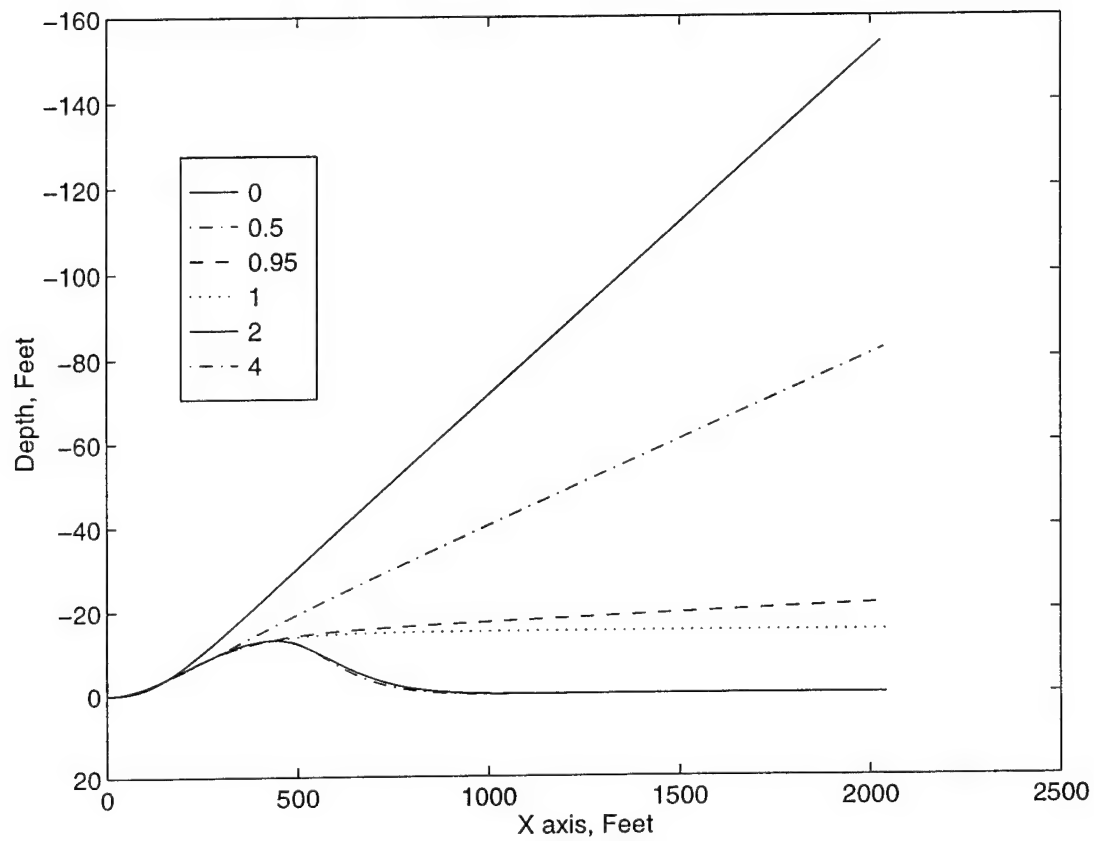


Figure 30. Nonlinear simulation of vertical plane response to a pure moment disturbance with a feedforward term based on nonlinear steady state

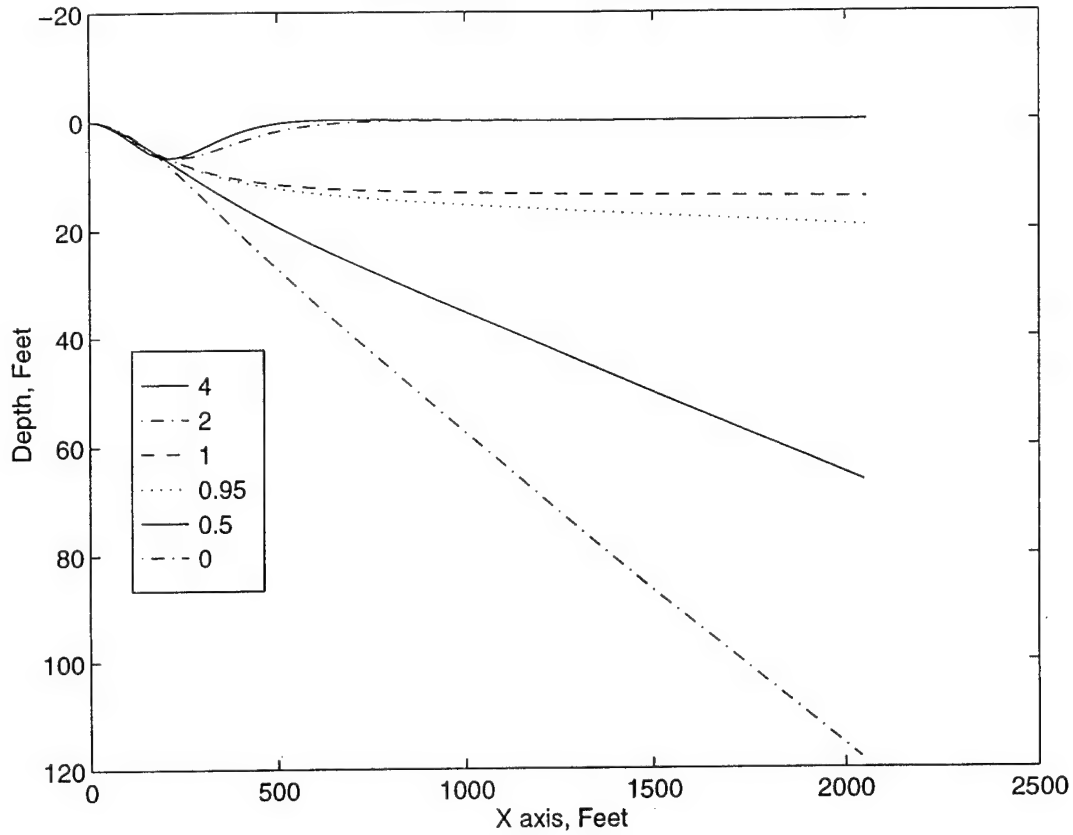


Figure 31. Nonlinear simulation of vertical plane response to a pure force disturbance with a feedforward term based on nonlinear steady state

e) Disturbance response with sliding mode integral control

Another means of eliminating steady state error is by the use of an integral control term. To accomplish this, an additional equation is added to the state space representation.

$$\dot{z}_I = z \quad (194)$$

This forces a zero steady state error in z , although there are some additional considerations with the use of integral control. The resulting control law, with the additional state, is:

$$\sigma = S_1 w + S_2 q + S_3 \theta + S_4 z + S_5 z_I \quad (195)$$

$$\delta = K_1 w + K_2 q + K_3 \theta + K_4 z + \eta K_s \text{sat} \text{sign} \left(\frac{\sigma}{\phi} \right) \quad (196)$$

$$|\delta| \leq 0.4 \quad (197)$$

Based on inspection of Equations (195) and (196) several conclusions can be drawn. First, because z is included in the proportional portion of the control law, values of the gain parameter which are less than critical will result in a steady state error in z for any controllable disturbance. Second, if there is a steady state error in z , the magnitude of the integral term, z_I , will tend to infinity. This can cause problems with changing conditions or pathkeeping as it will delay the control response to other errors.

At a condition of steady state, with the gain parameter greater than critical, the steady state error in z is zero. Because of this, the previously calculated values for steady state pitch angle, heave, and control deflection are still valid (Equations (174) through (177)). Moreover, because any controllable disturbance will result in a steady state condition these values apply for cases where the gain parameter is less than critical.

For conditions where the gain parameter is less than critical, the resulting control law is:

$$\delta = K_1 w + K_2 q + K_3 \theta + K_4 z + \eta K_s \text{sign}(\sigma) \quad (198)$$

And the steady state value of z is:

$$z_{ss} = \frac{\delta_{ss} - K_1 w_{ss} - K_3 \theta_{ss} - \eta K_s \text{sign}(\sigma)}{K_4} \quad (199)$$

Expressed in linear state space form for control law design, the representation for the SUBOFF at six knots is:

$$\begin{bmatrix} \dot{w} \\ \dot{q} \\ \dot{\theta} \\ \dot{z} \\ \dot{z}_I \end{bmatrix} = \begin{bmatrix} -0.0179 & 3.7101 & 0.0196 & 0 & 0 \\ 0.0006 & -0.068 & -0.0034 & 0 & 0 \\ 0 & 1 & 0 & 0 & 0 \\ 1 & 0 & -10.1269 & 0 & 0 \\ 0 & 0 & 0 & 1 & 0 \end{bmatrix} \begin{bmatrix} w \\ q \\ \theta \\ z \\ z_I \end{bmatrix} + \begin{bmatrix} -0.1009 \\ -0.0027 \\ 0 \\ 0 \\ 0 \end{bmatrix} \delta + \begin{bmatrix} F_d \\ M_d \\ 0 \\ 0 \\ 0 \end{bmatrix} \quad (200)$$

Utkin's method was applied to obtain a suitable control law. After some experimentation, the diagonal of the minimization matrix Q was selected as $Q_{11} = 100$, $Q_{22} = 100$, $Q_{33} = 100$, $Q_{44} = 1$, $Q_{55} = 0.01$. This yielded the following control law:

$$\sigma = 1.0w - 49.8158q - 12.7725\theta + 0.1050z + 0.0035z_I \quad (201)$$

$$\delta = -1.6009w + 161.0589q + 24.8125\theta - 0.0991z + K_s \eta s \text{at sign} \left(\frac{\sigma}{\phi} \right) \quad (202)$$

$$|\delta| \leq 0.4 \quad (203)$$

Simulations of the SUBOFF under sliding mode integral control with a moment disturbance are given in Figure 32. For this state space system, control law, and disturbance set the value of η_{crit} was (0.0484). Shown are five different values the ratio of the gain parameter to the critical gain parameter. For values of the ratio larger than about two, the system exhibited excessive oscillation before settling to zero depth error.

Simulations of the SUBOFF under sliding mode integral control with a force disturbance are given in Figure 33. For this state space system, control law, and disturbance set the value of η_{crit} was (0.0466). Shown are six different values the ratio of the gain parameter to the critical gain parameter. For values of the ratio larger than about two, the system exhibited excessive oscillation before settling to zero depth error.

f) *Sliding mode disturbance response conclusions*

Submarine vertical plane depth control using sliding mode control can be effectively achieved in the presence of disturbances. Sliding mode control is similar to linear state feedback in that the an external disturbance will result in a steady state depth error. However, if the gain parameters of the sliding mode control are not properly selected, a loss of depth control can occur.

Steady state error can be dealt with using feedforward or integral control. Integral control has several advantages. Application of integral control does not require knowledge of the disturbance. However, if the gain parameter is too small, windup of the integral term occurs. If the gain parameter is too large, excessive oscillations can be

introduced. The greatest advantage of integral control demonstrated was that gain parameters less than critical did not result in loss of depth stability.

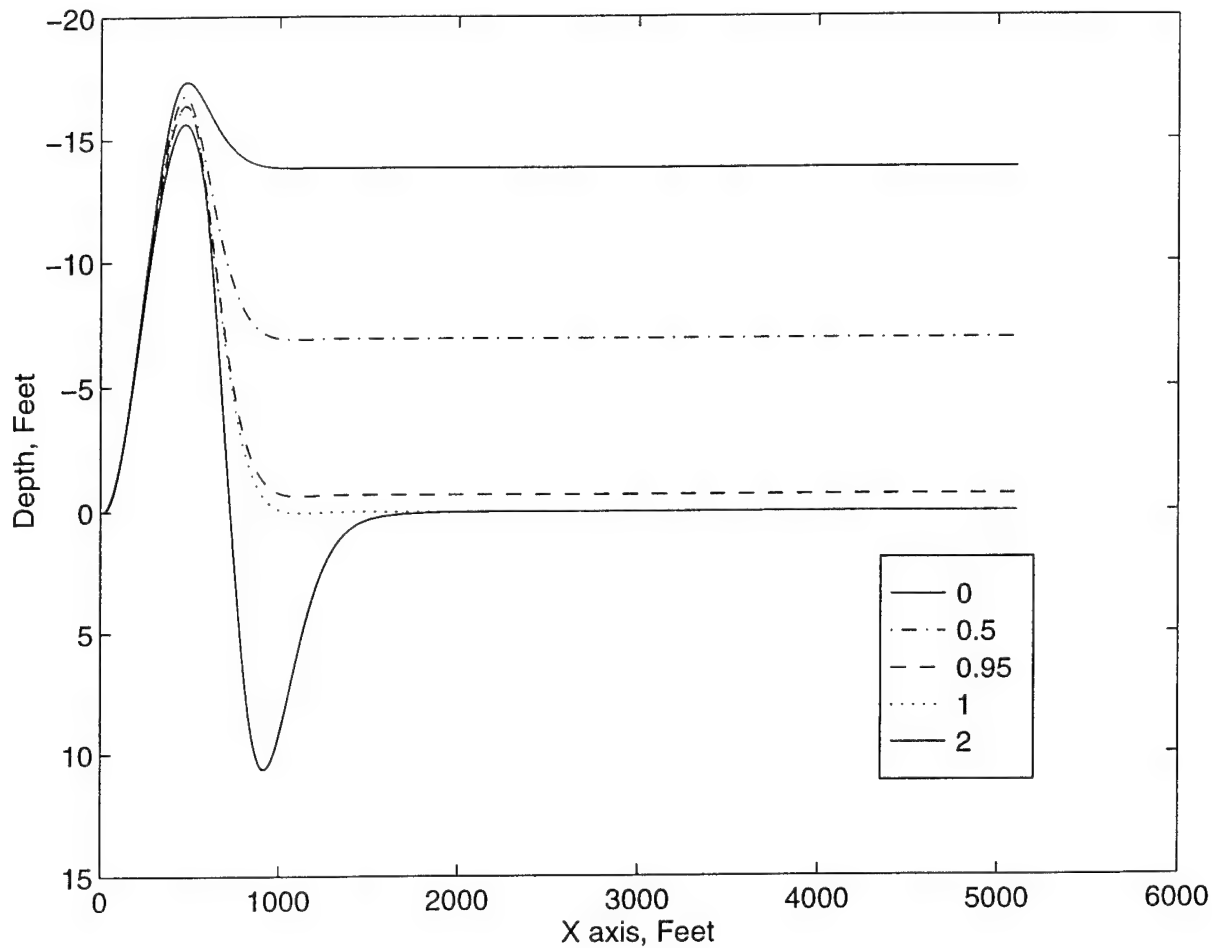


Figure 32. Nonlinear simulation of moment disturbance using sliding mode integral control

Feedforward control exhibited good disturbance compensation, assuming that the disturbances were measurable. Given the disturbances, feedforward values can be determined based upon the nonlinear equations of motion, requiring periodic nonlinear root finding, or upon the linear solution. Because of the computational expense of obtaining the nonlinear solution and the expected error in the hydrodynamic coefficients, a linear steady state solution is appropriate for feedforward computation.

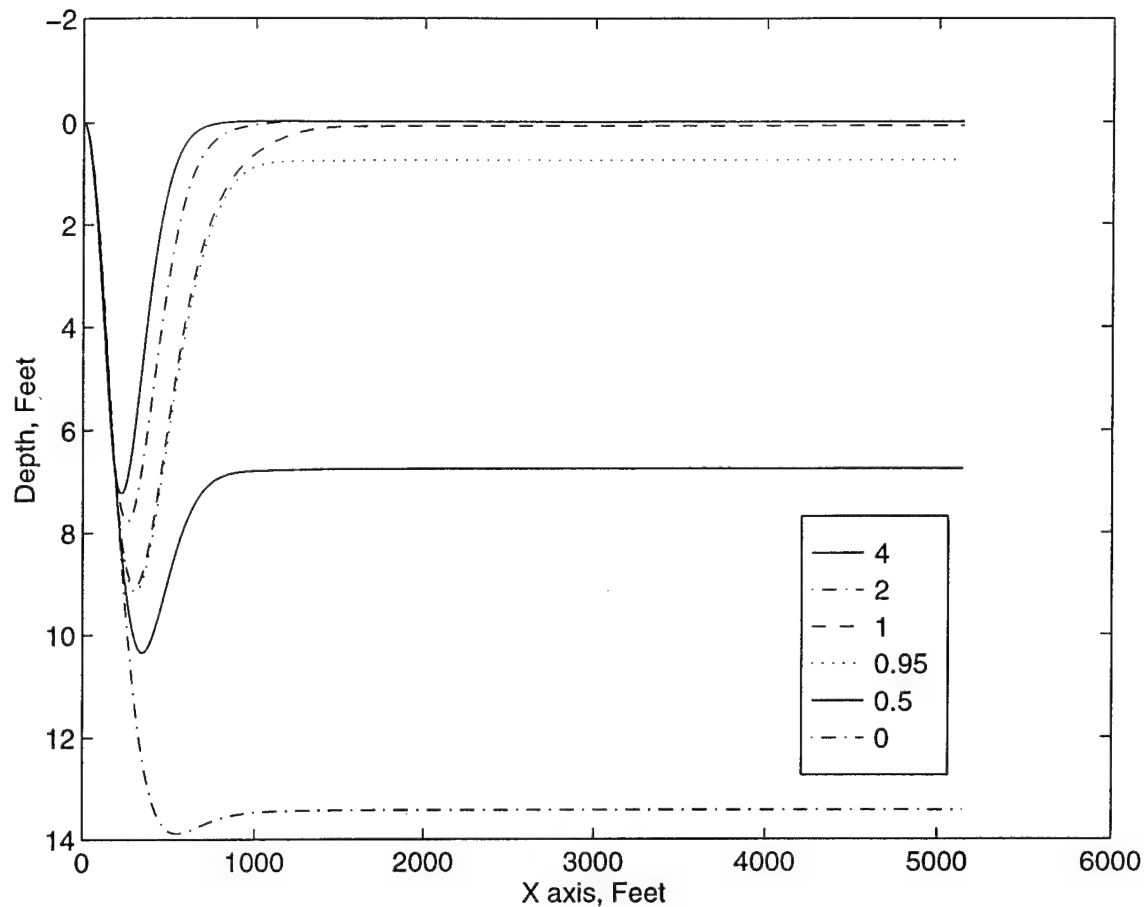


Figure 33. Nonlinear simulation of force disturbance using sliding mode integral control

C. MIMO SLIDING MODE CONTROL AT PERISCOPE DEPTH

1. Introduction

The purpose of using sliding mode control was to provide an alternate means of control which relied upon all the system states. The robust characteristics of sliding mode control were thought to be a good approximation to the human operators.

At periscope depth, experience dictates several desired conditions. First, the ship is trimmed heavy to counter the steady wave forces. Even more weight is brought on after this point to allow for a constant small positive trim angle, of several degrees. This provides reserve ballast which is made available by reducing the trim angle. Finally, in sea state three, it should be very possible to maintain depth within one foot of ordered depth.

The equations of motion used for this section are the nonlinear equations of submarine motion in the vertical plane. They are different from the equations used previously in this chapter, as they include both bow and stern planes. Also the force and moment disturbances used represent not only constant disturbances, like ships trim, but time varying wave forces as well. Repeated for convenience, the equations are:

$$\dot{w} = a_{11}uw + a_{12}uq + a_{13}\sin(\theta) + b_{11}u^2\delta_b + b_{12}u^2\delta_s + F_d \cos(\theta) + e_{11}q^2 + e_{12}qw \quad (204)$$

$$\dot{q} = a_{21}uw + a_{22}uq + a_{23}\sin(\theta) + b_{21}u^2\delta_b + b_{22}u^2\delta_s + M_d \cos(\theta) + e_{21}q^2 + e_{22}qw \quad (205)$$

$$\dot{\theta} = q \quad (206)$$

$$\dot{z} = w \cos(\theta) - u \sin(\theta) \quad (207)$$

$$\dot{x} = w \sin(\theta) + u \cos(\theta) \quad (208)$$

2. Basic sliding mode controller

The sliding mode controller is of the same form as before, although with the introduction of MIMO control some of the scalar terms become vectors or matrices. The form of the basic sliding mode controller is:

$$\sigma_1 = S_{11}w + S_{12}q + S_{13}\theta + S_{14}z \quad (209)$$

$$\sigma_2 = S_{21}w + S_{22}q + S_{23}\theta + S_{24}z \quad (210)$$

$$\delta_b = K_{11}w + K_{12}q + K_{13}\theta + \eta_1 K_{s11} \text{satsign}\left(\frac{\sigma_1}{\phi_1}\right) + \eta_2 K_{s12} \text{satsign}\left(\frac{\sigma_2}{\phi_2}\right) \quad (211)$$

$$\delta_s = K_{21}w + K_{22}q + K_{23}\theta + \eta_1 K_{s21} \text{satsign}\left(\frac{\sigma_1}{\phi_1}\right) + \eta_2 K_{s22} \text{satsign}\left(\frac{\sigma_2}{\phi_2}\right) \quad (212)$$

$$|\delta_b| \leq \delta_{\max} \quad (213)$$

$$|\delta_s| \leq \delta_{\max} \quad (214)$$

As an initial attempt, Utkin's method was used to determine a sliding mode control law. After some experimentation, the diagonal of the minimization matrix Q was selected as $Q_{11} = 100$, $Q_{22} = 100$, $Q_{33} = 100$, $Q_{44} = 1$. This resulted in the following control matrices:

$$K = \begin{bmatrix} 39.6585 & -632.81 & -404.54 & 0 \\ -24.6916 & 429.65 & 250.27 & 0 \end{bmatrix} \quad (215)$$

$$S = \begin{bmatrix} 1 & 0 \\ 0 & 1 \\ -0.0985 & 1.7281 \\ 0.0170 & -0.0985 \end{bmatrix} \quad (216)$$

$$K_s = \begin{bmatrix} 10.9711 & -405.06 \\ 3.083 & 252.10 \end{bmatrix} \quad (217)$$

The values of the gain and boundary layer thickness parameters were taken as:

$$\eta_1 = \eta_2 = \frac{1}{20} \quad (218)$$

$$\phi_1 = \phi_2 = 1 \quad (219)$$

A SIMULINK® model was developed to incorporate the submarine dynamics of Chapter II, the wave forces of Chapter III, and the MIMO sliding mode control law. Also included was the trim model from Chapter IV.

The model was used to simulate a step change in commanded depth from 140 feet to 50 feet in depth. To provide some realism in the trim condition, the submarine was trimmed to 25 thousand pounds heavy, with no moment correction. Wave force values for sea state three were used, with a relative heading of 180 degrees (head seas). Figure 35 shows the resulting path taken by the submarine.

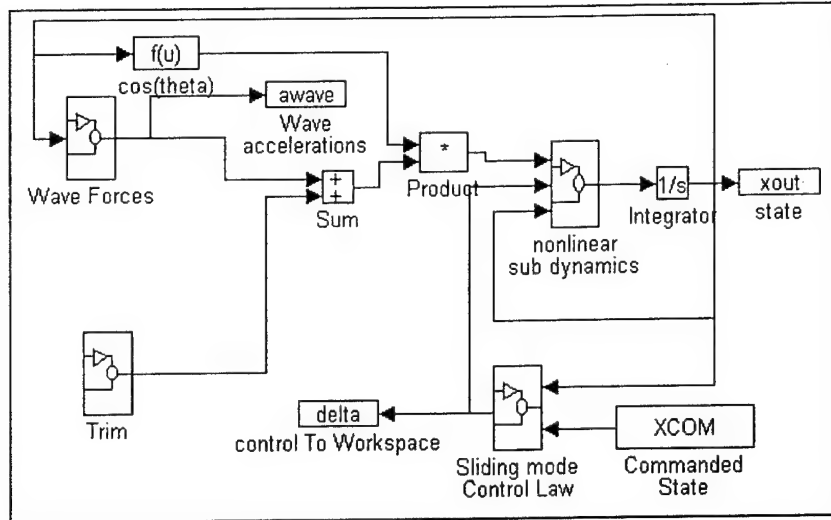


Figure 34. SIMULINK® model of submarine with wave forces and trim

At first glance, this control scheme fulfills most of the desired characteristics of a submarine depth controller. Periscope depth was achieved with no overshoot, and reasonable depth control was maintained. The trim condition was selected so that a steady state positive trim angle would exist at periscope depth. During the depth change, the maximum trim angle achieved was about ten degrees, which is also very consistent with actual submarine practice.

Inspection of Figure 36 shows some problems with this particular controller. The application of control effort was excessive. The main reason for this was the high frequency variations in w and q induced by the wave forces. Because of the combination of wave forces and trim, the commanded depth was not achieved. The average depth at periscope depth was 50.75 feet, as opposed to the commanded depth of 50 feet.

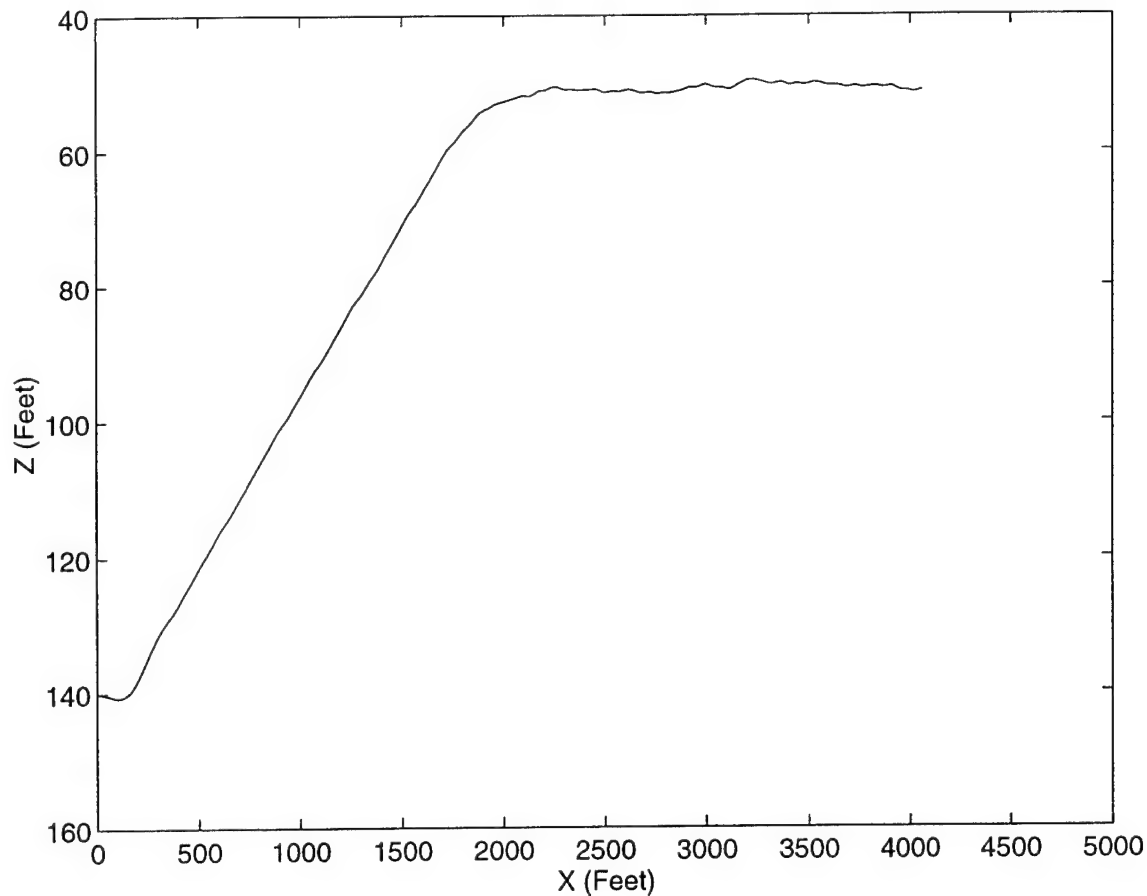


Figure 35. Basic sliding mode performance, step change approach to PD

Although the performance for the sea state three, head seas was adequate with this controller, it did not perform well with the other sea states or headings. Because of this, it was decided to use this control as a starting point for a performance optimization for each of the four sea state and direction cases available.

As was done for state feedback control, the MATLAB® CONSTR function was used to perform the optimizations. To provide a general set of design variables, the sliding mode linear quadratic regulator program was not used to determine the control law at each step of the optimization. Instead, the sliding surface itself was varied to change the control law.

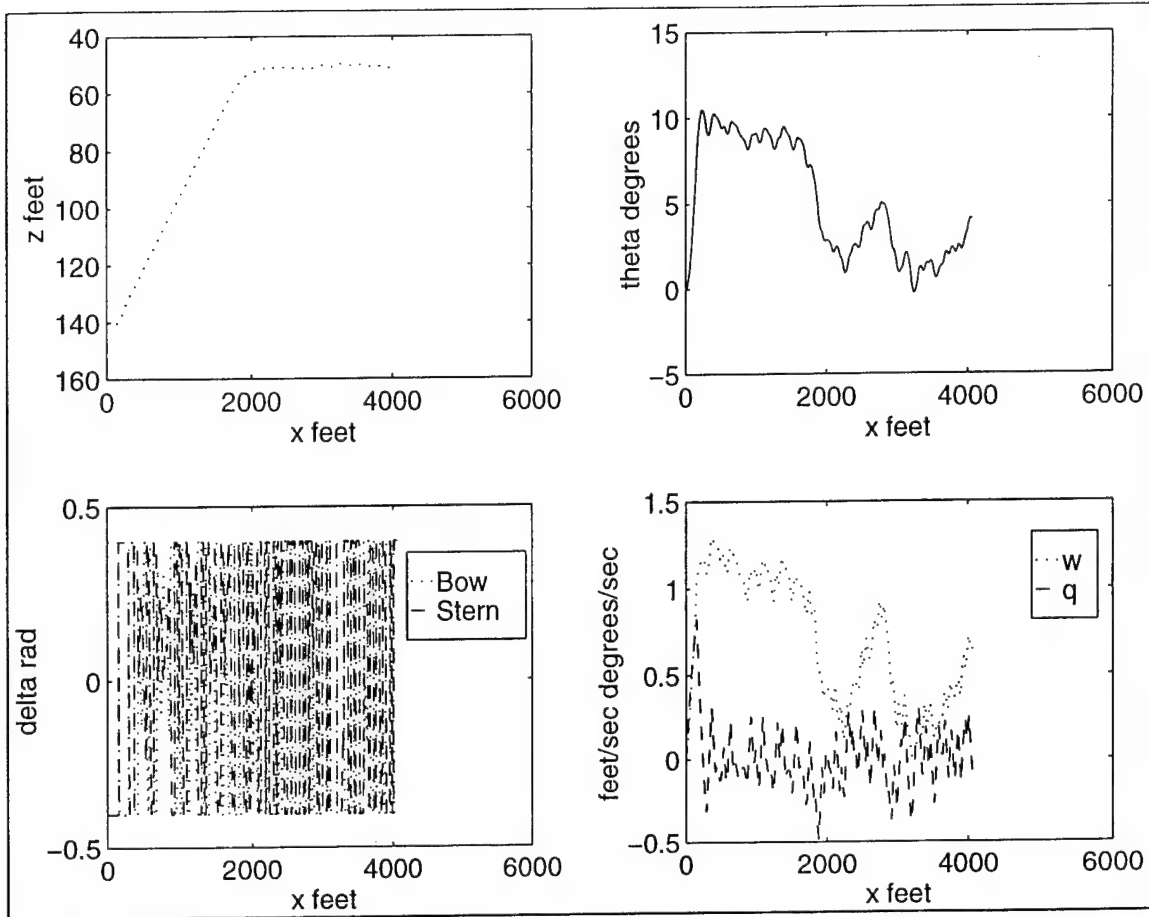


Figure 36. State parameters for basic sliding mode approach to periscope depth

The formal optimization statement is:

Minimize:

$$F(S_{31}, S_{32}, S_{41}, S_{42}, \eta_1, \eta_2, H, F) = \sqrt{\frac{\int_0^{t_f} (z - z_{mean})^2 dt}{t_f}} \quad (220)$$

where:

$z = \text{depth}$, determined by nonlinear simulation

$$z_{mean} = \frac{\int_0^{t_f} (z) dt}{t_f},$$

$H = \text{Ballast added to center of buoyancy, thousands of pounds}$

$F = \text{Ballast shifted from forward to aft, thousands of pounds}$

Subject to:

$$\text{real}(\text{eigenvalues}(A_{22} - A_{21}S_2^T)) \leq E_{\max} \quad (221)$$

Deviation from the mean value of depth vice the commanded was used because of the expected average depth error.

This approach was used for each of the four sea state cases. For sea state three (head

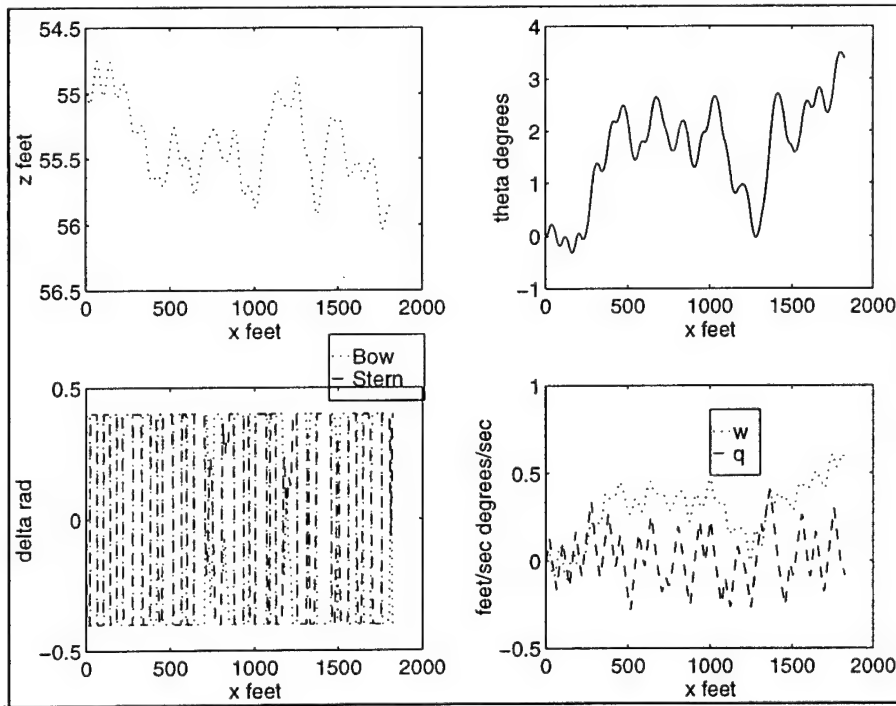


Figure 37. Simulation with basic sliding mode control in sea state three (head sea direction seas), the optimized response is shown in Figure 37. The results of the four optimizations are shown in Table 15. For the RMS error and maximum error, the optimized values are given, along with their percentage of the initial values. In all cases, use of the optimization resulted in reduction of the mean square depth error (measured from the average depth). Reduction of the maximum error was also achieved.

Sea State/Direction	3/head		3/beam		4/head		4/beam	
Initial Values								
S	1 0 -0.0985 0.0170	0 1 1.7281 -0.0985	1 0 -0.0985 0.0170	0 1 1.7281 -0.0985	1 0 -0.1388 0.0191	0 1 1.377 -0.694	1 0 -0.0932 0.0170	0 1 1.7281 -0.0903
K^T	39.658 -632.81 -404.54 0	-24.69 429.6 250.27 0	39.658 -632.81 -404.54 0	-24.69 429.6 250.27 0	27.88 -491.0 -285.23 0	-17.34 341.0 175.8 0	36.32 -632.77 -370.71 0	-22.61 429.7 229.21 0
η_1 / η_2	0.05/0.05		0.05/0.05		0.05/0.05		0.0445/0.0445	
H/F (10 ³ pounds)	20/0		20/0		20/0		20/0	
Mean Depth (feet)	53.46		49.55		52.83		54.53	
RMS Error (feet)	1.48		3.37		1.63		2.75	
Maximum Error (feet)	3.00		8.03		4.20		9.78	
Sliding surface eigenvalues	-0.8725 + 0.5063i -0.8725 - 0.5063i		-0.8725 + 0.5063i -0.8725 - 0.5063i		-0.6981 + 0.4820i -0.6981 - 0.4820i		-0.8726 + 0.4172i -0.8726 - 0.4172i	
Optimized Values								
S	1 0 -0.0816 0.0205	0 1 1.7244 -0.1203	1 0 -0.0196 0.0037	0 1 1.884 -0.0208	1 0 -0.1525 0.0176	0 1 1.3761 -0.0759	1 0 -0.933 0.0170	0 1 1.7281 -0.0903
K^T	48.50 -631.1 -494.0 0	-30.16 428.78 305.61 0	8.008 -695.15 -84.01 0	-5.124 469.2 52.11 0	30.475 -490.8 -311.5 0	-18.97 340.74 192.3 0	36.322 -632.76 -370.75 0	-22.615 429.67 229.24 0
η_1 / η_2	0.0488/0.0510		0.0457/0.0457		0.0501/0.0501		0.0446/0.0445	
H/F (10 ³ pounds)	19.9/0		19.6/0.0		20.0/0		20.0/0	
Mean Depth (feet)	55.44		57.61		55.53		54.57	
RMS Error (feet)	0.27 (18%)		0.84 (25%)		0.683 (42%)		1.43 (52%)	
Maximum Error (feet)	0.77 (26%)		2.36 (29%)		1.92 (46%)		4.14 (42%)	
Sliding surface eigenvalues	-0.8725 + 0.6945i -0.8725 - 0.6945i		-1.7649 -0.1229		-0.6968 + 0.5434i -0.6968 - 0.5434i		-0.8726 + 0.4173i -0.8726 - 0.4173i	

Table 15. Optimized basic sliding mode control law results and performance

3. Disturbance feedforward

The sliding mode control can be implemented with a disturbance feedforward to correct average depth error. This can be implemented inside or outside of the sliding surface. For this example, the disturbance feedforward was implemented inside the sliding surface calculation.

$$\sigma = S^T x + S_5 \quad (222)$$

Assuming that neither sliding surface is saturated, that control deflection is within limits, and using a linear analysis, the steady state value of the depth error can be written as a linear combination of the force and moment disturbances (Appendix B).

$$z_{ss} - z_{commanded} = C_1 F_d + C_2 M_d \quad (223)$$

To eliminate the depth error, it is necessary to apply the same amount of control effort that the steady state error provides within the sliding surface:

$$S_5 = (z_{ss} - z_{commanded}) \begin{bmatrix} S_{41} \\ S_{42} \end{bmatrix} \quad (224)$$

This results in the following control law:

$$\begin{bmatrix} \delta_{bp} \\ \delta_{sp} \end{bmatrix} = \begin{bmatrix} K_{11} & K_{12} & K_{13} & 0 \\ K_{21} & K_{22} & K_{23} & 0 \end{bmatrix} \begin{bmatrix} w - w_{commanded} \\ q - q_{commanded} \\ \theta - \theta_{commanded} \\ z - z_{commanded} \end{bmatrix} + \begin{bmatrix} K_{s11} & K_{s12} \\ K_{s21} & K_{s22} \end{bmatrix} \begin{bmatrix} \eta_1 \text{satsign}\left(\frac{\sigma_1}{\phi_1}\right) \\ \eta_2 \text{satsign}\left(\frac{\sigma_2}{\phi_2}\right) \end{bmatrix} \quad (225)$$

$$\begin{bmatrix} \sigma_1 \\ \sigma_2 \end{bmatrix} = \begin{bmatrix} 1 & 0 \\ 0 & 1 \\ S_{31} & S_{32} \\ S_{41} & S_{42} \end{bmatrix}^T \begin{bmatrix} w - w_{commanded} \\ q - q_{commanded} \\ \theta - \theta_{commanded} \\ z - z_{commanded} \end{bmatrix} + \begin{bmatrix} C_1 S_{41} & C_2 S_{41} \\ C_1 S_{42} & C_2 S_{42} \end{bmatrix} \begin{bmatrix} \hat{F}_d \\ \hat{M}_d \end{bmatrix} \quad (226)$$

$$|\delta| \leq \delta_{\max} \quad (227)$$

where the force and moment disturbances are filtered.

The initial sliding surface and gains from the basic sliding mode control law was used as the starting point for optimization. The formal optimization statement is:

$$F(S_{31}, S_{32}, S_{41}, S_{42}, \omega_{co}, \eta_1, \eta_2, H, F) = \sqrt{\frac{\int_0^{t_f} (z - z_{commanded})^2 dt}{t_f}} \quad (228)$$

Subject to:

$$real(eigenvalues(A_{22} - A_{21}S_2^T)) \leq E_{\max} \quad (229)$$

This approach was used for each of the four sea state cases. For sea state three (head seas), the optimized response is shown in Figure 38. The results of the four optimizations are shown in Table 16. For the RMS error and maximum error, the optimized values are given, along with their percentage of the initial values.

Sea State/Direction	3/head		3/beam		4/head		4/beam	
Initial Values								
S	1 0 -0.0985 0.0170	0 1 1.7281 -0.0985	1 0 -0.0985 0.0170	0 1 1.7281 -0.0985	1 0 -0.0985 0.0170	0 1 1.7281 -0.0985	1 0 -0.0985 0.0170	0 1 1.7281 -0.0985
K^T	39.658 -632.81 -404.54 0	-24.69 429.6 250.27 0	39.658 -632.81 -404.54 0	-24.69 429.6 250.27 0	39.658 -632.81 -404.54 0	-24.69 429.6 250.27 0	39.658 -632.81 -404.54 0	-24.69 429.6 250.27 0
ω_{co} (radians/second)	0.25		0.25		0.25		0.25	
η_1 / η_2	0.05/0.05		0.05/0.05		0.05/0.05		0.05/0.05	
H/F (10 ³ pounds)	20/0		20/0		20/0		20/0	
Mean Depth (feet)	55.28		54.99		55.10		53.41	
RMS Error (feet)	0.4181		1.50		1.01		7.04	
Maximum Error (feet)	1.225		3.85		3.50		18.75	
Sliding surface eigenvalues	-0.8725 + 0.5063i -0.8725 - 0.5063i		-0.8725 + 0.5063i -0.8725 - 0.5063i		-0.8725 + 0.5063i -0.8725 - 0.5063i		-0.8725 + 0.5063i -0.8725 - 0.5063i	
Optimized Values								
S	1 0 -0.0981 0.0166	0 1 1.7281 0.096	1 0 -0.1255 0.0400	0 1 2.1291 -0.0473	1 0 -1.9567 -0.0445	0 1 3.8086 -0.1476	1 0 -0.1167 -0.0155	0 1 1.8775 -0.0240
K^T	38.67 -632.8 -394.5 0	-24.08 429.65 244.1 0	19.16 -795.53 -196.91 0	-11.70 530.65 118.74 0	58.9 -1496.0 -599.1 0	-37.3 948.4 377.5 0	9.906 -693.54 -95.02 0	-5.992 467.3 60.9 0
ω_{co} (radians/second)	0.25		0.350		0.267		0.245	
η_1 / η_2	0.05/0.05		0.0542/0.0578		0.1853/0.0544		0.0596/0.0548	
H/F (10 ³ pounds)	20/0		20.2/-0.1		20.7/1.3		20.1/0.0	
Mean Depth (feet)	55.22		55.47		55.45		2.00	
RMS Error (feet)	0.405 (97%)		1.22 (81%)		1.01 (100%)		1.99 (28%)	
Maximum Error (feet)	1.36 (111%)		3.20 (83%)		2.52 (72%)		4.93 (26%)	
Sliding surface eigenvalues	-0.8723 + 0.4813i -0.8723 - 0.4813i		-1.8706 -0.2984		-3.4649 -0.2992		-1.7409 -0.1211	

Table 16. Optimized sliding mode control with disturbance feedforward results and performance

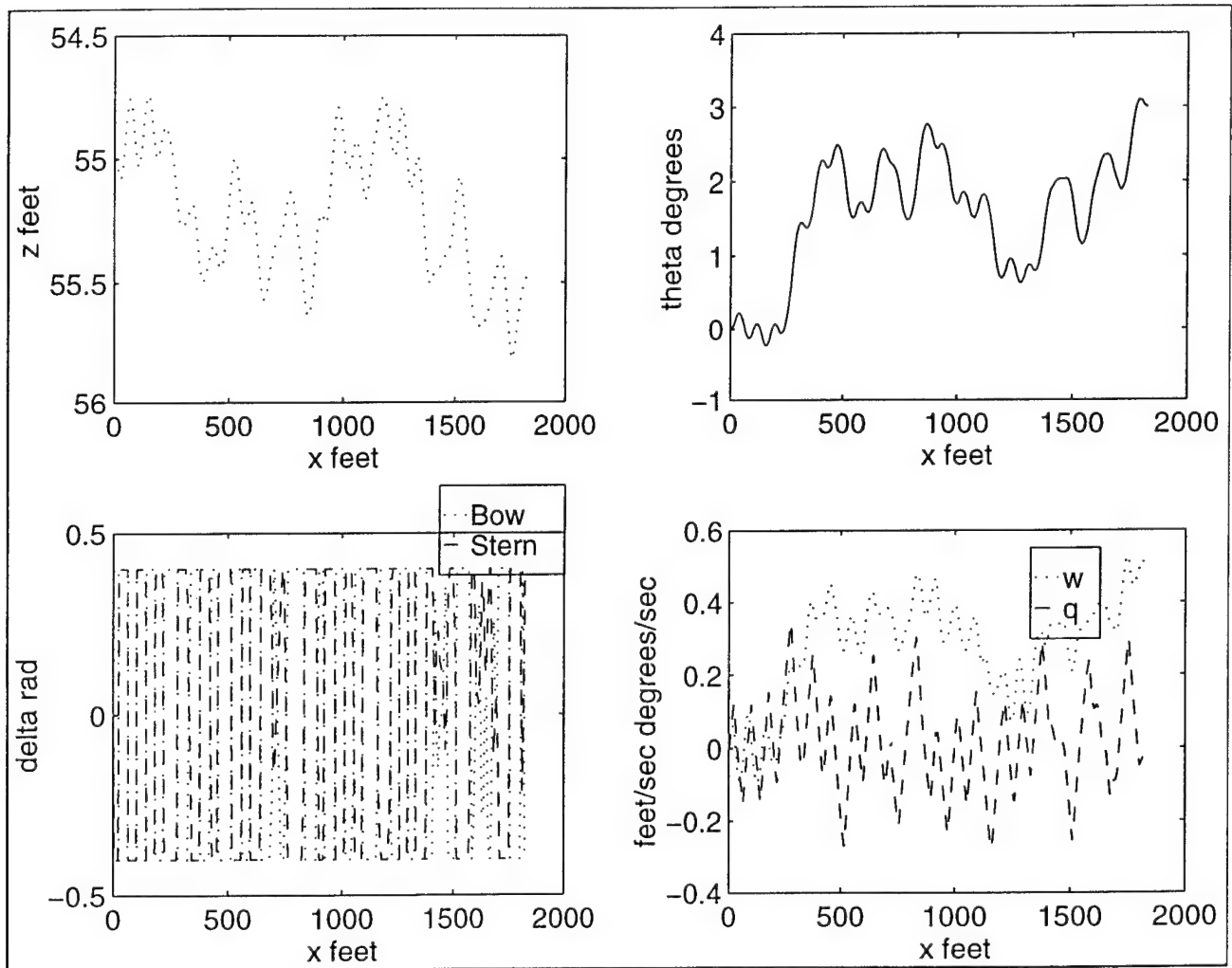


Figure 38. Simulation using sliding mode control with disturbance feedforward

4. Integral control

The sliding mode control law can be augmented with integral control on depth to remove the average depth error. This results in the following control law:

$$\begin{bmatrix} \delta_{bp} \\ \delta_{sp} \end{bmatrix} = \begin{bmatrix} K_{11} & K_{12} & K_{13} & K_{14} & 0 \\ K_{21} & K_{22} & K_{23} & K_{24} & 0 \end{bmatrix} \begin{bmatrix} w - w_{commanded} \\ q - q_{commanded} \\ \theta - \theta_{commanded} \\ z - z_{commanded} \\ z_I \end{bmatrix} + \begin{bmatrix} K_{s11} & K_{s12} \\ K_{s21} & K_{s22} \end{bmatrix} \begin{bmatrix} \eta_1 \text{satsign}\left(\frac{\sigma_1}{\phi_1}\right) \\ \eta_2 \text{satsign}\left(\frac{\sigma_2}{\phi_2}\right) \end{bmatrix} \quad (230)$$

$$\begin{bmatrix} \sigma_1 \\ \sigma_2 \end{bmatrix} = \begin{bmatrix} 1 & 0 \\ 0 & 1 \\ S_{31} & S_{32} \\ S_{41} & S_{42} \\ S_{51} & S_{52} \end{bmatrix}^T \begin{bmatrix} w - w_{commanded} \\ q - q_{commanded} \\ \theta - \theta_{commanded} \\ z - z_{commanded} \\ z_I \end{bmatrix} \quad (231)$$

$$|\delta| \leq \delta_{\max} \quad (232)$$

After a stable set of gains was determined, the controller was optimized to minimize the deviation from the commanded depth. The formal optimization statement is:

Minimize:

$$F(S_{31}, S_{32}, S_{41}, S_{42}, S_{51}, S_{52}, \eta_1, \eta_2, H, F) = \sqrt{\frac{\int_0^{t_f} (z - z_{commanded})^2 dt}{t_f}} \quad (233)$$

Subject to:

$$\text{real}(\text{eigenvalues}(A_{22} - A_{21}S_2^T)) \leq E_{\max} \quad (234)$$

This approach was used for each of the four sea state cases. For sea state three (head seas), the optimized response is shown in Figure 39. The results of the four optimizations are shown in Table 17.

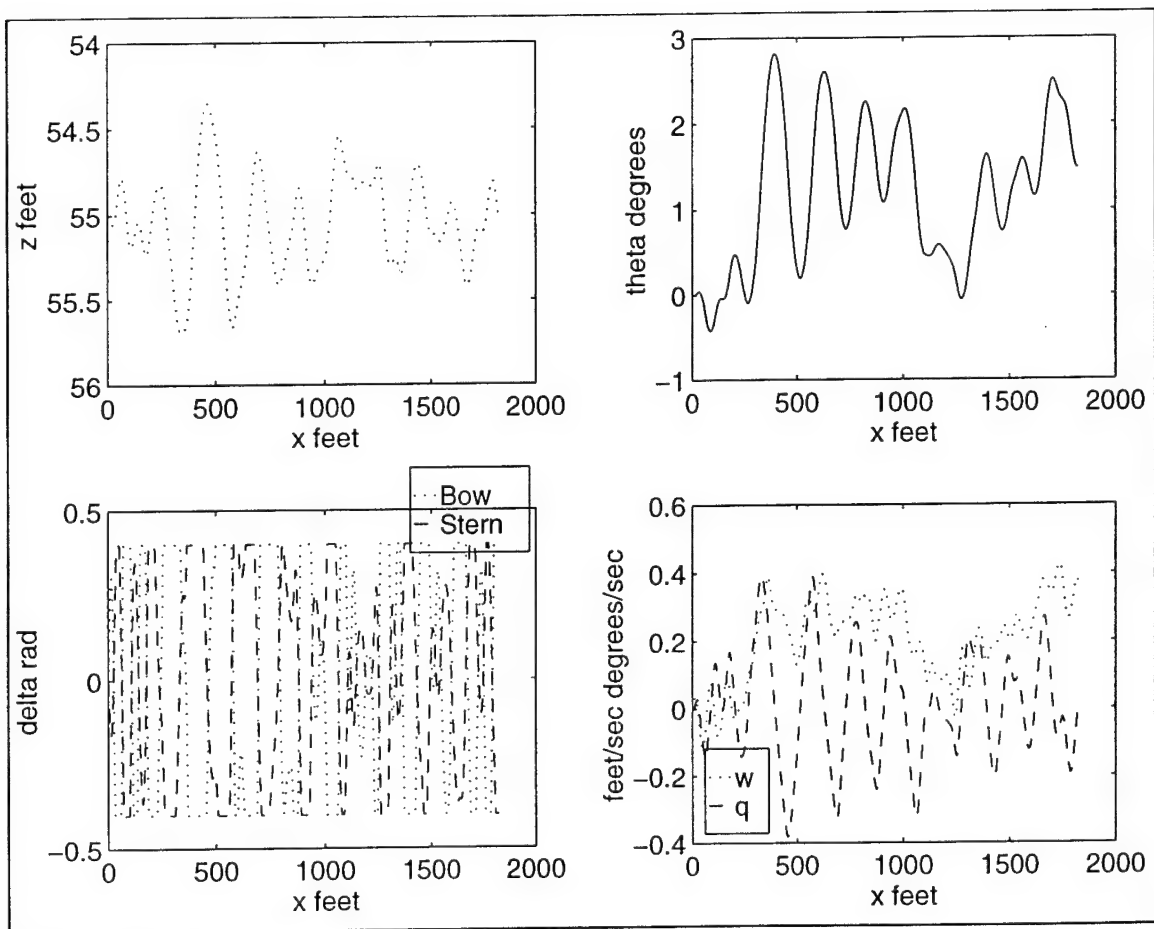


Figure 39. Simulation with sliding mode integral control in sea state three (head seas)

Sea State/Direction	3/head		3/beam		4/head		4/beam	
Initial Values								
S	1 0 -0.1038 0.0179 0.0005	0 1 1.7582 -0.1038 -0.0031	1 0 -0.1038 0.0179 0.0005	0 1 1.7582 -0.1038 -0.0031	1 0 -0.1038 0.0179 0.0005	0 1 1.7582 -0.1038 -0.0031	1 0 -0.1038 0.0179 0.0005	0 1 1.7582 -0.1038 -0.0031
K^T	41.79 -645.08 -426.14 1.268 0	-26.01 437.2 263.63 -0.7835 0	41.79 -645.08 -426.14 1.268 0	-26.01 437.2 263.63 -0.7835 0	41.79 -645.08 -426.14 1.268 0	-26.01 437.2 263.63 -0.7835 0	41.79 -645.08 -426.14 1.268 0	-26.01 437.2 263.63 -0.7835 0
η_1 / η_2	0.05/0.05		0.05/0.05		0.025/0.025		0.05/0.05	
H/F (10 ³ pounds)	20/0		20/0		20/0		20/0	
Mean Depth (feet)	54.82		54.80		55.00		54.73	
RMS Error (feet)	0.4671		1.47		0.707		13.3	
Maximum Error (feet)	1.14		4.23		2.03		31.62	
Sliding surface eigenvalues	-0.8722 + 0.5063i -0.8722 - 0.5063i -0.0316		-0.8722 + 0.5063i -0.8722 - 0.5063i -0.0316		-0.8722 + 0.5063i -0.8722 - 0.5063i -0.0316		-0.8722 + 0.5063i -0.8722 - 0.5063i -0.0316	
Optimized Values								
S	1 0 -0.0106 0.0195 0.0002	0 1 0.2485 -0.0202 -0.0010	1 0 -0.0233 0.0197 0.0001	0 1 0.5120 -0.0152 -0.0007	1 0 -0.0767 0.0118 0.0005	0 1 1.5995 -0.0766 -0.0031	1 0 -0.1428 0.0177 0.0003	0 1 3.7927 -0.0624 0.0006
K^T	7.931 -32.52 -83.24 0.3965 0	-4.920 56.91 50.04 -0.245 0	5.945 -139.4 -63.13 0.271 0	-3.682 123.3 37.51 -0.1681 0	30.73 -580.47 -314.13 1.266 0	-19.18 397.3 194.52 -0.783 0	25.0 -1469.6 -256.2 0.20 0	-15.6 950.0 157.8 0.10 0
η_1 / η_2	0.0468/0.0464		0.0461/0.0453		0.025/0.025		0.0436/0.0553	
H/F (10 ³ pounds)	19.6/-0.1		19.6/0.0		20.0/0.0		19.4/-0.1	
Mean Depth (feet)	54.98		55.01		55.02		55.16	
RMS Error (feet)	0.2345 (50%)		0.713 (49%)		0.693 (98%)		1.47 (11%)	
Maximum Error (feet)	0.789 (69%)		1.90 (45%)		1.92 (95%)		4.15 (13%)	
Sliding surface eigenvalues	-0.1090 + 0.4314i -0.1090 - 0.4314i -0.0500		-0.2418 + 0.2871i -0.2418 - 0.2871i -0.0481		-0.7834 + 0.3260i -0.7834 - 0.3260i -0.0446		-3.6194 -0.1971 0.0061	

Table 17. Optimized sliding mode integral control law results and performance

D. CONCLUDING REMARKS

A comparison between the quality of control achieved by sliding mode control could conclude that the sliding mode control was inferior to state feedback control. This comparison would, however, neglect the added benefits of sliding mode control. The robust character of sliding mode control with the ability to provide reliable control for submarine control given uncertain hydrodynamic coefficients has been demonstrated for the NPS autonomous underwater vehicle program (Hawkinson, 1990).

The sliding mode optimizations did not substantially reduce the control chatter and attendant high actuation rates. Variations of the sliding mode boundary thickness did not alleviate the chatter.

Table 18 gives a summary of the RMS error achieved by each of the sliding mode optimizations. For comparison, it also includes the full state feedback results from Chapter IV. Although these were larger than the corresponding full state feedback cases, the sliding mode control proved to be much more robust in response to step changes in commanded depth. The sliding surface eigenvalues exhibited much more damping than the corresponding cases of full state feedback control. Also, it seemed to provide a more realistic average pitch angle for periscope depth operations.

Sea State/Direction	3/Head	3/Beam	4/Head	4/Beam
Control Scheme				
Full State	0.037	0.2638	0.2683	1.24
Basic sliding mode	0.27	0.84	0.683	1.43
Full State with feedforward	0.0928	0.4121	0.400	0.792
Sliding mode with disturbance feedforward	0.405	1.22	1.01	1.99
Full State integral	0.0414	0.372	0.536	1.96
Sliding mode with integral control	0.2345	0.713	0.693	1.47

Table 18. Optimized RMS error (feet) of sliding mode control and full state feedback

VI. GRAPHICAL DISPLAY

A. INTRODUCTION

In conducting ship control at periscope depth, a submarine diving officer relies on a variety of indications, meters, and some verbal reports to maintain the ship within the required depth band. In addition to the displayed parameters, the ship's control party also has their inertial reference, or "the seat of the pants". It is perhaps the inertial reference which differentiates between great ship's control parties, and the merely adequate.

A submarine diving officer must track status of many ship's systems in addition to ship control. The items which the diving officer must monitor include:

- Mast positions
- Proximity of any portion of the ship to broaching (sail, rudder, mast fairing)
- Water depth (general terms)
- Ship's relationship to the submerged operating envelope
- Trim
- Speed
- Water density
- Ship's evolutions (trash disposal, ventilation, etc.)
- Towed array, floating wire antenna

In many cases, the tracking tool most used is the diving officer's mental picture. Unfortunately, the ability to keep a clear status on many issues varies with fatigue and among individuals. This chapter gives the current conditions of the interface between the diving officer and ship's control, and proposes a different display medium to improve operations.

B. CURRENT DIVING OFFICER INTERFACE

To maintain a complete status, the diving officer has few tools at his disposal. He must rely on looking around at several different panels to get mast status, soundings, and water density while supervising the planesman. If an unplanned event, for example broaching, occurs the only record for reconstruction is the memory of the operators.

The gauges and meters used for ship control, while designed with generally appropriate time constants, are not adaptable for a given circumstance. For the most part, the same indications are used for high speed transit, periscope depth, and tactical operations. Figure 40 and Figure 41 show some of the indications used on board the USS Nautilus (SSN 571). Although Nautilus is now a museum, the design of submarine ship's control panels has not changed significantly.

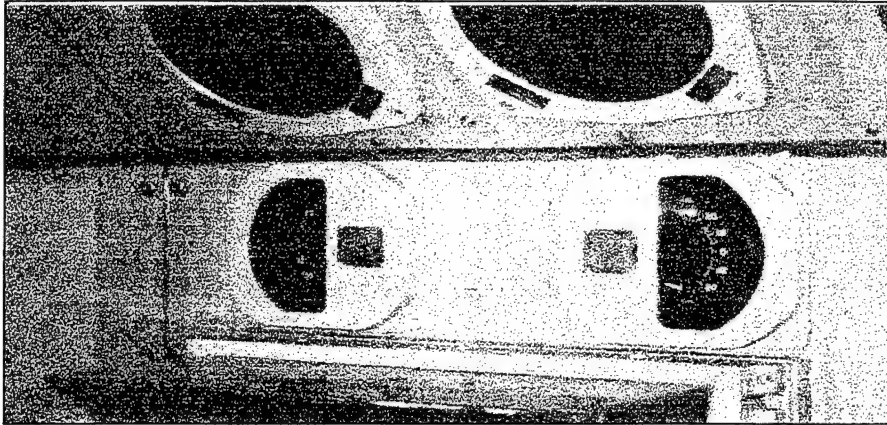


Figure 40. USS Nautilus planes position indications

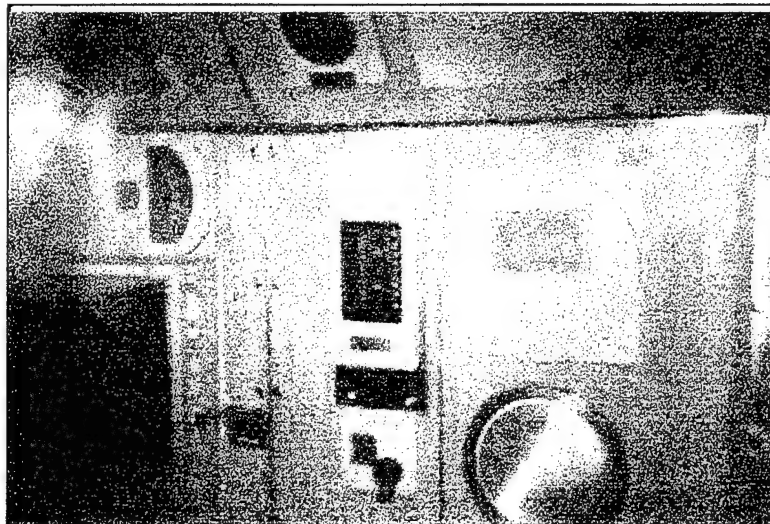


Figure 41. USS Nautilus pitch angle indication

The current system of ship status display is very reliable, with redundant indications for important items and some purely mechanical indicators. It falls short in the area of presenting an integrated status. It is the writers opinion that the display system degrades the performance of the ship's control party. With some parameters not displayed and others not conditioned for the

ship's operating mode, operation near the surface in heavy sea states is extremely difficult. Skilled operators rely upon the existing indications, as well as "the seat of their pants" to maintain depth. Even so, it is a solid accomplishment to keep from broaching during extended periscope depth operations.

Even more complex are operations in shallow water. The proximity to grounding complicates all aspects of ship control. The diving officer must be constantly aware of the water beneath the keel available for casualty recovery. Because nonzero pitch angles will cause one end of the ship to be deeper than indicated, this must also be accounted for.

C. PROPOSED DISPLAY

To incorporate the desired indications in a single display, a radically different approach is taken. Rather than rely on meters and gauges for the state of the ship, a screen is used. Figure 42 shows the proposed display. A crude version of this display was developed using the SIMULINK® Animation Toolbox® (Figure 43).

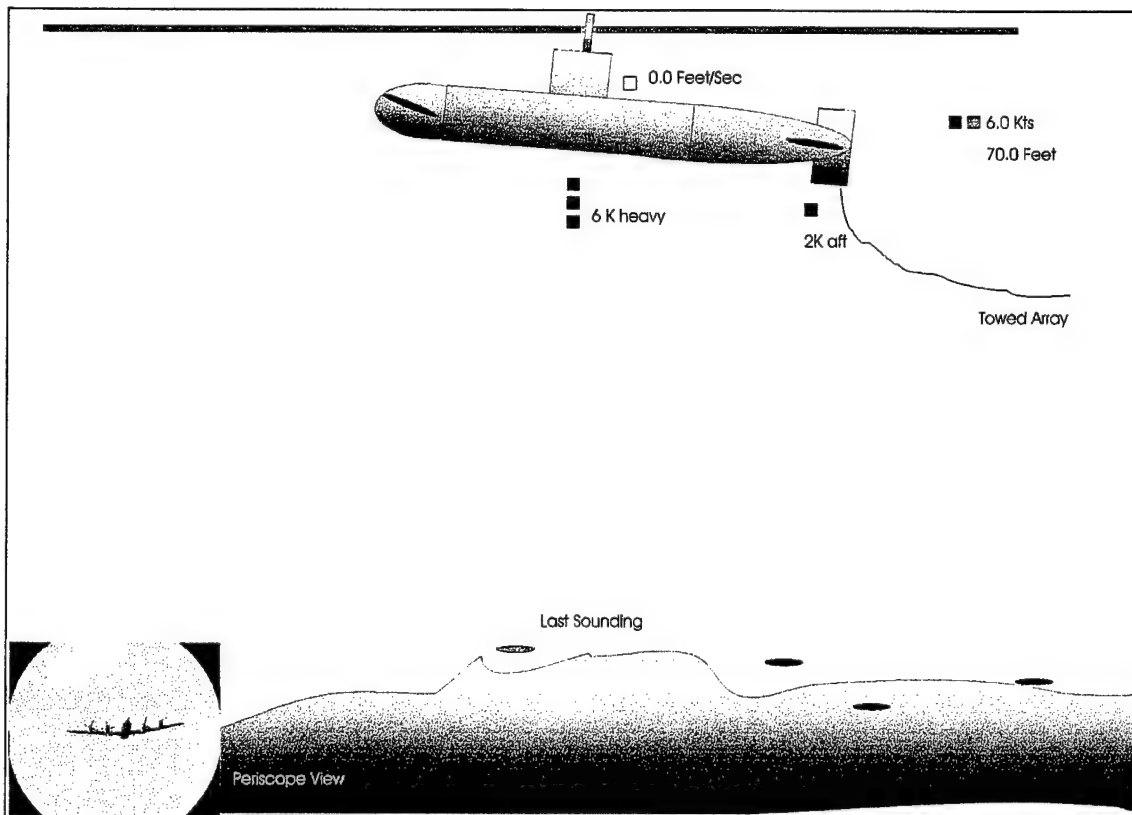


Figure 42. Proposed graphical display of submarine control status

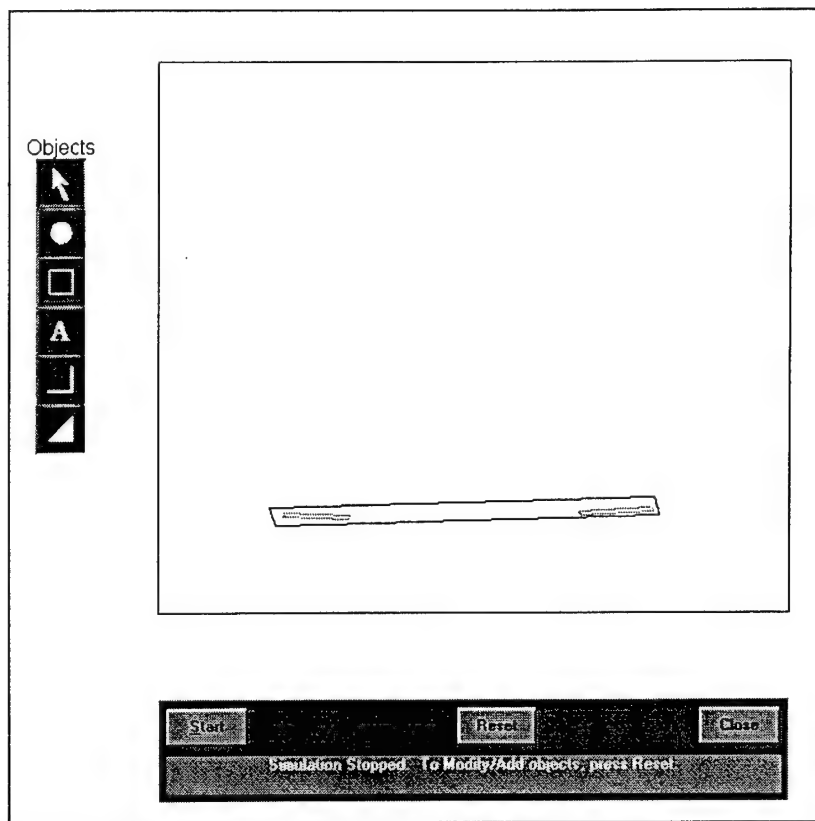


Figure 43. SIMULINK® animation of depth, pitch angle, and planes angles

By integrating the ship status into one display, numerous improvements can be realized. The relationship of the submarine to the bottom and the surface is clearly shown. With the bottom contour information from a database, the diving officer has a continuous sense of the ship's proximity to grounding. In addition as sounding data is obtained, it can be displayed.

The use of a digital display paradigm allows the display to be modified to support different operating modes. Because of the relationship between ship control and safety, the settings would be chosen based on a commanding officer approved doctrine. This would allow the operators to adjust the display system to best fit needs, and adapt it to new circumstances or missions. Alerts and alarms could readily added as the situation warranted.

To assist the diving officer in maintaining status on the wave forces, several bar graphs were added to show the net force that the ship's angle and planes were applying at a given time. These quantities would be filtered to provide a relevant average. Provided the averaging

interval was appropriate, this would queue the diving officer to order trim changes in response to changing environmental conditions.

The periscope video in the bottom left hand corner would provide critical feedback for the dive. This would make the scope's position relative to the surface apparent (another indication of depth), and allow the diving officer to be somewhat aware of the tactical situation. A close or new contact would prompt the diving officer to review mast exposure, which is also on the same display.

Safety of shallow water operations would be enhanced by presenting a clear picture of the ship's relationship to the bottom. During evasive action, the ship's control party and the Officer of the Deck would be working with common knowledge of available water beneath the keel, and the contour ahead of the ship.

Ship's status could be recorded, to allow playback for the reconstruction of unplanned events. Figure 44 shows a possible data architecture to support the display.

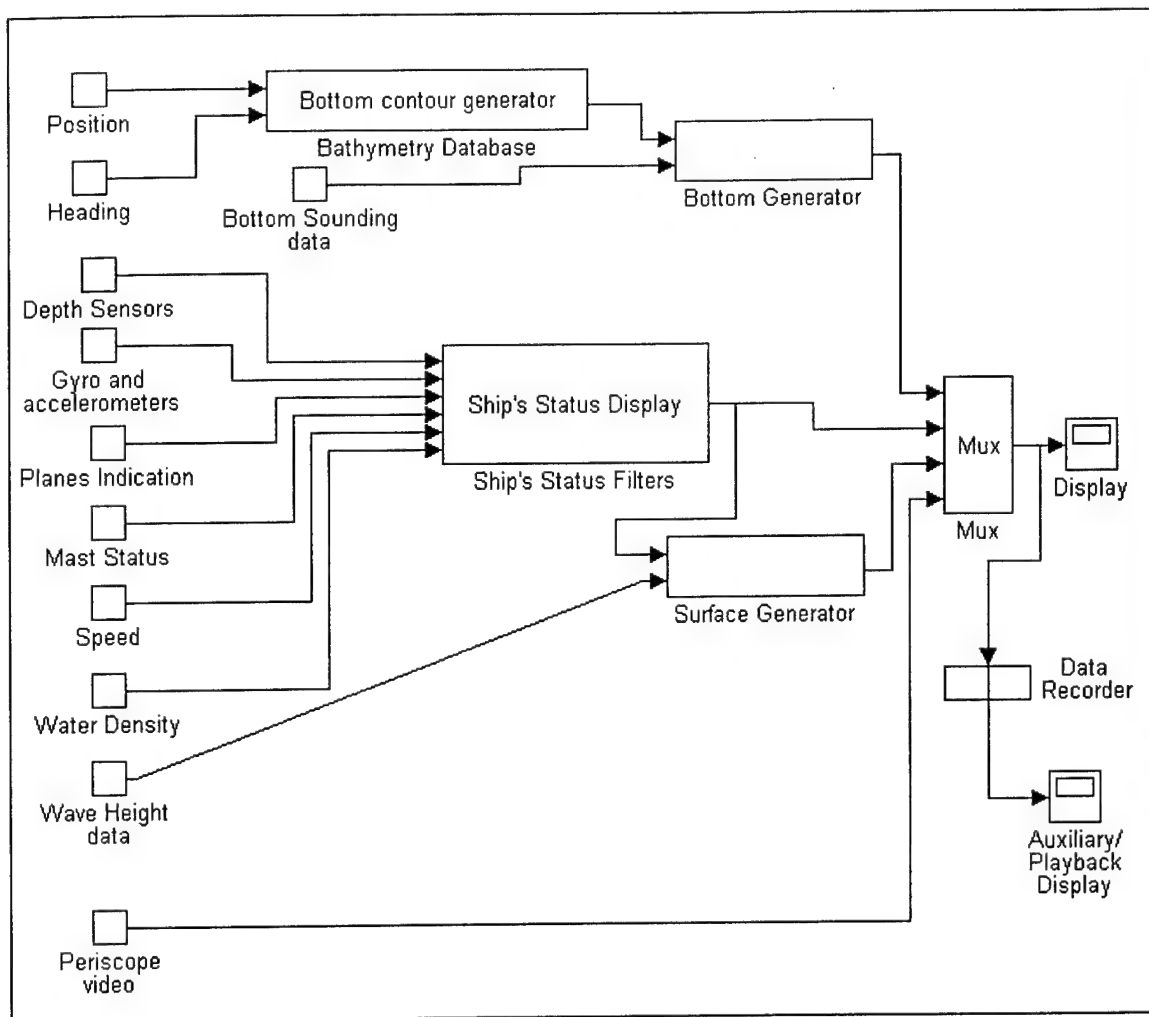


Figure 44. Graphical display data paths

D. CONCLUDING REMARKS

The integration of the pertinent ship parameters in one display should yield dramatic improvements in submarine periscope depth operations. The diving officers improved awareness should reduce fatigue levels, allow for slightly lower speeds for a given sea state (reducing mast feather), and enable a much more complete environmental picture for the ship's control party. This awareness should increase the confidence of the ship's control party during demanding shallow water operations, reduce the likelihood of grounding or broaching, and provide an improved level of support for the Officer of the Deck.

VII. CONCLUSIONS AND RECOMMENDATIONS

A. CONCLUSIONS

As additional states were added to the control laws, the level achieved by the control law optimizations generally improved. For the full state feedback control cases, the depth control exceeded, in the authors experience, what is achievable by manual control.

Ship's control parties use more information about the state of the ship than is available from the explicit indications. Also, the success of the disturbance feedforward control suggests that averaged net force and moment would be of value to the ship's control party.

Sliding mode control provided well damped dynamics, with a robust behavior in response to changes in commanded depth. Although sliding mode control did not achieve the very low RMS errors of full state feedback, the gains which it employed were smaller and more realistic.

B. RECOMMENDATIONS

Although very good depthkeeping was achieved with state feedback control, the optimization schemes used resulted in control surface chatter, and very high control surface rates. To improve the quality of the model and provide more realistic planesman action several features could be added to the control laws and optimization routines:

- Investigate other sea states, speeds and sea directions
- Incorporate control surface rate limits
- Include control surface chatter in the optimization objective functions
- Use of Kalman filtering to provide state estimation and filtering
- Investigate the use of depth rate for feedback control in place of heave

The application of a new display system to an operating submarine is a major undertaking. Recommended steps to find a new manual submarine depth control paradigm are:

- Application of system identification techniques to submarine operating data to investigate the nature of the human control

- Trials of a display onboard an appropriate submarine and or a submarine dive trainer
- Use of recorded submarine operating data to provide for “instant replay” training of ship’s control personnel

LIST OF REFERENCES

- Crook, T. P., "An Initial Assessment of Free Surface Effects on Submerged Bodies", Master's Thesis, Naval Postgraduate School, September 1994.
- Graham, D. and McRuer, D., "Retrospective Essay on Nonlinearities on Aircraft Flight Control", *Journal of Guidance, Control, and Dynamics*, Vol. 14, No. 6, pp. 1089-1098, November 1991.
- Hawkinson, T. D., "Multiple Input Sliding Mode Control for Autonomous Diving and Steering of Underwater Vehicles", Engineer's Thesis, Naval Postgraduate School, December 1990.
- Jackson, H. A., "Fundamentals of Submarine Concept Design", *SNAME paper*, October 1992.
- Musker, A. J., Loader, P. R., and Butcher, M. C., "Simulation of a Submarine Under Waves", *International Shipbuilding Progress*, Vol. 35, pp. 389-410, 1988.
- Ni, S. Y., Zhang, L., and Dai, Y. S., "Hydrodynamic Forces on a Moving Submerged Body in Waves", *International Shipbuilding Progress*, Vol. 41, pp. 95-111, 1994.
- O'Dea, J. F. and Barr, R. A., "Prediction of Wave-Induced First Order Motions and Second Order Forces and Moments During Submarine Maneuvers", *Technical Report 7611-1*, Hydronautics, Inc., September 1976.
- Roddy, R., "Investigations of the Stability and Control Characteristics of Several Configurations of the DARPA SUBOFF (DTRC Model 5470) from Captive-model Experiments", *DTRC/SHD-1298-08*, David Taylor Research Center, 1990.
- Sarpkaya, T. and Isaacson M., *Mechanics of Wave Forces on Offshore Structures*, Van Nostrand Reinhold Company, Inc., 1981.
- Smith, N.C., Crane, J.W., and Summey, D.C., "SDV Simulator Hydrodynamic Coefficients", *Naval Coastal Systems Center Technical Memorandum 231-78*, June 1978.
- Utkin, V.I., "Variable Structure Systems with Sliding Modes", *IEEE Transactions on Automatic Control*, Vol. AC-22, No. 2, April 1977.
- Vanderplaats, G. N., *Numerical Optimization Techniques for Engineering Design*, McGraw-Hill, Inc., 1984.

APPENDIX A

All computer code and SIMULINK® models used in this thesis are available from Professor Fotis Papoulias, Naval Postgraduate School. The computer programs and SIMULINK® models used were:

Programs:

SUBOFF.M¹- initializes SUBOFF hydrodynamic coefficients

AXNL.M¹- performs nonlinear $Ax + E[qq;wq]$ calculation

SMLQR¹.M- determines MIMO sliding mode control law using Utkin's method (LQR)

WF_INI.M- reads wave data files, processes

WFORCE.M- calculates wave forces for a given depth and time

SB_INI.M- initializes model variables for MIMO vertical plane submarine model

SBI_INI.M- initializes model variables for MIMO vertical plane submarine model with integral depth control

SB_SM.M- calculates MIMO SM control law from Q matrix

SB_SS.M- calculates MIMO SM control law from sliding surface

SB_SMFF.M- determines the feed forward matrix for a given sliding mode control law

SB_PD.M- state feedback control law

SB_Pdff.M- determines the feed forward matrix for a state feedback control law

OBJ2.M - Objective function for pitch / depth feedback optimizations

OPT2A.M- Optimization program for OBJ2.M and sea state three (head seas)

OPT2B.M- Optimization program for OBJ2.M and sea state three (beam seas)

OPT2C.M- Optimization program for OBJ2.M and sea state four (head seas)

OPT2D.M- Optimization program for OBJ2.M and sea state four (beam seas)

OBJ2ff.M - Objective function for pitch / depth feedback with disturbance feedforward optimizations

OPT2FFA.M- Optimization program for OBJ2FF.M and sea state three (head seas)

OPT2FFB.M- Optimization program for OBJ2FF.M and sea state three (beam seas)

OPT2FFC.M- Optimization program for OBJ2FF.M and sea state four (head seas)

¹ Given after list of programs

OPT2FFD.M- Optimization program for OBJ2FF.M and sea state four (beam seas)

OBJ2I.M - Objective function for pitch / depth feedback with integral depth control optimizations

OPT2IA.M- Optimization program for OBJ2I.M and sea state three (head seas)

OPT2IB.M- Optimization program for OBJ2I.M and sea state three (beam seas)

OPT2IC.M- Optimization program for OBJ2I.M and sea state four (head seas)

OPT2ID.M- Optimization program for OBJ2I.M and sea state four (beam seas)

OBJ3.M - Objective function for full state partial distribution feedback optimizations

OPT3A.M- Optimization program for OBJ3.M and sea state three (head seas)

OPT3B.M- Optimization program for OBJ3.M and sea state three (beam seas)

OPT3C.M- Optimization program for OBJ3.M and sea state four (head seas)

OPT3D.M- Optimization program for OBJ3.M and sea state four (beam seas)

OBJ3FF.M - Objective function for full state feedback with disturbance feedforward optimizations

OPT3FFA.M- Optimization program for OBJ3FF.M and sea state three (head seas)

OPT3FFB.M- Optimization program for OBJ3FF.M and sea state three (beam seas)

OPT3FFC.M- Optimization program for OBJ3FF.M and sea state four (head seas)

OPT3FFD.M- Optimization program for OBJ3FF.M and sea state four (beam seas)

OBJ3I.M - Objective function for full state feedback with integral depth control optimizations

OPT3IA.M- Optimization program for OBJ3I.M and sea state three (head seas)

OPT3IB.M- Optimization program for OBJ3I.M and sea state three (beam seas)

OPT3IC.M- Optimization program for OBJ3I.M and sea state four (head seas)

OPT3ID.M- Optimization program for OBJ3I.M and sea state four (beam seas)

OBJ3.M - Objective function for full state feedback optimizations

OPT4A.M- Optimization program for OBJ4.M and sea state three (head seas)

OPT4B.M- Optimization program for OBJ4.M and sea state three (beam seas)

OPT4C.M- Optimization program for OBJ4.M and sea state four (head seas)

OPT4D.M- Optimization program for OBJ4.M and sea state four (beam seas)

OBJ4FF.M - Objective function for full state partial distribution feedback with disturbance feedforward optimizations

OPT4FFA.M- Optimization program for OBJ4FF.M and sea state three (head seas)

OPT4FFB.M- Optimization program for OBJ4FF.M and sea state three (beam seas)

OPT4FFC.M- Optimization program for OBJ4FF.M and sea state four (head seas)
 OPT4FFD.M- Optimization program for OBJ4FF.M and sea state four (beam seas)
 OBJ4I.M - Objective function for full state partial distribution feedback with integral depth control optimizations
 OPT4IA.M- Optimization program for OBJ4I.M and sea state three (head seas)
 OPT4IB.M- Optimization program for OBJ4I.M and sea state three (beam seas)
 OPT4IC.M- Optimization program for OBJ4I.M and sea state four (head seas)
 OPT4ID.M- Optimization program for OBJ4I.M and sea state four (beam seas)
 OBJ7.M - Objective function for sliding mode control optimizations
 OPT7A.M- Optimization program for OBJ7.M and sea state three (head seas)
 OPT7B.M- Optimization program for OBJ7.M and sea state three (beam seas)
 OPT7C.M- Optimization program for OBJ7.M and sea state four (head seas)
 OPT7D.M- Optimization program for OBJ7.M and sea state four (beam seas)
 OBJ7FF.M - Objective function for sliding mode control with disturbance feedforward optimizations
 OPT7FFA.M- Optimization program for OBJ7FF.M and sea state three (head seas)
 OPT7FFB.M- Optimization program for OBJ7FF.M and sea state three (beam seas)
 OPT7FFC.M- Optimization program for OBJ7FF.M and sea state four (head seas)
 OPT7FFD.M- Optimization program for OBJ7FF.M and sea state four (beam seas)
 OBJ7I.M - Objective function for sliding mode control with integral depth control optimizations
 OPT7IA.M- Optimization program for OBJ7I.M and sea state three (head seas)
 OPT7IB.M- Optimization program for OBJ7I.M and sea state three (beam seas)
 OPT7IC.M- Optimization program for OBJ7I.M and sea state four (head seas)
 OPT7ID.M- Optimization program for OBJ7I.M and sea state four (beam seas)
 OBJ7.M - Objective function for full state feedback optimizations

Models:

SMSW.M- MIMO sliding mode control submarine control model, with wave forces and trim
 SMSWFF.M- Same as SMSW.M, with disturbance feedforward
 SMT.M- used for determining steady state response, does not return the x state
 PDSW.M- MIMO state feedback control submarine control model, with wave forces and trim

PDSWFF.M- Same as PDSW.M, with disturbance feedforward
PDT.M- used for determining steady state response, does not return the x state

Wave Force Data files:

For the first order motions / second order forces, each displacement / force is given in terms of a complex number.

Wave spectral data files

[wave frequency (rad/sec), $S(\omega)$ (), amplitude (feet), phase (rad)]

SPEC_A.TXT

SPEC_B.TXT

SPEC_C.TXT

SPEC_D.TXT

First order motions

[ω (rad/sec), $\omega_{\text{encounter}}$ (rad/sec), surge, sway, heave, pitch, yaw, roll]

LMOT_A.TXT

LMOT_B.TXT

LMOT_C.TXT

LMOT_D.TXT

Second order forces

[ω_1 (rad/sec), ω_2 (rad/sec), F_x , F_y , F_z , M_x , M_y , M_z]

FORC_A.TXT

FORC_B.TXT

FORC_C.TXT

FORC_D.TXT

SUBOFF.M

function [A,B,MMI,Emat, D,WS]=suboff(U);

% SDV hydrodynamic data, TM 231-78 page 6

ff=2; %fudge factor to make planes authority realistic for 300 ft sub

g=32.2; %

L=300; % feet

p=1.94; % slug/ft³;

m = 0.018296*0.5*p*L³;

Iz = 0.001084*0.5*p*L⁵;

Iy = 0.00108*0.5*p*L⁵;

mxg = -0.127467E-4;

W=m*g;

zgb=1; % feet

xgb=0; % feet

Mqdot = -0.000860*0.5*p*L⁵;

Mwdot = -0.000561*0.5*p*L⁴;

Mq = -0.003702*0.5*p*L⁴*U;

Mw = 0.010324*0.5*p*L³*U;

Mds = -ff*0.002409*0.5*p*L³*U²;

Mdb = -Mds/4;

Zqdot = -0.000633*0.5*p*L⁴;

Zwdot = -0.014529*0.5*p*L³;

Zq = -0.007545*0.5*p*L³*U;

Zw = -0.013910*0.5*p*L²*U;

Zds = -ff*0.005603*0.5*p*L²*U²;

Zdb = Zds/2;

% define mass matrix, compute mass matrix inverse

```

mm=eye(4);
mm(1,1)=m-Zwdot;
mm(1,2)=-Zqdot;
mm(2,1)=-Mwdot;
mm(2,2)=Iy-Mqdot;

A=zeros(4,4);
A(1,1)=Zw;
A(1,2)=m*U+Zq;
A(2,1)=Mw;
A(2,2)=Mq;
A(2,3)=-zgb*W;
A(3,2)=1;
A(4,1)=1;
A(4,3)=-U;

B=[ Zdb Zds;Mdb Mds;0 0;0 0];

MMI=inv(mm);

A=MMI*A;
B=MMI*B;
Emat=MMI(1:2,1:2)*[m*zgb,0;0,-m*zgb];

% diameter and surface area calculation

D=L/8.575;

WS=67.651*(L/13.9792)^2;

```

AXNLM

```
function ax=axnl(x)
```

```
global Amat Emat
```

```
n=max(size(x));
```

```
a=Amat;
```

```
a(4,1)=Amat(4,1)*cos(x(3));
```

```
x(3)=sin(x(3));
```

```
ax=a*x;
```

```
ax(1:2)=ax(1:2)+Emat*[x(2)^2;x(2)*x(1)];
```

SMLQR.M

```
function [k,s,ks,e]=smlqr(a,b,q)

%    [k,s,ks,e]=smlqr(a,b,q) determines the sliding
%    mode control law for the system
%     $\dot{x}=a*x+b*u$  where
%     $u=-kx-kn*satsgn(\sigma)$  and
%     $\sigma=s*x$ .  $q$  is a positive definite
%    symmetric weighting matrix
%    used in assigning error weights
%    (LQR) to the states. Uses Utkin's method
%    as detailed in Hawkinson pp10-17
```

```
[n,m]=size(b);
```

```
% do transformation if required
if norm(b(m+1:n,1:m))>eps^0.5
```

```
    [t,b1]=qr(b);
    b1=b1(1:m,1:m);
    t=t';
```

```
else
```

```
    t=eye(n);
    b1=b(1:m,1:m);
```

```
end
```

```
q=t*q*t';
a=t*a*t';
```

```
q11=q(1:m,1:m);
q12=q(1:m,m+1:n);
q21=q(m+1:n,1:m);
q22=q(m+1:n,m+1:n);
```

```
a11=a(1:m,1:m);
a12=a(1:m,m+1:n);
a21=a(m+1:n,1:m);
a22=a(m+1:n,m+1:n);
```

```
as=a22-a21*inv(q11)*q12;
qs=q22-q21*inv(q11)*q12;
```

```
kt=are(as,a21*inv(q11)*(a21') ,qs);
```

```
c2=(inv(q11)*(q12+a21')*kt)';
```

```
k=-[inv(b1)*(a11+c2'*a21),inv(b1)*(a12+c2'*a22)]*t;
```

```
s=rref([eye(m); c2]'*t)';
```

```
ks=-inv(s'*b);
```

```
e=eig([a+[b1;zeros(n-m,m)]*k*t']);
```


APPENDIX B

MAPLE® Solutions

Determination of MIMO state feedback control steady state

Determination of MIMO sliding mode control steady state

This maple script determines the steady state response in the vertical plane using MIMO state feedback control. Constant disturbances are assumed and the linear equations of motion applied to find the steady state depth error. It is also assumed that both control deflections are less than maximum.

EQ1 and EQ2 are the heave and pitch linear equations of motion
 > EQ1:=(a11*w*u+a13*theta+b11*u^2*d1+b12*u^2*d2)+Fd;

$$EQ1 := a11 w u + a13 \theta + b11 u^2 d1 + b12 u^2 d2 + Fd$$

> EQ2 :=(a21*w*u+a23*theta+b21*u^2*d1+b22*u^2*d2)+Md;

$$EQ2 := a21 w u + a23 \theta + b21 u^2 d1 + b22 u^2 d2 + Md$$

> readlib(isolate);

> w := theta*u;

$$w := \theta u$$

The linear state feedback laws at steady state are:

> d1 := K11*w+K13*theta+K14*z;

$$d1 := K11 \theta u + K13 \theta + K14 z$$

> d2 := K21*w+K23*theta+K14*z;

$$d2 := K21 \theta u + K23 \theta + K14 z$$

After the application of the control laws, the equations of heavy and pitch become:

> EQ1=0;

$$a11 \theta u^2 + a13 \theta + b11 u^2 (K11 \theta u + K13 \theta + K14 z) + b12 u^2 (K21 \theta u + K23 \theta + K14 z) + Fd = 0$$

> EQ2=0;

$$a21 \theta u^2 + a23 \theta + b21 u^2 (K11 \theta u + K13 \theta + K14 z) + b22 u^2 (K21 \theta u + K23 \theta + K14 z) + Md = 0$$

Remove z from EQ1 and EQ2

> F1:=coeff(collect(expand(EQ1),z),z,1);

$$F1 := b12 u^2 K14 + b11 u^2 K14$$

> F2:=coeff(collect(expand(EQ2),z),z,1);

$$F2 := b22 u^2 K14 + b21 u^2 K14$$

> EQ3:=simplify(EQ1-EQ2*F1/F2);

$$EQ3 := (a11 \theta u^2 b22 + a11 \theta u^2 b21 + b11 u^3 K11 \theta b22 + b11 u^2 K13 \theta b22 + a13 \theta b22 + a13 \theta b21 - a23 \theta b11 + Fd b22 + Fd b21 - Md b12 - Md b11 + b12 u^3 K21 \theta b21 + b12 u^2 K23 \theta b21 - a21 \theta u^2 b12 - a21 \theta u^2 b11 - b21 u^3 K11 \theta b12 - b21 u^2 K13 \theta b12 - b22 u^3 K21 \theta b11 - b22 u^2 K23 \theta b11 - a23 \theta b12) / (b22 + b21)$$

> isolate(EQ3,theta);

$$\theta = (-Fd b22 - Fd b21 + Md b12 + Md b11) / (a11 u^2 b22 + a11 u^2 b21 + b11 u^3 K11 b22 + b11 u^2 K13 b22 + a13 b22 + a13 b21 - a23 b11 + b12 u^3 K21 b21 + b12 u^2 K23 b21)$$

$$-a21 u^2 b12 - a21 u^2 b11 - b21 u^3 K11 b12 - b21 u^2 K13 b12 - b22 u^3 K21 b11 - b22 u^2 K23 b11 - a23 b12)$$

Find the steady state value of theta by setting EQ3=0

> thetass:=coeff(collect(EQ3,theta),theta,0)/coeff(collect(EQ3,theta),theta,1);

$$\text{thetass} := (Fd b22 + Fd b21 - Md b12 - Md b11) / (a11 u^2 b22 + a11 u^2 b21 + b11 u^3 K11 b22 + b11 u^2 K13 b22 + a13 b22 + a13 b21 - a23 b11 + b12 u^3 K21 b21 + b12 u^2 K23 b21 - a21 u^2 b12 - a21 u^2 b11 - b21 u^3 K11 b12 - b21 u^2 K13 b12 - b22 u^3 K21 b11 - b22 u^2 K23 b11 - a23 b12)$$

Substitute thetass into EQ1 and solve for steady state z

> temp:=coeff(collect(EQ1,z),z,0)/coeff(collect(EQ1,z),z,1);

$$\text{temp} := \frac{a11 \theta u^2 + a13 \theta + b11 u^2 (K11 \theta u + K13 \theta) + b12 u^2 (K21 \theta u + K23 \theta) + Fd}{b12 u^2 K14 + b11 u^2 K14}$$

> zss :=

> coeff(collect(temp,theta),theta,1)*thetass+coeff(collect(temp,theta),theta,0)

> ;

$$\begin{aligned} \text{zss} := & (a13 + b11 u^2 (K11 u + K13) + b12 u^2 (K21 u + K23) + a11 u^2) \\ & (Fd b22 + Fd b21 - Md b12 - Md b11) / ((b12 u^2 K14 + b11 u^2 K14) (a11 u^2 b22 \\ & + a11 u^2 b21 + b11 u^3 K11 b22 + b11 u^2 K13 b22 + a13 b22 + a13 b21 - a23 b11 \\ & + b12 u^3 K21 b21 + b12 u^2 K23 b21 - a21 u^2 b12 - a21 u^2 b11 - b21 u^3 K11 b12 \\ & - b21 u^2 K13 b12 - b22 u^3 K21 b11 - b22 u^2 K23 b11 - a23 b12)) \\ & + \frac{Fd}{b12 u^2 K14 + b11 u^2 K14} \end{aligned}$$

Determine the coefficients C1 and C2 such that zss=C1*Fd+C2*Md

> C1:=simplify(coeff(collect(expand(zss),Fd),Fd,1));

$$\begin{aligned} C1 := & (2 a11 u^2 b22 + 2 a11 u^2 b21 - a21 u^2 b12 - a21 u^2 b11 - a23 b12 + 2 a13 b21 \\ & - a23 b11 + 2 a13 b22 + 2 b11 u^3 K11 b22 + 2 b11 u^2 K13 b22 - b21 u^3 K11 b12 \\ & + 2 b12 u^3 K21 b21 + 2 b12 u^2 K23 b21 - b22 u^3 K21 b11 - b22 u^2 K23 b11 \\ & - b21 u^2 K13 b12 + b12 u^2 K23 b22 + b11 u^3 K11 b21 + b12 u^3 K21 b22 + b11 u^2 K13 b21) \\ & / (u^2 K14 (b12 + b11) (a11 u^2 b22 + a11 u^2 b21 + b11 u^3 K11 b22 + b11 u^2 K13 b22 \\ & + a13 b22 + a13 b21 - a23 b11 + b12 u^3 K21 b21 + b12 u^2 K23 b21 - a21 u^2 b12 \\ & - a21 u^2 b11 - b21 u^3 K11 b12 - b21 u^2 K13 b12 - b22 u^3 K21 b11 - b22 u^2 K23 b11 \\ & - a23 b12)) \end{aligned}$$

> C2:=simplify(coeff(collect(expand(zss),Md),Md,1));

$$C2 := - (a13 + b11 u^3 K11 + b11 u^2 K13 + b12 u^3 K21 + b12 u^2 K23 + a11 u^2) / (($$

$$\begin{aligned}
& a_{11} u^2 b_{22} + a_{11} u^2 b_{21} + b_{11} u^3 K_{11} b_{22} + b_{11} u^2 K_{13} b_{22} + a_{13} b_{22} + a_{13} b_{21} - a_{23} b_{11} \\
& + b_{12} u^3 K_{21} b_{21} + b_{12} u^2 K_{23} b_{21} - a_{21} u^2 b_{12} - a_{21} u^2 b_{11} - b_{21} u^3 K_{11} b_{12} \\
& - b_{21} u^2 K_{13} b_{12} - b_{22} u^3 K_{21} b_{11} - b_{22} u^2 K_{23} b_{11} - a_{23} b_{12} \big) u^2 K_{14} \big)
\end{aligned}$$

Check that $zss = C_1 * Fd + C_2 * Md$
 $> eq6 := \text{simplify}(zss - C_1 * Fd - C_2 * Md);$

$eq6 := 0$

This maple script determines the steady state response in the vertical plane with basic MIMO sliding mode control. Constant disturbances are assumed and the linear equations of motion applied to find the steady state depth error. It is also assumed that both control deflections are less than maximum and that neither sliding surface is saturated.

EQ1 and EQ2 are the heave and pitch linear equations of motion

> EQ1:=(a11*w*u+a13*theta+b11*u^2*d1+b12*u^2*d2)+Fd;

$$EQ1 := a11 w u + a13 \theta + b11 u^2 d1 + b12 u^2 d2 + Fd$$

> EQ2 :=(a21*w*u+a23*theta+b21*u^2*d1+b22*u^2*d2)+Md;

$$EQ2 := a21 w u + a23 \theta + b21 u^2 d1 + b22 u^2 d2 + Md$$

> readlib(isolate):

> w := theta*u;

$$w := \theta u$$

The linear state feedback laws at steady state are:

> d1 := K11*w+K13*theta+Ks11*etal*sigma1/phi1+Ks12*eta2*sigma2/phi2;

$$d1 := K11 \theta u + K13 \theta + \frac{Ks11 \text{ etal } \sigma1}{\phi1} + \frac{Ks12 \text{ eta2 } \sigma2}{\phi2}$$

> d2 := K21*w+K23*theta+Ks21*etal*sigma1/phi1+Ks22*eta2*sigma2/phi2;

$$d2 := K21 \theta u + K23 \theta + \frac{Ks21 \text{ etal } \sigma1}{\phi1} + \frac{Ks22 \text{ eta2 } \sigma2}{\phi2}$$

> sigma1:=S11*w+S13*theta+S14*z;

$$\sigma1 := S11 \theta u + S13 \theta + S14 z$$

> sigma2:=S21*w+S23*theta+S24*z;

$$\sigma2 := S21 \theta u + S23 \theta + S24 z$$

After the application of the control laws, the equations of heavy and pitch become:

> EQ1=0;

$$a11 \theta u^2 + a13 \theta + b11 u^2 \left(K11 \theta u + K13 \theta + \frac{Ks11 \text{ etal } (S11 \theta u + S13 \theta + S14 z)}{\phi1} + \frac{Ks12 \text{ eta2 } (S21 \theta u + S23 \theta + S24 z)}{\phi2} \right) + b12 u^2 \left(K21 \theta u + K23 \theta + \frac{Ks21 \text{ etal } (S11 \theta u + S13 \theta + S14 z)}{\phi1} + \frac{Ks22 \text{ eta2 } (S21 \theta u + S23 \theta + S24 z)}{\phi2} \right) + Fd = 0$$

> EQ2=0;

$$a21 \theta u^2 + a23 \theta + b21 u^2 \left(K11 \theta u + K13 \theta + \frac{Ks11 \text{ etal } (S11 \theta u + S13 \theta + S14 z)}{\phi1} + \frac{Ks12 \text{ eta2 } (S21 \theta u + S23 \theta + S24 z)}{\phi2} \right) + b22 u^2 \left(K21 \theta u + K23 \theta + \frac{Ks21 \text{ etal } (S11 \theta u + S13 \theta + S14 z)}{\phi1} + \frac{Ks22 \text{ eta2 } (S21 \theta u + S23 \theta + S24 z)}{\phi2} \right) + Md = 0$$

Remove z from EQ1 and EQ2

> F1:=coeff(collect(expand(EQ1),z),z,1);

$$F1 := \frac{b11 u^2 Ks12 eta2 S24}{phi2} + \frac{b11 u^2 Ks11 etal S14}{phil} + \frac{b12 u^2 Ks22 eta2 S24}{phi2} + \frac{b12 u^2 Ks21 etal S14}{phil}$$

> F2:=coeff(collect(expand(EQ2),z),z,1);

$$F2 := \frac{b21 u^2 Ks12 eta2 S24}{phi2} + \frac{b21 u^2 Ks11 etal S14}{phil} + \frac{b22 u^2 Ks22 eta2 S24}{phi2} + \frac{b22 u^2 Ks21 etal S14}{phil}$$

> EQ3:=simplify(EQ1-EQ2*F1/F2);

$$\begin{aligned} EQ3 := & - \left(-b11 u^3 Ks11 etal S11 \theta b22 Ks22 eta2 S24 - b11 u^3 K11 \theta phil b22 Ks22 eta2 S24 \right. \\ & - b11 u^2 Ks11 etal S13 \theta b22 Ks22 eta2 S24 - b11 u^3 Ks12 eta2 S21 \theta b22 Ks21 etal S14 \\ & - b11 u^2 Ks12 eta2 S23 \theta b22 Ks21 etal S14 - b11 u^3 K11 \theta phi2 b22 Ks21 etal S14 \\ & - b11 u^2 K13 \theta phil b22 Ks22 eta2 S24 - b11 u^2 K13 \theta phi2 b22 Ks21 etal S14 \\ & - a11 \theta u^2 phil b21 Ks12 eta2 S24 - a11 \theta u^2 phi2 b21 Ks11 etal S14 \\ & - a11 \theta u^2 phil b22 Ks22 eta2 S24 - a11 \theta u^2 phi2 b22 Ks21 etal S14 \\ & - a13 \theta phil b21 Ks12 eta2 S24 - a13 \theta phi2 b21 Ks11 etal S14 \\ & - a13 \theta phil b22 Ks22 eta2 S24 - a13 \theta phi2 b22 Ks21 etal S14 \\ & - b12 u^3 K21 \theta phil b21 Ks12 eta2 S24 - b12 u^3 K21 \theta phi2 b21 Ks11 etal S14 \\ & - b12 u^2 K23 \theta phil b21 Ks12 eta2 S24 - b12 u^2 K23 \theta phi2 b21 Ks11 etal S14 \\ & - b12 u^3 Ks21 etal S11 \theta b21 Ks12 eta2 S24 - b12 u^2 Ks21 etal S13 \theta b21 Ks12 eta2 S24 \\ & - b12 u^3 Ks22 eta2 S21 \theta b21 Ks11 etal S14 - b12 u^2 Ks22 eta2 S23 \theta b21 Ks11 etal S14 \\ & - Fd phil b21 Ks12 eta2 S24 - Fd phi2 b21 Ks11 etal S14 - Fd phil b22 Ks22 eta2 S24 \\ & - Fd phi2 b22 Ks21 etal S14 + a21 \theta u^2 phil b11 Ks12 eta2 S24 \\ & + a21 \theta u^2 phi2 b11 Ks11 etal S14 + a21 \theta u^2 phil b12 Ks22 eta2 S24 \\ & + a21 \theta u^2 phi2 b12 Ks21 etal S14 + a23 \theta phil b11 Ks12 eta2 S24 \\ & + a23 \theta phi2 b11 Ks11 etal S14 + a23 \theta phil b12 Ks22 eta2 S24 \\ & + a23 \theta phi2 b12 Ks21 etal S14 + b21 u^3 K11 \theta phil b12 Ks22 eta2 S24 \\ & + b21 u^3 K11 \theta phi2 b12 Ks21 etal S14 + b21 u^2 K13 \theta phil b12 Ks22 eta2 S24 \\ & + b21 u^2 K13 \theta phi2 b12 Ks21 etal S14 + b21 u^3 Ks11 etal S11 \theta b12 Ks22 eta2 S24 \\ & + b21 u^2 Ks11 etal S13 \theta b12 Ks22 eta2 S24 + b21 u^3 Ks12 eta2 S21 \theta b12 Ks21 etal S14 \\ & + b21 u^2 Ks12 eta2 S23 \theta b12 Ks21 etal S14 + b22 u^3 K21 \theta phil b11 Ks12 eta2 S24 \\ & \left. + b22 u^3 K21 \theta phi2 b11 Ks11 etal S14 + b22 u^2 K23 \theta phil b11 Ks12 eta2 S24 \right) \end{aligned}$$

$$\begin{aligned}
& + b22 u^2 K23 \theta \text{ phi2 } b11 Ks11 \text{ etal } S14 + b22 u^3 Ks21 \text{ etal } S11 \theta b11 Ks12 \text{ eta2 } S24 \\
& + b22 u^2 Ks21 \text{ etal } S13 \theta b11 Ks12 \text{ eta2 } S24 + b22 u^3 Ks22 \text{ eta2 } S21 \theta b11 Ks11 \text{ etal } S14 \\
& + b22 u^2 Ks22 \text{ eta2 } S23 \theta b11 Ks11 \text{ etal } S14 + Md \text{ phi1 } b11 Ks12 \text{ eta2 } S24 \\
& + Md \text{ phi2 } b11 Ks11 \text{ etal } S14 + Md \text{ phi1 } b12 Ks22 \text{ eta2 } S24 + Md \text{ phi2 } b12 Ks21 \text{ etal } S14 \Big) / (\\
& b21 Ks12 \text{ eta2 } S24 \text{ phi1 } + b21 Ks11 \text{ etal } S14 \text{ phi2 } + b22 Ks22 \text{ eta2 } S24 \text{ phi1 } \\
& + b22 Ks21 \text{ etal } S14 \text{ phi2 })
\end{aligned}$$

> isolate(EQ3, theta);

$$\begin{aligned}
\theta = & (Fd \text{ phi1 } b21 Ks12 \text{ eta2 } S24 + Fd \text{ phi2 } b21 Ks11 \text{ etal } S14 + Fd \text{ phi1 } b22 Ks22 \text{ eta2 } S24 \\
& + Fd \text{ phi2 } b22 Ks21 \text{ etal } S14 - Md \text{ phi1 } b11 Ks12 \text{ eta2 } S24 - Md \text{ phi2 } b11 Ks11 \text{ etal } S14 \\
& - Md \text{ phi1 } b12 Ks22 \text{ eta2 } S24 - Md \text{ phi2 } b12 Ks21 \text{ etal } S14) / (\\
& - b11 u^3 Ks11 \text{ etal } S11 b22 Ks22 \text{ eta2 } S24 - b11 u^3 K11 \text{ phi1 } b22 Ks22 \text{ eta2 } S24 \\
& - b11 u^3 Ks12 \text{ eta2 } S21 b22 Ks21 \text{ etal } S14 - b11 u^2 Ks12 \text{ eta2 } S23 b22 Ks21 \text{ etal } S14 \\
& - a11 u^2 \text{ phi1 } b21 Ks12 \text{ eta2 } S24 - b11 u^2 Ks11 \text{ etal } S13 b22 Ks22 \text{ eta2 } S24 \\
& - b11 u^3 K11 \text{ phi2 } b22 Ks21 \text{ etal } S14 - b11 u^2 K13 \text{ phi1 } b22 Ks22 \text{ eta2 } S24 \\
& - b11 u^2 K13 \text{ phi2 } b22 Ks21 \text{ etal } S14 - a13 \text{ phi2 } b21 Ks11 \text{ etal } S14 \\
& - a11 u^2 \text{ phi2 } b21 Ks11 \text{ etal } S14 - a11 u^2 \text{ phi1 } b22 Ks22 \text{ eta2 } S24 \\
& - a11 u^2 \text{ phi2 } b22 Ks21 \text{ etal } S14 - a13 \text{ phi1 } b21 Ks12 \text{ eta2 } S24 \\
& - b12 u^2 K23 \text{ phi2 } b21 Ks11 \text{ etal } S14 - a13 \text{ phi1 } b22 Ks22 \text{ eta2 } S24 \\
& - a13 \text{ phi2 } b22 Ks21 \text{ etal } S14 - b12 u^3 K21 \text{ phi1 } b21 Ks12 \text{ eta2 } S24 \\
& - b12 u^3 K21 \text{ phi2 } b21 Ks11 \text{ etal } S14 - b12 u^2 K23 \text{ phi1 } b21 Ks12 \text{ eta2 } S24 \\
& + a21 u^2 \text{ phi2 } b12 Ks21 \text{ etal } S14 + a23 \text{ phi1 } b11 Ks12 \text{ eta2 } S24 \\
& + a23 \text{ phi2 } b11 Ks11 \text{ etal } S14 - b12 u^3 Ks21 \text{ etal } S11 b21 Ks12 \text{ eta2 } S24 \\
& - b12 u^2 Ks21 \text{ etal } S13 b21 Ks12 \text{ eta2 } S24 - b12 u^3 Ks22 \text{ eta2 } S21 b21 Ks11 \text{ etal } S14 \\
& - b12 u^2 Ks22 \text{ eta2 } S23 b21 Ks11 \text{ etal } S14 + a21 u^2 \text{ phi1 } b11 Ks12 \text{ eta2 } S24 \\
& + a21 u^2 \text{ phi2 } b11 Ks11 \text{ etal } S14 + a21 u^2 \text{ phi1 } b12 Ks22 \text{ eta2 } S24 \\
& + b21 u^3 Ks12 \text{ eta2 } S21 b12 Ks21 \text{ etal } S14 + b21 u^2 Ks12 \text{ eta2 } S23 b12 Ks21 \text{ etal } S14 \\
& + b22 u^3 K21 \text{ phi1 } b11 Ks12 \text{ eta2 } S24 + b22 u^3 K21 \text{ phi2 } b11 Ks11 \text{ etal } S14 \\
& + a23 \text{ phi1 } b12 Ks22 \text{ eta2 } S24 + a23 \text{ phi2 } b12 Ks21 \text{ etal } S14 \\
& + b21 u^3 K11 \text{ phi1 } b12 Ks22 \text{ eta2 } S24 + b21 u^3 K11 \text{ phi2 } b12 Ks21 \text{ etal } S14 \\
& + b21 u^2 K13 \text{ phi1 } b12 Ks22 \text{ eta2 } S24 + b21 u^2 K13 \text{ phi2 } b12 Ks21 \text{ etal } S14 \\
& + b21 u^3 Ks11 \text{ etal } S11 b12 Ks22 \text{ eta2 } S24 + b21 u^2 Ks11 \text{ etal } S13 b12 Ks22 \text{ eta2 } S24 \\
& + b22 u^2 K23 \text{ phi1 } b11 Ks12 \text{ eta2 } S24 + b22 u^2 K23 \text{ phi2 } b11 Ks11 \text{ etal } S14
\end{aligned}$$

$+ b22 u^3 Ks21 \text{ etal } S11 b11 Ks12 \text{ eta2 } S24 + b22 u^2 Ks21 \text{ etal } S13 b11 Ks12 \text{ eta2 } S24$
 $+ b22 u^3 Ks22 \text{ eta2 } S21 b11 Ks11 \text{ etal } S14 + b22 u^2 Ks22 \text{ eta2 } S23 b11 Ks11 \text{ etal } S14)$

Find the steady state value of theta by setting EQ3=0
> thetass:=simplify(coeff(collect(EQ3,theta),theta,0)/coeff(collect(EQ3,theta),
> theta,1));

$thetass := (Md \text{ phi2 } b11 Ks11 \text{ etal } S14 + Md \text{ phi1 } b12 Ks22 \text{ eta2 } S24$
 $+ Md \text{ phi2 } b12 Ks21 \text{ etal } S14 - Fd \text{ phi1 } b21 Ks12 \text{ eta2 } S24 + Md \text{ phi1 } b11 Ks12 \text{ eta2 } S24$
 $- Fd \text{ phi1 } b22 Ks22 \text{ eta2 } S24 - Fd \text{ phi2 } b22 Ks21 \text{ etal } S14 - Fd \text{ phi2 } b21 Ks11 \text{ etal } S14) / ($
 $- b11 u^3 Ks11 \text{ etal } S11 b22 Ks22 \text{ eta2 } S24 - b11 u^3 K11 \text{ phi1 } b22 Ks22 \text{ eta2 } S24$
 $- b11 u^3 Ks12 \text{ eta2 } S21 b22 Ks21 \text{ etal } S14 - b11 u^2 Ks12 \text{ eta2 } S23 b22 Ks21 \text{ etal } S14$
 $- a11 u^2 \text{ phi1 } b21 Ks12 \text{ eta2 } S24 - b11 u^2 Ks11 \text{ etal } S13 b22 Ks22 \text{ eta2 } S24$
 $- b11 u^3 K11 \text{ phi2 } b22 Ks21 \text{ etal } S14 - b11 u^2 K13 \text{ phi1 } b22 Ks22 \text{ eta2 } S24$
 $- b11 u^2 K13 \text{ phi2 } b22 Ks21 \text{ etal } S14 - a13 \text{ phi2 } b21 Ks11 \text{ etal } S14$
 $- a11 u^2 \text{ phi2 } b21 Ks11 \text{ etal } S14 - a11 u^2 \text{ phi1 } b22 Ks22 \text{ eta2 } S24$
 $- a11 u^2 \text{ phi2 } b22 Ks21 \text{ etal } S14 - a13 \text{ phi1 } b21 Ks12 \text{ eta2 } S24$
 $- b12 u^2 K23 \text{ phi2 } b21 Ks11 \text{ etal } S14 - a13 \text{ phi1 } b22 Ks22 \text{ eta2 } S24$
 $- a13 \text{ phi2 } b22 Ks21 \text{ etal } S14 - b12 u^3 K21 \text{ phi1 } b21 Ks12 \text{ eta2 } S24$
 $- b12 u^3 K21 \text{ phi2 } b21 Ks11 \text{ etal } S14 - b12 u^2 K23 \text{ phi1 } b21 Ks12 \text{ eta2 } S24$
 $+ a21 u^2 \text{ phi2 } b12 Ks21 \text{ etal } S14 + a23 \text{ phi1 } b11 Ks12 \text{ eta2 } S24$
 $+ a23 \text{ phi2 } b11 Ks11 \text{ etal } S14 - b12 u^3 Ks21 \text{ etal } S11 b21 Ks12 \text{ eta2 } S24$
 $- b12 u^2 Ks21 \text{ etal } S13 b21 Ks12 \text{ eta2 } S24 - b12 u^3 Ks22 \text{ eta2 } S21 b21 Ks11 \text{ etal } S14$
 $- b12 u^2 Ks22 \text{ eta2 } S23 b21 Ks11 \text{ etal } S14 + a21 u^2 \text{ phi1 } b11 Ks12 \text{ eta2 } S24$
 $+ a21 u^2 \text{ phi2 } b11 Ks11 \text{ etal } S14 + a21 u^2 \text{ phi1 } b12 Ks22 \text{ eta2 } S24$
 $+ b21 u^3 Ks12 \text{ eta2 } S21 b12 Ks21 \text{ etal } S14 + b21 u^2 Ks12 \text{ eta2 } S23 b12 Ks21 \text{ etal } S14$
 $+ b22 u^3 K21 \text{ phi1 } b11 Ks12 \text{ eta2 } S24 + b22 u^3 K21 \text{ phi2 } b11 Ks11 \text{ etal } S14$
 $+ a23 \text{ phi1 } b12 Ks22 \text{ eta2 } S24 + a23 \text{ phi2 } b12 Ks21 \text{ etal } S14$
 $+ b21 u^3 K11 \text{ phi1 } b12 Ks22 \text{ eta2 } S24 + b21 u^3 K11 \text{ phi2 } b12 Ks21 \text{ etal } S14$
 $+ b21 u^2 K13 \text{ phi1 } b12 Ks22 \text{ eta2 } S24 + b21 u^2 K13 \text{ phi2 } b12 Ks21 \text{ etal } S14$
 $+ b21 u^3 Ks11 \text{ etal } S11 b12 Ks22 \text{ eta2 } S24 + b21 u^2 Ks11 \text{ etal } S13 b12 Ks22 \text{ eta2 } S24$
 $+ b22 u^2 K23 \text{ phi1 } b11 Ks12 \text{ eta2 } S24 + b22 u^2 K23 \text{ phi2 } b11 Ks11 \text{ etal } S14$
 $+ b22 u^3 Ks21 \text{ etal } S11 b11 Ks12 \text{ eta2 } S24 + b22 u^2 Ks21 \text{ etal } S13 b11 Ks12 \text{ eta2 } S24$
 $+ b22 u^3 Ks22 \text{ eta2 } S21 b11 Ks11 \text{ etal } S14 + b22 u^2 Ks22 \text{ eta2 } S23 b11 Ks11 \text{ etal } S14)$

Substitute thetass into EQ1 and solve for steady state z

> temp:=coeff(collect(EQ1,z),z,0)/coeff(collect(EQ1,z),z,1);

$$\begin{aligned} \text{temp} := & \left(a11 \theta u^2 + a13 \theta \right. \\ & + b11 u^2 \left(K11 \theta u + K13 \theta + \frac{Ks11 \text{etal} (S11 \theta u + S13 \theta)}{\text{phil}} + \frac{Ks12 \text{eta2} (S21 \theta u + S23 \theta)}{\text{phi2}} \right) \\ & + b12 u^2 \left(K21 \theta u + K23 \theta + \frac{Ks21 \text{etal} (S11 \theta u + S13 \theta)}{\text{phil}} + \frac{Ks22 \text{eta2} (S21 \theta u + S23 \theta)}{\text{phi2}} \right) \\ & \left. + Fd \right) / \left(\right. \\ & b11 u^2 \left(\frac{Ks11 \text{etal} S14}{\text{phil}} + \frac{Ks12 \text{eta2} S24}{\text{phi2}} \right) + b12 u^2 \left(\frac{Ks21 \text{etal} S14}{\text{phil}} + \frac{Ks22 \text{eta2} S24}{\text{phi2}} \right) \left. \right) \end{aligned}$$

> zss :=

> coeff(collect(temp,theta),theta,1)*thetass+coeff(collect(temp,theta),theta,0)

> ;

$$\begin{aligned} \text{zss} := & \left(a13 + b11 u^2 \left(K11 u + K13 + \frac{Ks11 \text{etal} (S11 u + S13)}{\text{phil}} + \frac{Ks12 \text{eta2} (S21 u + S23)}{\text{phi2}} \right) \right. \\ & + b12 u^2 \left(K21 u + K23 + \frac{Ks21 \text{etal} (S11 u + S13)}{\text{phil}} + \frac{Ks22 \text{eta2} (S21 u + S23)}{\text{phi2}} \right) + a11 u^2 \left. \right) (\\ & Md \text{phi2} b11 Ks11 \text{etal} S14 + Md \text{phil} b12 Ks22 \text{eta2} S24 + Md \text{phi2} b12 Ks21 \text{etal} S14 \\ & - Fd \text{phil} b21 Ks12 \text{eta2} S24 + Md \text{phil} b11 Ks12 \text{eta2} S24 - Fd \text{phil} b22 Ks22 \text{eta2} S24 \\ & - Fd \text{phi2} b22 Ks21 \text{etal} S14 - Fd \text{phi2} b21 Ks11 \text{etal} S14) / \left(\right. \\ & \left(b11 u^2 \left(\frac{Ks11 \text{etal} S14}{\text{phil}} + \frac{Ks12 \text{eta2} S24}{\text{phi2}} \right) + b12 u^2 \left(\frac{Ks21 \text{etal} S14}{\text{phil}} + \frac{Ks22 \text{eta2} S24}{\text{phi2}} \right) \right) \left. \right) (\\ & - b11 u^3 Ks11 \text{etal} S11 b22 Ks22 \text{eta2} S24 - b11 u^3 K11 \text{phil} b22 Ks22 \text{eta2} S24 \\ & - b11 u^3 Ks12 \text{eta2} S21 b22 Ks21 \text{etal} S14 - b11 u^2 Ks12 \text{eta2} S23 b22 Ks21 \text{etal} S14 \\ & - a11 u^2 \text{phil} b21 Ks12 \text{eta2} S24 - b11 u^2 Ks11 \text{etal} S13 b22 Ks22 \text{eta2} S24 \\ & - b11 u^3 K11 \text{phi2} b22 Ks21 \text{etal} S14 - b11 u^2 K13 \text{phil} b22 Ks22 \text{eta2} S24 \\ & - b11 u^2 K13 \text{phi2} b22 Ks21 \text{etal} S14 - a13 \text{phi2} b21 Ks11 \text{etal} S14 \\ & - a11 u^2 \text{phi2} b21 Ks11 \text{etal} S14 - a11 u^2 \text{phil} b22 Ks22 \text{eta2} S24 \\ & - a11 u^2 \text{phi2} b22 Ks21 \text{etal} S14 - a13 \text{phil} b21 Ks12 \text{eta2} S24 \\ & - b12 u^2 K23 \text{phi2} b21 Ks11 \text{etal} S14 - a13 \text{phil} b22 Ks22 \text{eta2} S24 \\ & - a13 \text{phi2} b22 Ks21 \text{etal} S14 - b12 u^3 K21 \text{phil} b21 Ks12 \text{eta2} S24 \\ & - b12 u^3 K21 \text{phi2} b21 Ks11 \text{etal} S14 - b12 u^2 K23 \text{phil} b21 Ks12 \text{eta2} S24 \\ & + a21 u^2 \text{phi2} b12 Ks21 \text{etal} S14 + a23 \text{phil} b11 Ks12 \text{eta2} S24 \\ & + a23 \text{phi2} b11 Ks11 \text{etal} S14 - b12 u^3 Ks21 \text{etal} S11 b21 Ks12 \text{eta2} S24 \\ & - b12 u^2 Ks21 \text{etal} S13 b21 Ks12 \text{eta2} S24 - b12 u^3 Ks22 \text{eta2} S21 b21 Ks11 \text{etal} S14 \end{aligned}$$

$$\begin{aligned}
& -b12 u^2 Ks22 eta2 S23 b21 Ks11 eta1 S14 + a21 u^2 phi1 b11 Ks12 eta2 S24 \\
& + a21 u^2 phi2 b11 Ks11 eta1 S14 + a21 u^2 phi1 b12 Ks22 eta2 S24 \\
& + b21 u^3 Ks12 eta2 S21 b12 Ks21 eta1 S14 + b21 u^2 Ks12 eta2 S23 b12 Ks21 eta1 S14 \\
& + b22 u^3 K21 phi1 b11 Ks12 eta2 S24 + b22 u^3 K21 phi2 b11 Ks11 eta1 S14 \\
& + a23 phi1 b12 Ks22 eta2 S24 + a23 phi2 b12 Ks21 eta1 S14 \\
& + b21 u^3 K11 phi1 b12 Ks22 eta2 S24 + b21 u^3 K11 phi2 b12 Ks21 eta1 S14 \\
& + b21 u^2 K13 phi1 b12 Ks22 eta2 S24 + b21 u^2 K13 phi2 b12 Ks21 eta1 S14 \\
& + b21 u^3 Ks11 eta1 S11 b12 Ks22 eta2 S24 + b21 u^2 Ks11 eta1 S13 b12 Ks22 eta2 S24 \\
& + b22 u^2 K23 phi1 b11 Ks12 eta2 S24 + b22 u^2 K23 phi2 b11 Ks11 eta1 S14 \\
& + b22 u^3 Ks21 eta1 S11 b11 Ks12 eta2 S24 + b22 u^2 Ks21 eta1 S13 b11 Ks12 eta2 S24 \\
& + b22 u^3 Ks22 eta2 S21 b11 Ks11 eta1 S14 + b22 u^2 Ks22 eta2 S23 b11 Ks11 eta1 S14) \Big)
\end{aligned}$$

$$+ \frac{Fd}{b11 u^2 \left(\frac{Ks11 eta1 S14}{phi1} + \frac{Ks12 eta2 S24}{phi2} \right) + b12 u^2 \left(\frac{Ks21 eta1 S14}{phi1} + \frac{Ks22 eta2 S24}{phi2} \right)}$$

Determine the coefficients C1 and C2 such that zss=C1*Fd+C2*Md

> C1:= simplify(coeff(collect(expand(zss),Fd),Fd,1));

$$\begin{aligned}
C1 := & - \left(2 phi2^2 phi1 a13 b22 Ks21 eta1 S14 + 2 phi2 phi1^2 a13 b21 Ks12 eta2 S24 \right. \\
& + 2 phi2 phi1^2 a13 b22 Ks22 eta2 S24 + 2 phi2^2 phi1 a13 b21 Ks11 eta1 S14 \\
& + phi2 phi1^2 b11 u^3 K11 b21 Ks12 eta2 S24 + 2 phi2 phi1^2 b11 u^3 K11 b22 Ks22 eta2 S24 \\
& + phi2 phi1 b11 u^2 Ks11 eta1 S13 b21 Ks12 eta2 S24 \\
& + 2 phi2 phi1 b11 u^2 Ks11 eta1 S13 b22 Ks22 eta2 S24 \\
& + 2 phi2 phi1 b11 u^3 Ks11 eta1 S11 b22 Ks22 eta2 S24 \\
& + 2 phi2^2 phi1 b11 u^2 K13 b22 Ks21 eta1 S14 + phi2^2 phi1 b11 u^2 K13 b21 Ks11 eta1 S14 \\
& + 2 phi2 phi1^2 b11 u^2 K13 b22 Ks22 eta2 S24 + phi2^2 phi1 b11 u^3 K11 b21 Ks11 eta1 S14 \\
& + phi2 phi1 b11 u^3 Ks11 eta1 S11 b21 Ks12 eta2 S24 \\
& + phi2 phi1^2 b11 u^2 K13 b21 Ks12 eta2 S24 + 2 phi2^2 phi1 b11 u^3 K11 b22 Ks21 eta1 S14 \\
& + 2 phi2 phi1 b11 u^3 Ks12 eta2 S21 b22 Ks21 eta1 S14 \\
& + phi2 phi1 b11 u^3 Ks12 eta2 S21 b21 Ks11 eta1 S14 \\
& + phi2 phi1 b11 u^2 Ks12 eta2 S23 b21 Ks11 eta1 S14 \\
& + 2 phi2 phi1 b11 u^2 Ks12 eta2 S23 b22 Ks21 eta1 S14 \\
& + 2 phi2 phi1^2 b12 u^3 K21 b21 Ks12 eta2 S24 \\
& \left. + 2 phi2 phi1 b12 u^3 Ks21 eta1 S11 b21 Ks12 eta2 S24 \right)
\end{aligned}$$

$$\begin{aligned}
& + \phi^2 \phi^2 b_{12} u^2 K_{23} b_{22} K_{s22} \eta^2 S_{24} + 2 \phi^2 \phi^2 b_{12} u^2 K_{23} b_{21} K_{s12} \eta^2 S_{24} \\
& + 2 \phi^2 \phi^2 \phi b_{12} u^3 K_{21} b_{21} K_{s11} \eta^2 S_{14} + \phi^2 \phi^2 \phi b_{12} u^3 K_{21} b_{22} K_{s21} \eta^2 S_{14} \\
& + \phi^2 \phi^2 b_{12} u^3 K_{21} b_{22} K_{s22} \eta^2 S_{24} + 2 \phi^2 \phi^2 \phi b_{12} u^2 K_{23} b_{21} K_{s11} \eta^2 S_{14} \\
& + \phi^2 \phi^2 \phi b_{12} u^2 K_{23} b_{22} K_{s21} \eta^2 S_{14} \\
& + \phi^2 \phi^2 \phi b_{12} u^2 K_{s21} \eta^2 S_{13} b_{22} K_{s22} \eta^2 S_{24} \\
& + 2 \phi^2 \phi^2 \phi b_{12} u^2 K_{s21} \eta^2 S_{13} b_{21} K_{s12} \eta^2 S_{24} \\
& + \phi^2 \phi^2 \phi b_{12} u^3 K_{s21} \eta^2 S_{11} b_{22} K_{s22} \eta^2 S_{24} \\
& + \phi^2 \phi^2 \phi b_{12} u^3 K_{s22} \eta^2 S_{21} b_{22} K_{s21} \eta^2 S_{14} \\
& + 2 \phi^2 \phi^2 \phi b_{12} u^3 K_{s22} \eta^2 S_{21} b_{21} K_{s11} \eta^2 S_{14} \\
& + \phi^2 \phi^2 \phi b_{12} u^2 K_{s22} \eta^2 S_{23} b_{22} K_{s21} \eta^2 S_{14} \\
& + 2 \phi^2 \phi^2 \phi b_{12} u^2 K_{s22} \eta^2 S_{23} b_{21} K_{s11} \eta^2 S_{14} \\
& + 2 \phi^2 \phi^2 \phi^2 a_{11} u^2 b_{21} K_{s12} \eta^2 S_{24} + 2 \phi^2 \phi^2 \phi^2 a_{11} u^2 b_{22} K_{s22} \eta^2 S_{24} \\
& + 2 \phi^2 \phi^2 \phi^2 a_{11} u^2 b_{22} K_{s21} \eta^2 S_{14} + 2 \phi^2 \phi^2 \phi^2 a_{11} u^2 b_{21} K_{s11} \eta^2 S_{14} \\
& + \phi^2 \phi^2 b_{11} u^3 K_{s11} \eta^2 S_{11} b_{22} K_{s21} S_{14} + \phi^2 \phi^2 b_{11} u^3 K_{s11}^2 \eta^2 S_{11} b_{21} S_{14} \\
& + \phi^2 \phi^2 b_{11} u^2 K_{s12}^2 \eta^2 S_{23} b_{21} S_{24} + \phi^2 \phi^2 b_{11} u^2 K_{s12} \eta^2 S_{23} b_{22} K_{s22} S_{24} \\
& + \phi^2 \phi^2 b_{11} u^2 K_{s11} \eta^2 S_{13} b_{22} K_{s21} S_{14} + \phi^2 \phi^2 b_{11} u^2 K_{s11}^2 \eta^2 S_{13} b_{21} S_{14} \\
& + \phi^2 \phi^2 b_{11} u^3 K_{s12}^2 \eta^2 S_{21} b_{21} S_{24} + \phi^2 \phi^2 b_{11} u^3 K_{s12} \eta^2 S_{21} b_{22} K_{s22} S_{24} \\
& + \phi^2 \phi^2 b_{12} u^2 K_{s21}^2 \eta^2 S_{13} b_{22} S_{14} + \phi^2 \phi^2 b_{12} u^2 K_{s21} \eta^2 S_{13} b_{21} K_{s11} S_{14} \\
& + \phi^2 \phi^2 b_{12} u^3 K_{s22} \eta^2 S_{21} b_{21} K_{s12} S_{24} + \phi^2 \phi^2 b_{12} u^3 K_{s22}^2 \eta^2 S_{21} b_{22} S_{24} \\
& + \phi^2 \phi^2 b_{12} u^3 K_{s21}^2 \eta^2 S_{11} b_{22} S_{14} + \phi^2 \phi^2 b_{12} u^3 K_{s21} \eta^2 S_{11} b_{21} K_{s11} S_{14} \\
& + \phi^2 \phi^2 b_{12} u^2 K_{s22} \eta^2 S_{23} b_{21} K_{s12} S_{24} + \phi^2 \phi^2 b_{12} u^2 K_{s22}^2 \eta^2 S_{23} b_{22} S_{24} \\
& - \phi^2 \phi^2 \phi a_{21} u^2 b_{12} K_{s21} \eta^2 S_{14} - \phi^2 \phi^2 \phi^2 a_{23} b_{11} K_{s12} \eta^2 S_{24} \\
& - \phi^2 \phi^2 \phi^2 a_{23} b_{11} K_{s11} \eta^2 S_{14} - \phi^2 \phi^2 \phi^2 a_{21} u^2 b_{11} K_{s12} \eta^2 S_{24} \\
& - \phi^2 \phi^2 \phi^2 a_{21} u^2 b_{11} K_{s11} \eta^2 S_{14} - \phi^2 \phi^2 \phi^2 a_{21} u^2 b_{12} K_{s22} \eta^2 S_{24} \\
& - \phi^2 \phi^2 \phi b_{21} u^3 K_{s12} \eta^2 S_{21} b_{12} K_{s21} \eta^2 S_{14} \\
& - \phi^2 \phi^2 \phi b_{21} u^2 K_{s12} \eta^2 S_{23} b_{12} K_{s21} \eta^2 S_{14} \\
& - \phi^2 \phi^2 \phi^2 b_{22} u^3 K_{21} b_{11} K_{s12} \eta^2 S_{24} - \phi^2 \phi^2 \phi^2 b_{22} u^3 K_{21} b_{11} K_{s11} \eta^2 S_{14} \\
& - \phi^2 \phi^2 \phi^2 a_{23} b_{12} K_{s22} \eta^2 S_{24} - \phi^2 \phi^2 \phi^2 a_{23} b_{12} K_{s21} \eta^2 S_{14} \\
& - \phi^2 \phi^2 \phi^2 b_{21} u^3 K_{11} b_{12} K_{s22} \eta^2 S_{24} - \phi^2 \phi^2 \phi^2 b_{21} u^3 K_{11} b_{12} K_{s21} \eta^2 S_{14} \\
& - \phi^2 \phi^2 \phi^2 b_{21} u^2 K_{13} b_{12} K_{s22} \eta^2 S_{24} - \phi^2 \phi^2 \phi^2 b_{21} u^2 K_{13} b_{12} K_{s21} \eta^2 S_{14}
\end{aligned}$$

$$\begin{aligned}
& -\phi i2 \phi i1 b21 u^3 Ks11 \text{ etal } S11 b12 Ks22 \text{ eta2 } S24 \\
& -\phi i2 \phi i1 b21 u^2 Ks11 \text{ etal } S13 b12 Ks22 \text{ eta2 } S24 \\
& -\phi i2 \phi i1^2 b22 u^2 K23 b11 Ks12 \text{ eta2 } S24 - \phi i2^2 \phi i1 b22 u^2 K23 b11 Ks11 \text{ etal } S14 \\
& -\phi i2 \phi i1 b22 u^3 Ks21 \text{ etal } S11 b11 Ks12 \text{ eta2 } S24 \\
& -\phi i2 \phi i1 b22 u^2 Ks21 \text{ etal } S13 b11 Ks12 \text{ eta2 } S24 \\
& -\phi i2 \phi i1 b22 u^3 Ks22 \text{ eta2 } S21 b11 Ks11 \text{ etal } S14 \\
& -\phi i2 \phi i1 b22 u^2 Ks22 \text{ eta2 } S23 b11 Ks11 \text{ etal } S14) / (u^2 (\phi i1 b11 Ks12 \text{ eta2 } S24 \\
& + \phi i2 b11 Ks11 \text{ etal } S14 + \phi i1 b12 Ks22 \text{ eta2 } S24 + \phi i2 b12 Ks21 \text{ etal } S14) (\\
& -b11 u^3 Ks11 \text{ etal } S11 b22 Ks22 \text{ eta2 } S24 - b11 u^3 K11 \phi i1 b22 Ks22 \text{ eta2 } S24 \\
& -b11 u^3 Ks12 \text{ eta2 } S21 b22 Ks21 \text{ etal } S14 - b11 u^2 Ks12 \text{ eta2 } S23 b22 Ks21 \text{ etal } S14 \\
& -a11 u^2 \phi i1 b21 Ks12 \text{ eta2 } S24 - b11 u^2 Ks11 \text{ etal } S13 b22 Ks22 \text{ eta2 } S24 \\
& -b11 u^3 K11 \phi i2 b22 Ks21 \text{ etal } S14 - b11 u^2 K13 \phi i1 b22 Ks22 \text{ eta2 } S24 \\
& -b11 u^2 K13 \phi i2 b22 Ks21 \text{ etal } S14 - a13 \phi i2 b21 Ks11 \text{ etal } S14 \\
& -a11 u^2 \phi i2 b21 Ks11 \text{ etal } S14 - a11 u^2 \phi i1 b22 Ks22 \text{ eta2 } S24 \\
& -a11 u^2 \phi i2 b22 Ks21 \text{ etal } S14 - a13 \phi i1 b21 Ks12 \text{ eta2 } S24 \\
& -b12 u^2 K23 \phi i2 b21 Ks11 \text{ etal } S14 - a13 \phi i1 b22 Ks22 \text{ eta2 } S24 \\
& -a13 \phi i2 b22 Ks21 \text{ etal } S14 - b12 u^3 K21 \phi i1 b21 Ks12 \text{ eta2 } S24 \\
& -b12 u^3 K21 \phi i2 b21 Ks11 \text{ etal } S14 - b12 u^2 K23 \phi i1 b21 Ks12 \text{ eta2 } S24 \\
& + a21 u^2 \phi i2 b12 Ks21 \text{ etal } S14 + a23 \phi i1 b11 Ks12 \text{ eta2 } S24 \\
& + a23 \phi i2 b11 Ks11 \text{ etal } S14 - b12 u^3 Ks21 \text{ etal } S11 b21 Ks12 \text{ eta2 } S24 \\
& -b12 u^2 Ks21 \text{ etal } S13 b21 Ks12 \text{ eta2 } S24 - b12 u^3 Ks22 \text{ eta2 } S21 b21 Ks11 \text{ etal } S14 \\
& -b12 u^2 Ks22 \text{ eta2 } S23 b21 Ks11 \text{ etal } S14 + a21 u^2 \phi i1 b11 Ks12 \text{ eta2 } S24 \\
& + a21 u^2 \phi i2 b11 Ks11 \text{ etal } S14 + a21 u^2 \phi i1 b12 Ks22 \text{ eta2 } S24 \\
& + b21 u^3 Ks12 \text{ eta2 } S21 b12 Ks21 \text{ etal } S14 + b21 u^2 Ks12 \text{ eta2 } S23 b12 Ks21 \text{ etal } S14 \\
& + b22 u^3 K21 \phi i1 b11 Ks12 \text{ eta2 } S24 + b22 u^3 K21 \phi i2 b11 Ks11 \text{ etal } S14 \\
& + a23 \phi i1 b12 Ks22 \text{ eta2 } S24 + a23 \phi i2 b12 Ks21 \text{ etal } S14 \\
& + b21 u^3 K11 \phi i1 b12 Ks22 \text{ eta2 } S24 + b21 u^3 K11 \phi i2 b12 Ks21 \text{ etal } S14 \\
& + b21 u^2 K13 \phi i1 b12 Ks22 \text{ eta2 } S24 + b21 u^2 K13 \phi i2 b12 Ks21 \text{ etal } S14 \\
& + b21 u^3 Ks11 \text{ etal } S11 b12 Ks22 \text{ eta2 } S24 + b21 u^2 Ks11 \text{ etal } S13 b12 Ks22 \text{ eta2 } S24 \\
& + b22 u^2 K23 \phi i1 b11 Ks12 \text{ eta2 } S24 + b22 u^2 K23 \phi i2 b11 Ks11 \text{ etal } S14
\end{aligned}$$

$$\begin{aligned}
& + b22 u^3 Ks21 \text{ etal } S11 b11 Ks12 \text{ eta2 } S24 + b22 u^2 Ks21 \text{ etal } S13 b11 Ks12 \text{ eta2 } S24 \\
& + b22 u^3 Ks22 \text{ eta2 } S21 b11 Ks11 \text{ etal } S14 + b22 u^2 Ks22 \text{ eta2 } S23 b11 Ks11 \text{ etal } S14 \Big) \Big) \\
> C2 := \text{simplify}(\text{coeff}(\text{collect}(\text{expand}(zss), Md), Md, 1)); \\
C2 := & (Ks11 \text{ etal } \phi^2 b11 u^3 S11 + Ks11 \text{ etal } \phi^2 b11 u^2 S13 + \text{etal } \phi^2 u^2 S13 b12 Ks21 \\
& + \text{etal } \phi^2 u^3 S11 b12 Ks21 + \phi^2 b11 \phi^1 u^3 K11 + \phi^2 b11 \phi^1 u^2 K13 + \phi^2 \phi^1 a13 \\
& + \phi^2 \phi^1 b12 u^2 K23 + \phi^2 \phi^1 a11 u^2 + \phi^2 \phi^1 b12 u^3 K21 \\
& + b11 \phi^1 u^3 Ks12 \text{ eta2 } S21 + b11 \phi^1 u^2 Ks12 \text{ eta2 } S23 + \phi^1 b12 u^2 Ks22 \text{ eta2 } S23 \\
& + \phi^1 b12 u^3 Ks22 \text{ eta2 } S21) / ((-b11 u^3 Ks11 \text{ etal } S11 b22 Ks22 \text{ eta2 } S24 \\
& - b11 u^3 K11 \phi^1 b22 Ks22 \text{ eta2 } S24 - b11 u^3 Ks12 \text{ eta2 } S21 b22 Ks21 \text{ etal } S14 \\
& - b11 u^2 Ks12 \text{ eta2 } S23 b22 Ks21 \text{ etal } S14 - a11 u^2 \phi^1 b21 Ks12 \text{ eta2 } S24 \\
& - b11 u^2 Ks11 \text{ etal } S13 b22 Ks22 \text{ eta2 } S24 - b11 u^3 K11 \phi^2 b22 Ks21 \text{ etal } S14 \\
& - b11 u^2 K13 \phi^1 b22 Ks22 \text{ eta2 } S24 - b11 u^2 K13 \phi^2 b22 Ks21 \text{ etal } S14 \\
& - a13 \phi^2 b21 Ks11 \text{ etal } S14 - a11 u^2 \phi^2 b21 Ks11 \text{ etal } S14 \\
& - a11 u^2 \phi^1 b22 Ks22 \text{ eta2 } S24 - a11 u^2 \phi^2 b22 Ks21 \text{ etal } S14 \\
& - a13 \phi^1 b21 Ks12 \text{ eta2 } S24 - b12 u^2 K23 \phi^2 b21 Ks11 \text{ etal } S14 \\
& - a13 \phi^1 b22 Ks22 \text{ eta2 } S24 - a13 \phi^2 b22 Ks21 \text{ etal } S14 \\
& - b12 u^3 K21 \phi^1 b21 Ks12 \text{ eta2 } S24 - b12 u^3 K21 \phi^2 b21 Ks11 \text{ etal } S14 \\
& - b12 u^2 K23 \phi^1 b21 Ks12 \text{ eta2 } S24 + a21 u^2 \phi^2 b12 Ks21 \text{ etal } S14 \\
& + a23 \phi^1 b11 Ks12 \text{ eta2 } S24 + a23 \phi^2 b11 Ks11 \text{ etal } S14 \\
& - b12 u^3 Ks21 \text{ etal } S11 b21 Ks12 \text{ eta2 } S24 - b12 u^2 Ks21 \text{ etal } S13 b21 Ks12 \text{ eta2 } S24 \\
& - b12 u^3 Ks22 \text{ eta2 } S21 b21 Ks11 \text{ etal } S14 - b12 u^2 Ks22 \text{ eta2 } S23 b21 Ks11 \text{ etal } S14 \\
& + a21 u^2 \phi^1 b11 Ks12 \text{ eta2 } S24 + a21 u^2 \phi^2 b11 Ks11 \text{ etal } S14 \\
& + a21 u^2 \phi^1 b12 Ks22 \text{ eta2 } S24 + b21 u^3 Ks12 \text{ eta2 } S21 b12 Ks21 \text{ etal } S14 \\
& + b21 u^2 Ks12 \text{ eta2 } S23 b12 Ks21 \text{ etal } S14 + b22 u^3 K21 \phi^1 b11 Ks12 \text{ eta2 } S24 \\
& + b22 u^3 K21 \phi^2 b11 Ks11 \text{ etal } S14 + a23 \phi^1 b12 Ks22 \text{ eta2 } S24 \\
& + a23 \phi^2 b12 Ks21 \text{ etal } S14 + b21 u^3 K11 \phi^1 b12 Ks22 \text{ eta2 } S24 \\
& + b21 u^3 K11 \phi^2 b12 Ks21 \text{ etal } S14 + b21 u^2 K13 \phi^1 b12 Ks22 \text{ eta2 } S24 \\
& + b21 u^2 K13 \phi^2 b12 Ks21 \text{ etal } S14 + b21 u^3 Ks11 \text{ etal } S11 b12 Ks22 \text{ eta2 } S24 \\
& + b21 u^2 Ks11 \text{ etal } S13 b12 Ks22 \text{ eta2 } S24 + b22 u^2 K23 \phi^1 b11 Ks12 \text{ eta2 } S24 \\
& + b22 u^2 K23 \phi^2 b11 Ks11 \text{ etal } S14 + b22 u^3 Ks21 \text{ etal } S11 b11 Ks12 \text{ eta2 } S24 \\
& + b22 u^2 Ks21 \text{ etal } S13 b11 Ks12 \text{ eta2 } S24 + b22 u^3 Ks22 \text{ eta2 } S21 b11 Ks11 \text{ etal } S14
\end{aligned}$$

$$+ b_{22} u^2 K_{s22} \eta_{a2} S_{23} b_{11} K_{s11} \eta_{a1} S_{14}) u^2)$$

Check that $zss = C1 \cdot Fd + C2 \cdot Md$

> eq6 := simplify(zss - C1 * Fd - C2 * Md);

eq6 := 0

>

INITIAL DISTRIBUTION LIST

- | | | |
|----|--|---|
| 1. | Defense Technical Information Center
8725 John J. Kingman Rd., STE 0944
Ft. Belvoir, VA 22060-6218 | 2 |
| 2. | Dudley Knox Library
Naval Postgraduate School
411 Dyer Rd.
Monterey, CA 93943-5101 | 2 |
| 3. | Chairman, Code ME/Mc
Department of Mechanical Engineering
Naval Postgraduate School
Monterey, CA 93943-5000 | 1 |
| 4. | Mr. Randy Dean
Johns Hopkins University Applied Physics Laboratory
Mail Stop 13-N422
Johns Hopkins Road
Laurel, MD 20723-609 | 2 |
| 5. | Naval Engineering Curricular Office, Code 34
Naval Postgraduate School
Monterey, CA 93943-5000 | 1 |
| 6. | Professor F. A. Papoulias, Code ME/Pa
Department of Mechanical Engineering
Naval Postgraduate School
Monterey, CA 93943-5000 | 5 |
| 7. | LT John Tolliver
HC 67 Box 64
Loma, MT
59460 | 4 |